NTNU
Norwegian University of
Science and Technology

Physical Modeling of Debris Flow by Varying Sediment Concentration

Rosy Nhuchhen Pradhan

Physical Modeling of Debris Flow by Varying Sediment Concentration

Rosy Nhuchhen Pradhan

NORWEGIAN UNIVERSITY OF SCIENCE AND TECHNOLOGY

DEPARTMENT OF CIVIL AND ENVIRONMENTAL ENGINEERING

Report Title: PHYSICAL MODELING OF DEBRIS FLOW BY VARYING SEDIMENT CONCENTRATION	Date: 10.06.2017		
	Number of pages (incl. appendices): 155		
	Master Thesis	X	Project Work	
Name: Rosy Nhuchhen Pradhan			
Professor in charge/supervisor: Steinar Nordal, NTNU			
Other external professional contacts/supervisors: Vikas Thakur, NTNU			

Abstract

Debris flow is one of the destructive geohazards occurring typically in the steep topography induced mostly by heavy rainfall events. As the existing soil mass on the steep terrain receives a rainfall or water from any source, the effective stress of the soil reduces due to rise in pore pressure, which ultimately disturbs its stability and thus soil mass liquefies and flows. The flow may take an increasing amount of debris with it. The flowing mixture of sediments and water may hit infrastructure downslope and cause damage to property with loss of lives and large economical losses.

It is not possible to accurately predict the risk of and forces involved in a possible debris flow that may hit a building or a facility in a hazardous area. However, assuming that a certain volume of soil and water turns unstable high up in a certain slope the probability of potential damage can be quantified by predicting the velocity, impact forces, runout distance of the debris flow and flow height of debris flow. Observations and measurements from actual debris flow events can be helpful to evaluate the risk and calibrate our simulation tools for debris flow. But in many cases lack of field data makes this quite challenging. Data obtained from physical modeling of debris flow under controlled conditions in a laboratory therefore offers valuable information for improving our understanding and predictions.

A series of laboratory large scale model tests on debris flow has been conducted for this thesis. The objective is to study the effect of change in sediment concentration on the resulting velocity, flow height, deposition height, runout distance. Segregation of the sediment such that larger particles separate from finer particles during flow is also studied. The results are to be used for calibration of numerical models simulating the flow.

The thesis includes a literature review focusing on the basic mechanism, physics, and characteristics of the debris flow. Six debris slide tests on almost dry material are done. Forty debris flow tests on wet material are made, with varying the total volume of the flowing mass and the sediment concentration (i.e. the amount of added water). It is found that the tests resembled the real debris flow event and support existing knowledge and theory of debris flow. The main findings are summarized as:

- A distinct variation is observed in velocity and runout length as a function of sediment concentration.
- The velocity and runout length also varies with the amount (total volume) of debris material used in the test.
- For a larger material volume, the variation in velocity and runout length as a function of sediment concentration is less pronounced. The energy dissipation is rapid for flow with smaller volume.
- The runout length of the debris slide increases when the material gets more coarse, (larger average grain size). The coarser particles will also travel faster and further in the deposition area compared to the fines in the same mass.
- The surge height in the transport zone increases as the sediment concentration increases. In the deposition area, the surge height decreases as the sediment concentration increases.
- The variation in surge height with concentration varies more in the transport zone and deposition zone when larger volumes of the material used in the test.
- Inspection of the deposition mass after the debris flow, reveal that the mass separates with inverse grading during the flow unless the mass has a very low concentration.
- Degree of coarseness of the grain size at beginning of deposition area increases with decreasing volume and increasing concentration while it's vice versa at end of deposition area.
- Forces measured in the test on a cylinder is close to expected values based on simple formulas based on hydrodynamics.

Keywords: Debris Flow, Physical Modeling, Sediment Concentration, Debris flow parameters

MASTERS DEGREE THESIS
Spring 2017
Rosy Nhuchhen Pradhan
PHYSICAL MODELING OF DEBRIS FLOW BY VARYING SEDIMENT CONCENTRATION

BACKGROUND

Debris flows are water dominated earth slides that occur in steep slopes, normally exceeding 15º, due to heavy rainfall. The terrain surface may become unstable and a debris flow may start. The flowing mass may increase in volume by eroding the underlying soil and take organic material including trees and other debris into a destructive, heavy, flowing mass. The flowing mixture will be denoted a debris flow. The potential for loss of lives and damage to property, closure of roads and railroads may be large. Norway is the country with steep mountainsides that receive heavy rainfall every year. Occasionally local rainfall can be extremely intense. Due to climate change, the precipitation and rainfall intensity may increase significantly in certain areas. This increases the debris flow hazard. The suggested MSc study relates to two research programs that both aim to reduce the risk related to debris flows, the E39 project initiated by the Norwegian Public Roads Administration (NPRA) and the Klima 2050, Centre for Innovative Research, funded by the Norwegian Research Council.

A series of laboratory large scale model tests on debris flow is suggested for this MSc thesis by Rosy Nhuchhen Pradhan. The objective is to study the effect of change in sediment concentration on the resulting velocity, flow height, deposition height, runout distance for debris flows. The aim is to add to our understanding of the mechanics of the flowing material and to generate measurements, which can be used to calibrate numerical simulation tools for debris flow modeling.

An existing 1: 20 model scale test facility in the NTNU laboratory is to be used for the tests. The model has been used by previous MSc students since 2009 for testing the behavior of the flowing material and for tests on check dams, baffles, deflection structures and other debris flow breakers. A PhD study by Ashenafi Lulseged Yifru has started under the E39 project. The suggested tests by Rosy Nhuchhen Pradhan is to be performed in cooperation with Ashenafi Lulseged Yifru, who also will be a discussion partner in this work.
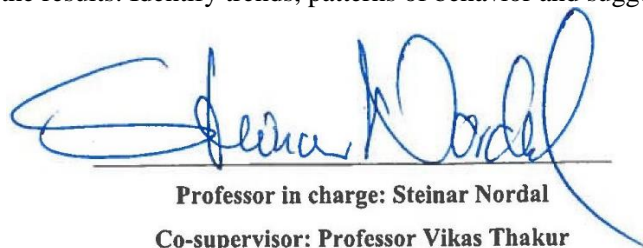
TASK

The main aim of the study is to systematically vary and study the effect of the amount of water in the flowing material (the debris) and the effect of the total volume of the debris flow mixture used in the test. Focus should be on observing velocities, flow heights, runout distances, mass separation during flow etc.

The model has not been used for a while and a new instrumentation system needs to be installed with cameras and optical sensors for determination of flow heights.

Task description

- Perform a literature study
- Prepare the model for testing with instrumentation
- Study the soil to be used in the test – run a few pilot tests
- Plan a series of tests to study the effect of concentration (how wet the debris is)
- Plan some tests to study the effect of changing the total volume of debris used during testing
- Run the tests and record results
- Study and present the results: Identify trends, patterns of behavior and suggest conclusions.

Professor in charge: Steinar Nordal

Co-supervisor: Professor Vikas Thakur

Department of Civil and Environmental Engineering, NTNU

Date: 10.06.2017

Preface

This Master thesis is submitted as the partial fulfillment of the MSc in Geotechnics and Geohazards at Department of Civil and Environmental Engineering, Norwegian University of Science and Technology (NTNU). This study was conducted during spring semester of 2017. The thesis is based on the experimental data obtained by test conducted in physical model in hydraulics laboratory at NTNU. The suggested MSc study relates to two research programs that both aim to reduce the risk related to debris flows, the E39 project initiated by the Norwegian Public Roads Administration (NPRA) and the Klima 2050, Centre for Innovative Research, funded by the Norwegian Research Council.

Trondheim, 2017-10-06

Rosy Nhuchhen Pradhan

Acknowledgment

Summary and Conclusions

Debris flow is the natural hazard occurring in the mountainous topography. The geography of Norway mostly consists of sloppy terrain with higher steepness. The country receives heavy rainfall every year which is in fact the main triggering factor for the debris flow. Therefore, debris flow has been one of the danger to human life and properties in Norway. To prevent the damage caused by debris flow, proper design of countermeasures is necessary and for this better understanding of debris flow is important. This Master thesis includes the study of debris flow mechanism, basic physics, and its characteristics. Several criteria have been proposed in many literatures for its classification but the most common types are: muddy type which is turbulent and granular or stony type which is less turbulent or laminar. Most of the experimental study existing till now are conducted with muddy flow than with the granular flow. However, the granular flow study is equally important as it can cause severe damage as it carries big bolder with it in suspension. Unlike debris avalanche where only the sliding surface is liquified, debris flow has whole mass liquified in presence of ample water. The rise in pore pressure due to water reduces its effective stress, causes instability of soil mass, and tends it to flow as one phase fluid. The debris flow stops due to either of the two mechanisms: due to reduce in pore pressure and gain in effective stress or due to dissipation of kinetic energy into heat energy. The decrease in sediment concentration of debris flow results in the change in its state to hyper-concentrated flow.

The main objective of this thesis is to study the effect of change in the sediment concentration and change in the volume of debris flow on its parameters: velocity, flow height, deposition height, grain size distribution in deposition area and runout length. A debris flow simulation has been done using physical model of 1:20 scale. To study the change in runout length of the debris slide with varying grain size of material, six tests with debris slide has been conducted using material with two different grain size distribution, one with coarser and other with finer particles. Forty other tests have been conducted for simulating debris flow with varying volume and sediment concentration among which two tests were done with force measurement to evaluate the existing analytical methods for force measurement. The sample for sieve analysis has been taken at the beginning and end of deposition area for each test with debris flow. As some material was left inside the box after every test, the concentration of flow and the mass of solid and water contributing in the flow was not same as the initially intended values. To obtain the actual values of these parameters, the weight of material left inside the box was measured in each test and sample was taken for water content measurement for every test.

The velocity of the debris flow for the test conducted lies within the range of down- scaled velocity of real debris flow event. However, the flow height did not meet the range provided for down- scaled flow height of the real debris flow event. This may be because of the lower volume of mixture used in the test or wider flow channel. Despite of this, the behavior of the debris flow and its character resembled with the actual debris flow event.

The test results revealed that the effect on velocity and runout length due to change in sediment volumetric concentration is more significant for flow with small volume debris flow mixture while the effect due to change in volume of flow mixture, is more for high concentrated flow. The slope of trend line of energy head is steep for debris flow with lower volumes of mixture, thus energy dissipation is rapid for flow with smaller volume. Due to cohesive nature of the fine particles, the material with fine particles have more yield strength than one with less fine particles which is demonstrated by the result of smaller or almost no runout length increment for debris slide with increasing mass of humid material. The surge height in the transport zone increases as the sediment concentration increases which is vice versa for surge height in the deposition area. The effect of concentration change in surge height at upstream (transport zone) and downstream (deposition area) is more for debris flow with high volume and surge height downstream increases as total volume increases. Inverse grading is observed for debris flow, while no distinct grading is observed for hyper-concentrated flow. The degree of coarseness of material increases from the beginning to end of deposition area. The degree of coarseness of the deposits at the beginning increases with decreasing volume and increasing concentration and it is just the opposite at end of deposition area. Force measured in test is close to existing mixed model of hydrostatic and hydrodynamic model.

In conclusion, the test results satisfied the existing concept and character of the debris flow. The trend of change of runout length, flow heights, deposition height, grain size distribution with change in sediment concentration or change in volume of mixture supported the existing theory. The force measurement satisfied the existing analytical methods. Thus, the test results can be used to calibrate the numerical simulating tool for simulation of real debris flow phenomena.

TABLE OF CONTENTS

List of Figures

List of Tables

Abbreviations

3D- Three dimensional

Cu- Coefficient of Uniformity

Cv- Volumetric concentration of sediment

D_{50}- 50% pass diameter in sieve analysis

dps- Data per second

F_{gm}- Gravitational force of the model

F_{gp}- Gravitational force of the prototype

F_m- Force acting on the model

F_p- Force action on the prototype

fps- Frames per second

GSD- Grain size distribution

h_m- Flow height of model

h_p- Flow height of prototype

i.e.- That is

kg- Kilogram

L_m- Characteristics length of the model

L_p- Characteristics length of the prototype

Lr- Ratio of the linear dimension of the model and the prototype

m- Meter

M_b – Weight of the bowl

M_{ds}- Weight of dry sample

M_{lb}- Weight of material left in the box

mm- millimeter

M_p - Weight of the plastic bag

Ms- Mass of the solid/ debris flow material

M_{sb} – Weight of the dry sample with bowl

M_{sbox}- Weight of the dry solid left in the box

M_{sp} - Weight of the sample with plastic bag

M_{sw} - Wet sample

M_{wbox}- Weight of the water left in the box

Mw-Mass of the water

M_{ws}- Weight of the water content in sample

NPRA- Norwegian Public Road Administration

s- Seconds

t- Time

v_m- Velocity of model

v_p- Velocity of prototype

Vs- Volume of the dry solids/ debris flow material

Vw- Volume of the liquid phase/ water

w- Water content

ρs- Density of solid/ debris flow material

ρw- Density of water

1 INTRODUCTION

Debris flow is one of the common geohazard, that occurs in mountainous terrain and takes life and properties of human being every year. Because of its destructive nature, the more advance study on this topic is necessary to counteract it. Thinking of this fact, a study on it has been conducted for this Master's thesis. This chapter includes the background of the debris flow, the objectives of the thesis and the structure of the thesis.

1.1 Background

Debris flow is defined as a flow of mixture of sediment and water in a way such that it acts as a flow of continuous fluid driven by gravity and it achieves large movement from the enlarged void space saturated with water or slurry (Takahashi, 2007b). According to Stiny (1910), debris flow is a flood in mountain torrent, that carries suspended load and transports bulk amount of bedload and the increase in amount of sediment carried by flow leads it to change into viscous mass comprising of water, soil, sand, gravel, rocks and wood mixture flowing like a lava into a valley. Debris flow involves the water charged, predominantly coarse-grained inorganic and organic material that flow rapidly down a steep, confined, preexisting channel (VanDine, 1985). Debris flow consist of less than 30% of silt and finer particles (Oldrich Hungr, Evans, Bovis, & Hutchinson, 2001).

The debris flow is initiated by either of these causes: landslide that turns into debris flow, collapse of naturally built dam that checks a gully or the heavy landslide that leads to disturb the stability of accumulated debris and thus turn into a flow (Takahashi, 1981). The latest cause is the most common (Takahashi, 1981). Earthquake can also initiate the flow which is more destructive (Varnes, 1978). However without water, debris flow cannot occur (Calligaris & Zini, 2012). The characteristics of the debris flow is its extreme capacity of sediment transport, destructive occurrences, high – sediment concentration, varied range of grain size, high velocity and short movement period (Cui, Zeng, & Lei, 2015). The flow is unsteady and non-uniform, often last for less than 15 minutes and the flow speed can exceed 10 m/s (Iverson, 1997). The velocity that has been observed ranges from 0.5 m/s to 20 m/s(Costa, 1984). The total sediment concentrations typically is more than 50% by volume which is slightly different than those of static, unconsolidated sediment masses(Iverson, 1997).

The research in climate suggest that Norway should expect more rainfall in the coming years (Frekhaug, 2015). The study by Jaedicke, Lied, and Kronholm (2009) defines that Norway has 30% of total land area covered by mountains and 6.7% has a slope more than 30 degrees. As

debris flow occurs on the slope with steepness of more than 15º- 20º (Costa, 1984), Norway is very prone to debris flow hazards. Debris flow are hazardous because of the level of difficulty in predictability, intense impact forces and their ability to deposit huge amount of sediment mass in inundated areas (Prochaska, Santi, Higgins, & Cannon, 2008). Huge damage can be caused when they flow out onto the alluvial fan and reaches the human settlement zone (Takahashi, 1981).

In previous days, people cope with debris flow hazards by avoiding area exposed to this hazard. However, this method is no longer satisfying as fast rate of development causes settlement in hazardous areas without time to build experience and understanding to the debris flow hazard. So, the importance of prediction and prevention of debris flow hazards and related phenomena conducted by geologist, geotechnical engineers, and hydrologist with deep knowledge in debris flow studies is increasing. Even though prevention can be done by placing the infrastructures away from hazard zones and adopting preventive measures, in most of the cases, there is a certain tolerance of placing the facilities in hazard zone based on the concept of acceptable risk. This is one of the big challenge to debris flow specialist. So, the expert is not responsible to talk about acceptable risk instead is responsible to predict the probability of occurrence, magnitudes, runout distances, velocities, impact forces and associated potential damage and other parameter that is needed to quantify risk (Jakob & Hungr, 2005)

Even though these phenomena causes considerable damage, debris flow is still poorly understood despite having existing basis knowledge regarding their recognition and propagation (Coussot & Meunier, 1996). The knowledge and understanding of the areas prone to inundation, deposition thickness and the velocity of flow helps to define the hazardous area and to propose the structural and non- structural intervention measures (Boniello, Calligaris, Lapasin, & Zini, 2010). The factors that should be understood before controlling the debris flow generation process are: from where, in what way, how much water and sediments are given (Takahashi, 2007e).

The experimental study on the effects of change in the volumetric sediment concentration and total volume of debris flow in the flow parameters namely: velocity, flow height, runout length and grading of depositional area, have been conducted for this thesis. Few tests have been conducted with force measurement to calibrate the existing analytical impact force measuring methods. The aim of the thesis is to generate a data of debris flow parameters which can help

to calibrate the existing or newly developed debris flow simulating tool. This can be supportive to design effective protective structure against debris flow.

The term debris flow material used in this thesis refers only to sediment (granular) material; the debris flow mixture refers to the mixture of granular material and the water; debris slide refers to the sliding phenomena of the humid solid material without any present of additional water; debris flow refers to the flow of mixture of granular material and water; total volume refers to the total volume of debris flow mixture; the concentration or sediment concentration refers to the volumetric sediment concentration of the debris flow.

1.2 Objectives

The main objective of this study is:

- To get an idea that how the change in concentration of the sediment or the total volume debris flow will affect the flow parameters of debris flow such as runout, velocity, and flow height.

The results of the thesis: runout length of debris flow, velocity of debris flow front, flow heights, grain size distribution in deposition area can help to calibrate any numerical model for debris flow.

The sub-objectives of this study are:

1. Study of debris flow and its mechanism

2. Understanding the modeling approaches to study the debris flow

3. Understanding the energy transformation of the debris flow and impact forces created by debris flow

4. Understanding the effect of grain size variation in the runout distance of debris slide

5. Study of the variation in the flow height, deposition pattern and height, grain size distribution in depositional area, velocity, energy line and runout of debris flow caused by change in volumetric concentration of the sediment or total volume of debris flow.

1.3   Structure of the Thesis

The other chapters of the thesis are structured as follow:

Chapter 2 includes the literature review regarding debris flow and its mechanism, physics and theory related to the debris flow, modeling of debris flow, energy transformation of debris flow, and impact force of debris flow.

Chapter 3 presents the physical model used for conducting experiment, the test equipment used, the test setup, test plans and material used for debris flow experiment.

Chapter 4 describes the results and analysis obtained from experimental data.

Chapter 5 includes the discussion of the results in relation to the objectives.

Chapter 6 contains the conclusion and recommendation for future work.

2 LITERATURE REVIEW

To fulfill the main objective mentioned in Section 1.2 , the sufficient knowledge and understanding of debris flow phenomena is necessary. For this purpose, the literature study has been conducted throughout the duration of the thesis. This chapters includes the literature review on the debris flow and debris flow mechanism, the basic theory behind the debris flow phenomena, modeling laws to simulate debris flow, energy transformation and impact force of debris flow.

2.1 Debris flow

The term debris can be defined as loose unsorted material with low plasticity such as generated by mass wasting processes, weathering processes of residual soil, glacier transport, volcanic explosion(e.g. granular pyroclastic deposits) (Oldrich Hungr et al., 2001). Debris flow material usually consist of coarse fragment, unlike the mud flow that consist of 50% sand, slit or clay sized particles, and occurs due to heavy rainfall or from melting of snow or frozen soil (Varnes, 1978). Among various type of mass movement that involves water and sediments, occurring on steep slopes in hilly range, debris flow is specific movement that includes large volume of highly concentrated viscous water debris mixture flowing through a stream channel (Coussot & Meunier, 1996) and moves like wet concrete mixture (Calligaris & Zini, 2012) . The concentration of the sediment by volume in debris flow ranges from 50-70% (Iverson, 1997). The condition initially required for most of debris flow are: mass of unconsolidated fine-grained rock and soil debris that act as source for debris flow, steep slope and significant amount of moisture (Costa, 1984). Thus, debris flow have high concentration, shows non-Newtonian dispersion with high apparent viscosity, bulk density and have yield strength and thus flow in laminar pattern (Fisher, 1971). The typical characteristics of the debris flow defined by Johnson and Rodine (1984) is as:

> *"A wall of boulders, rocks of all sizes, and oozing mud suddenly appear around the bend in a canyon preceded by a thunderous roar. As the boulder-choked wall passes, the channel remains filled with a debris-laden torrent of mud and boulders clanking and grinding together. The debris flows across an alluvial fan, engulfing structures and cars in its path, covering roads, fields and pastures with a blanket of muck, and slowly coming to a stop as the debris spreads in a lobate form with steep terminal snout and margins."*

Table 2-1 Classification of landslide of flow type (Oldrich Hungr et al., 2001) adopted from (Sherchan, 2016)

Material	Water content[1]	Special condition	Velocity	Name
Silt, Sand, Gravel, Debris (talus)	dry, moist or saturated	- no excess pore-pressure, - limited volume	various	*Non-liquefied sand (silt, gravel, debris) flow*
Silt, Sand, Debris, Weak rock[2]	saturated at rupture surface	- liquefiable material[3], - constant water content	Ex. rapid	*Sand (silt, debris, rock) flow slide*
Sensitive clay	at or above liquid limit	- liquefaction *in situ*,[3] - constant water content[4]	Ex. rapid	*Clay flow slide*
Peat	saturated	- excess pore-pressure	Slow to very rapid	*Peat flow*
Clay or Earth	near plastic limit	- slow movements, - plug flow (sliding)	< Rapid	*Earth flow*
Debris	saturated	- established channel[5], - increased water content[4]	Ex. rapid	*Debris flow*
Mud	at or above liquid limit	-fine-grained debris flow	> Very rapid	*Mud flow*
Debris	free water present	- flood[6]	Ex. rapid	*Debris flood*
Debris	partly or fully saturated	- no established channel[5], - relatively shallow, steep source	Ex. rapid	*Debris avalanche*
Fragmented Rock	various, mainly dry	- intact rock at source, - large volume[7]	Ex. rapid	*Rock avalanche*

1 Water content of material in the vicinity of the rupture surface at the time of failure
2 Highly porous, weak rock (examples: weak, chalk, weathered tuff, pumice).
3 The presence of full or partial in situ liquefaction of the source material of the flow slide may be observed or implied.
4 Relative to in situ source material.
5 Presence or absence of a defined channel over a large part of the path, and an established deposition landform(fan). Debris flow is recurrent phenomenon within its path while debris avalanche is not.
6 Peak discharge of the same order as that of a major flood or an accidental flood. Significant tractive forces of free-flowing water. Presence of floating debris.
7 Volume greater than 10,000 m^3 approximately. Mass flow, contrasting with fragmental rock fall.

Table 2-2 Velocity scale for Landslide classification (Cruden & Varnes, 1996)

Velocity class	Description	Velocity (m/sec)	Typical velocity
7	Extremely Rapid	5	5 m/sec
6	Very Rapid	0.05	3 m/min
5	Rapid	5×10^{-4}	1.8 m/hr
4	Moderate	5×10^{-6}	13 m/month
3	Slow	5×10^{-8}	1.6 m/year
2	Very Slow	5×10^{-10}	16 mm/year
1	Extremely Slow		

Oldrich Hungr et al. (2001) differentiated debris slide from debris flow and defines dry or non-liquefied debris slide as the flow of loose dry or moist, sorted or unsorted granular material without any significant excess pore pressure due to which the granular materials tend to fail by shallow planar sliding. The sliding mass will decelerate and stop as the kinetic friction force, which is the product of load acting perpendicular to the slip surface and the kinetic friction coefficient, is greater than the gravitational driving forces (Takahashi, 2007e). The classification of the landslides according to Oldrich Hungr et al. (2001) is shown in Table 2-1. Table 2-2 gives the velocity scale mentioned in Table 2-1.

Figure 2-1 illustrates that the water content goes on increasing while the volumetric sediment concentration goes on decreasing as the landslide changes its form to debris avalanche and then to debris flow. Especially in the steep slope, the cohesion decreases and the mass moves more rapid as the water content rises (Varnes, 1978). Figure 2-1 shows that when the water content increases the debris flow changes its form to hyper-concentrated flow. The hyper concentrated flow mostly consist of the fine particles (Takahashi, 2007e) and has volumetric concentration of sediment in between 20% to 60% (T. C. Pierson, 2005).
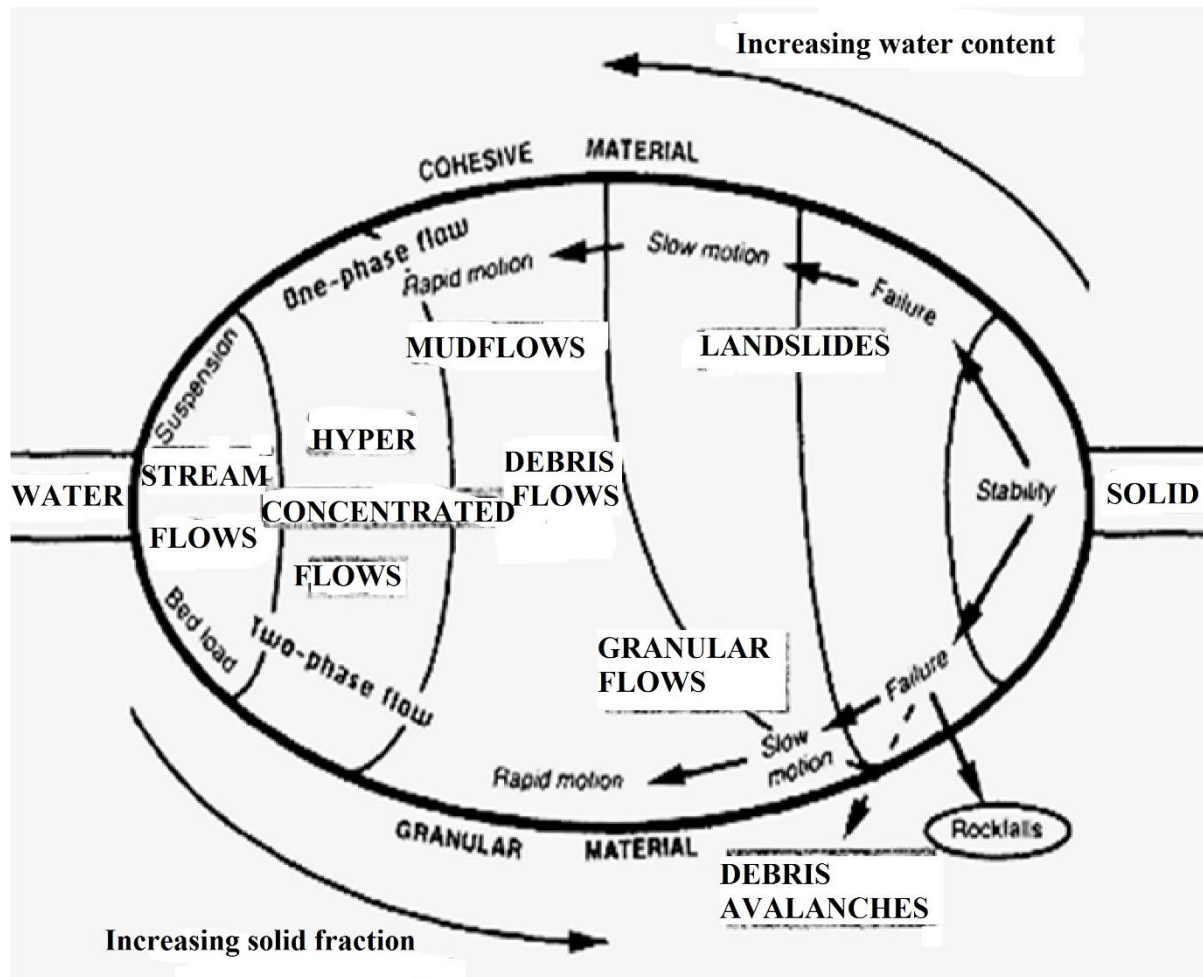
Figure 2-1 Mass movements classification on hilly slopes as based on solid fraction and material type (Coussot & Meunier, 1996)

Since the mechanical character such as velocity and flow depth relies on the boundary and initial conditions and they vary between different event, it is not sure that if they can be relevant basis for classification (Coussot & Meunier, 1996). Hence, Takahashi (2007e) has given the clear difference between debris avalanche and debris flow based on their initiation process ,and explains that both the debris avalanche and debris flow is derived from the liquefaction process of landslide. However, debris avalanche is caused due to the liquefaction of only lower part of the slipping body whereas debris flow is result of whole mass being liquified (Takahashi, 2007e) and debris avalanches can be defined as mass movement of granular material originating from rocky or burst of granular mass (Coussot & Meunier, 1996).

According to Coussot and Meunier (1996), the debris flow is the strongly transient viscous flow, usually consist of periodic surge of thick debris acting as slurry and interval between them is comparatively small whereas the normal or hyper concentrated stream flow is a flow where local flow intensity such as discharge and flow depth fluctuates gradually with time and

space. Based on the feature of debris flow, specifically velocity, flow nature and deposition character, debris flow can be said as a phenomena lies in between hyper concentrated flows and landslides (Calligaris & Zini, 2012). The relative velocity of the two-main element of debris flow: water and solid is small, but in the hyper concentrated stream flow, there is significant difference between the average velocity of the coarsest solid particle and water-solid suspension that flows around coarse particle (Coussot & Meunier, 1996). Thus, debris flow is the single-phase flow where fluid and solids mixture flows together as continuous fluid and the properties are denoted by fluid particle interaction effects whereas hyper concentrated flow is two phase flow where the fluid and solid flow as an independent component (Takahashi, 2007d).

The classifications of the debris flow have been done on various basis in different literatures. Coussot and Meunier (1996) has suggested two types of debris flow based on the solid fraction and material type: muddy debris flow where fine particle fraction containing clay is above 10% and granular debris flows where fine particle fraction is less and there is no direct contact to contribute to mass movement.

Based on the interaction of solid particle with the fluid during debris flow, Takahashi (2007e) has categorized debris flow into inertial debris flow and viscous debris flow. The inertial debris flow contains water and coarse particles where buffer effect of interstitial fluid leads to moderate the particle collisions and mass effect leads acceleration of the surrounding fluid (Takahashi, 2007e). Viscous debris flow contains fine particles like silt and clay, move like slurry and viscosity in the interstitial fluid is significant and thus flow is more laminar (Takahashi, 2007e). The buoyancy is common mechanism between inertial and viscous debris flow (Takahashi, 2007e).

Takahashi (2007e) classified debris flow, based on the stress dominancy, as Coulomb friction dominated quasi-static debris flow and dynamic debris flow. Dynamic debris flow is further classified as stony type; turbulent- muddy type debris flow; and viscous debris flow which are described below as by Takahashi (2007e) and these are described below based on Takahashi (2007e).

- **Stony type debris flow**- Grain collision stress is dominant in these types of flow. The flow consists of the boulder larger than 1 m in diameter. It is characterized by the accumulation of the big stones at the front part with little water and the back parts is more like liquid. The depth of the flow becomes large abruptly with almost no

preceding flow. The velocity is distributed laterally and the central part of the flow behaves like Bingham fluid flow. The flow contains less percentage of fines ranging from 1-10% of clay and silt and more percentage of gravel (10-60%) and sand (30-40%). The particle concentration and flow depth is maximum at the flow front. The density ranges from 1 gm/cm^3 to 1.5 gm/cm^3.

- **Turbulent-muddy-type debris flow-** Turbulent mixing stress is dominant in these kinds of flow. The flow is generated as the rainfall erodes the thick mountain cover of the ash from the active volcano. These kinds of debris flow have mainly fine ash, and some huge boulders and has different character than the stony type and are very turbulent from front to the back end of flow. The solid concentration ranges from 35-42% and the average diameter of solid is in between 0.3 mm to 1 mm.

- **Viscous debris flow-** Here, viscous stress of the slurry is dominating. The viscous debris flow doesn't have accumulation of big boulders at the front unlike stony type debris flow. The materials in debris flows resumes the characters of the source area. There is no particle segregation effect seen in the process of motion as the deposition has almost same particle size distribution as the debris flows. It is kind of mixture of slurry and coarse particle bigger than 0.1 mm. It consists 20-30% fine particles by weight with size less than 0.1 mm. The density of slurry ranges from 1.3-1.5 g/cm^3. It can be defined as the flow with dispersed coarse particles with concentration of coarse particles more than 50% by volume.

Among these types of the debris flow mixture, the debris flow of the test conducted for study in this thesis shows the behavior of stony type and viscous type.

2.2   Debris flow mechanism

The mechanism of the debris flow in overall includes the mechanism of initiation process of debris flow till it gets deposited as a debris fan.

Takahashi (2007c) classified the mechanical causes of the debris flow initiation in three types:

i.   Debris flow generated by the erosion of the deposit on the gully bed due to supply of water from outside which then turns as dense concentrated mixture

ii.   Debris flow initiated from landslide mass because of water stored in the sliding mass or by the water supplied from external source

iii.   Debris flow generated due to sudden burst of the debris dam.

There are two principle triggering mechanism for debris flow as explained in "Håndbok v139: Flom- og sørpeskred" 2014). The first, which is most common in slope of Norway, is the erosion of the surface terrain when the force exerted by the flowing water exceeds the erosion resistance of the particles on the surface in ("Håndbok v139: Flom- og sørpeskred," 2014). As the erosion rate and transport capacity of water becomes sufficiently large, the content of mass in the water will increase and develop into debris flow. Another mechanism is due to mixing of the sliding mass with the water released from outer source ("Håndbok v139: Flom- og sørpeskred," 2014). Figure 2-2 illustrates these two mechanisms in pictorial way.

The NPRA has not accounted the debris flow occurred due to dam burst into separate classification and has taken it under the classification group as debris flow generated due to erosion of bed caused by flowing water.
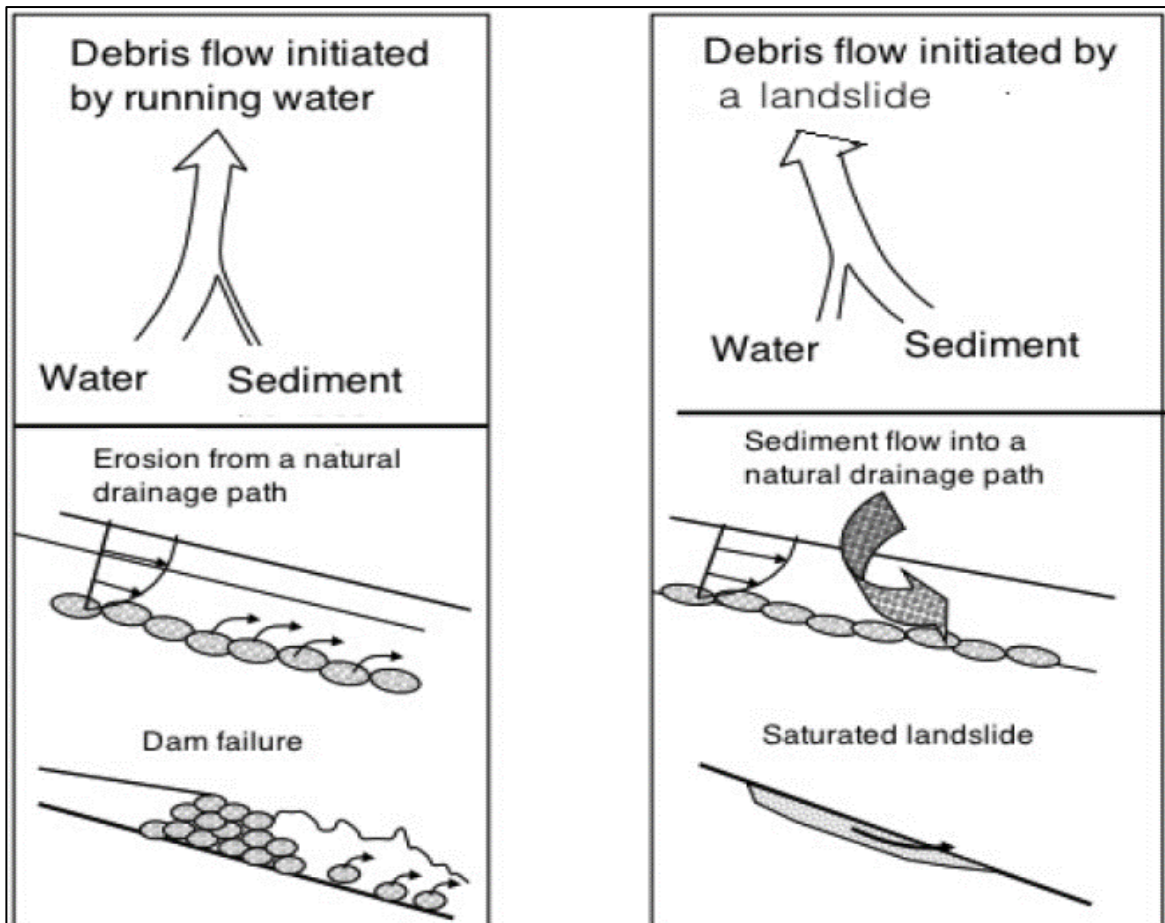
Figure 2-2 Triggering mechanism of debris flow as described in ("Håndbok v139: Flom- og sørpeskred," 2014) translated by Laache (2016)

The first and second figure describes the debris flow initiated by the running water and from the landslide respectively.

The initiation of the debris flow due to liquefaction of the existing slide is illustrated in Figure 2-3. As observed in Figure 2-3, the debris flow is generated just as the torrent deposits liquefies. Then, the torrent deposit resting on the weak and unstable structure collapses under rapid loading and the disturbed mass becomes debris flow as it comes in contact with the water. The liquefaction occurs usually in meta stable granular soil (Kyoji Sassa & hui Wang, 2005).
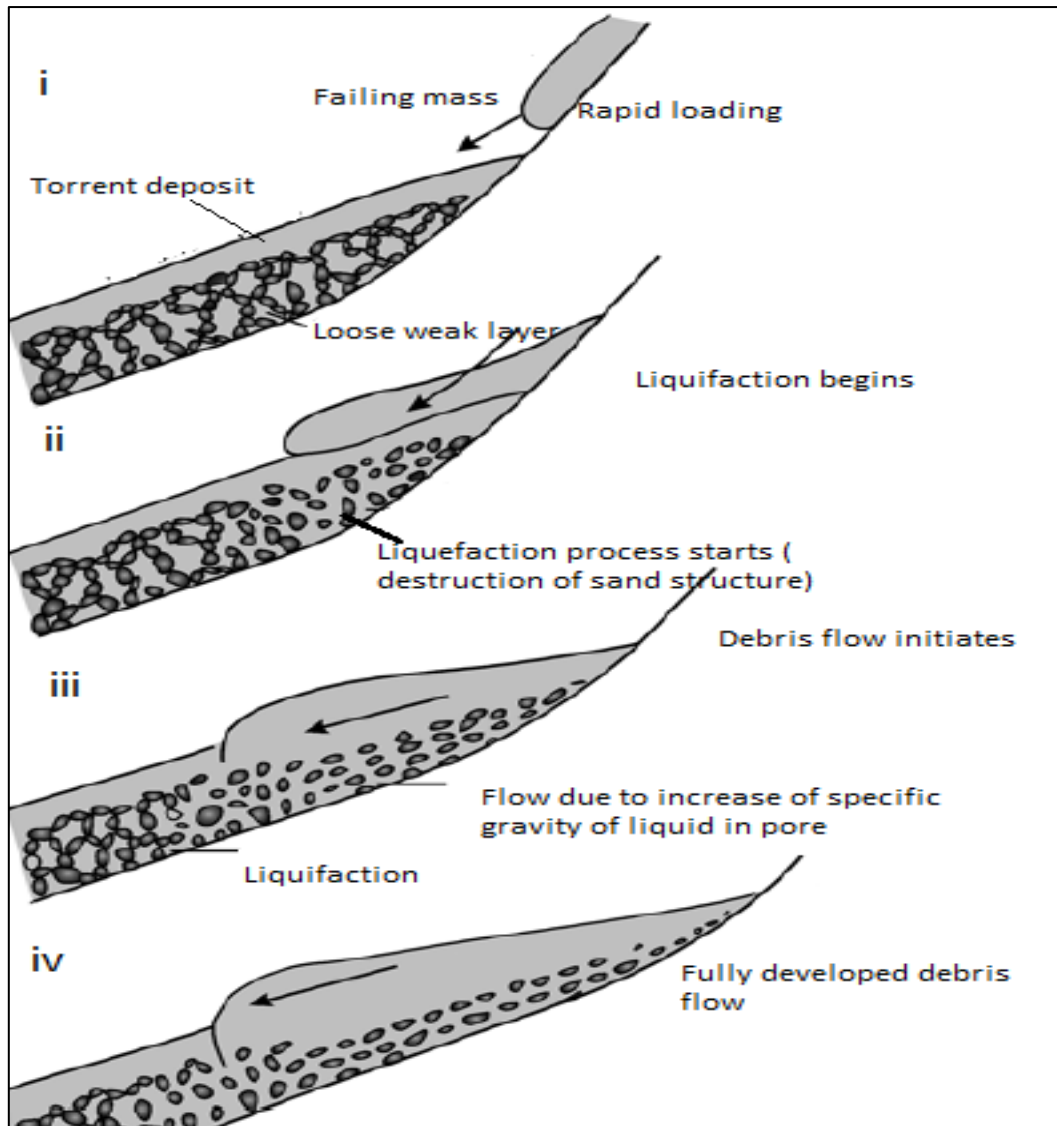
Figure 2-3 Illustration of the initiation of debris flows due to liquefaction of the slides (K Sassa, Kaibori, & Kitera, 1985)

Takahashi (2007c) has described the mechanism of formation of the debris flow by surface water runoff in different stress distribution cases based on Coulomb criteria. Figure 2-4 illustrates the six stress distribution cases in sediment layer that has been considered for explaining the mechanism. D is the thickness and θ is the slope angle, h_o is depth of water flowing. If "τ" is the stress that act to drag the block downwards and "τ_r" is the resisting stress, at any depth "a" measured from the surface of the sediment layer.

$$\tau = g \sin \theta \; (C(\sigma - \rho)a + \rho(a + h_o)) \qquad (2.1)$$

$$\tau_r = g \cos \theta \; (C(\sigma - \rho)a) \tan \emptyset + c \qquad (2.2)$$

In Equation (2.1) and (2.2) , C is the maximum concentration as linear concentration tends to infinity. The linear concentration is the ratio of diameter of grain to the average free dispersion distance (R. A. Bagnold, 1954), ρ is the pore pressure, g is the acceleration due to gravity, $\emptyset$ is the internal friction angle. The value of $\emptyset$ is in between $20°$ to $45°$ (Hutter, Svendsen, & Rickenmann, 1994).
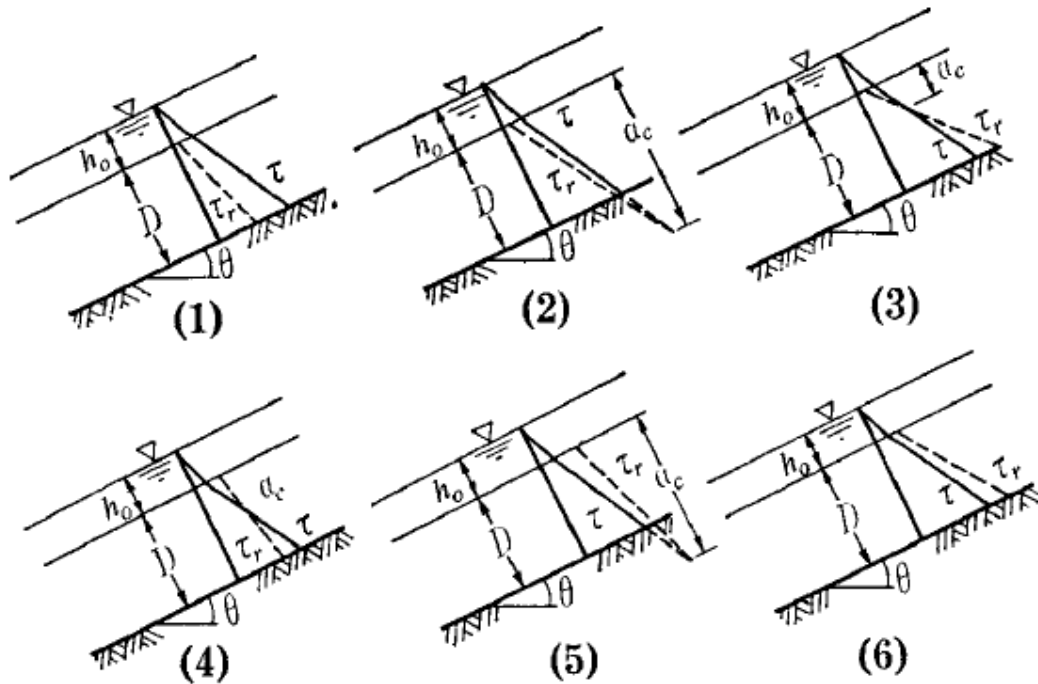
Figure 2-4 Stress distribution in sediment layer in varying conditions (Takahashi, 2007c)

In Figure 2-4 , for the case 1, 2 and 4 the whole mass is unstable as τ exceeded τ_r. However, in case 5 and 6, τ_r is greater than τ. In case 3, the sediment layer is stable but the top portion of thickness a_c is not stable.

Depending on the topography and geological nature of their location, there are two forms of debris occurrence: Hillslope (open-slope debris flows) and Channelized debris flows (Nettleton, Martin, Hencher, & Moore, 2005). Hillslope debris flow makes their way by itself as it moves down the valley before depositing the material on the lower area with small gradient (Cruden & Varnes, 1996). The deposition area consist of channels and levees (Nettleton et al., 2005). Channelized debris flow moves along the confined or channelized path which is a first order or the second order drainage channel or an existing gully that controls the flow direction (Oldrich Hungr et al., 2001) or the valleys, depression hollows (Nettleton et al., 2005). This is proven by the scouring seen along gully path and the cone shaped depositional area (Oldrich Hungr et al., 2001). The flows usually has high density around 80% solids by weight (Cruden & Varnes, 1996) and can carry big boulders even of some meters in diameter (Nettleton et al.,

2005). The apex of the debris depositional fan has widen channel and the debris flow front consist of finer liquefied debris traveling behind and stop as hit by thick boulders on the front (Oldrich Hungr et al., 2001).

Figure 2-5 illustrates the difference in flow path between Hillslope debris flow and Channelized debris flow.
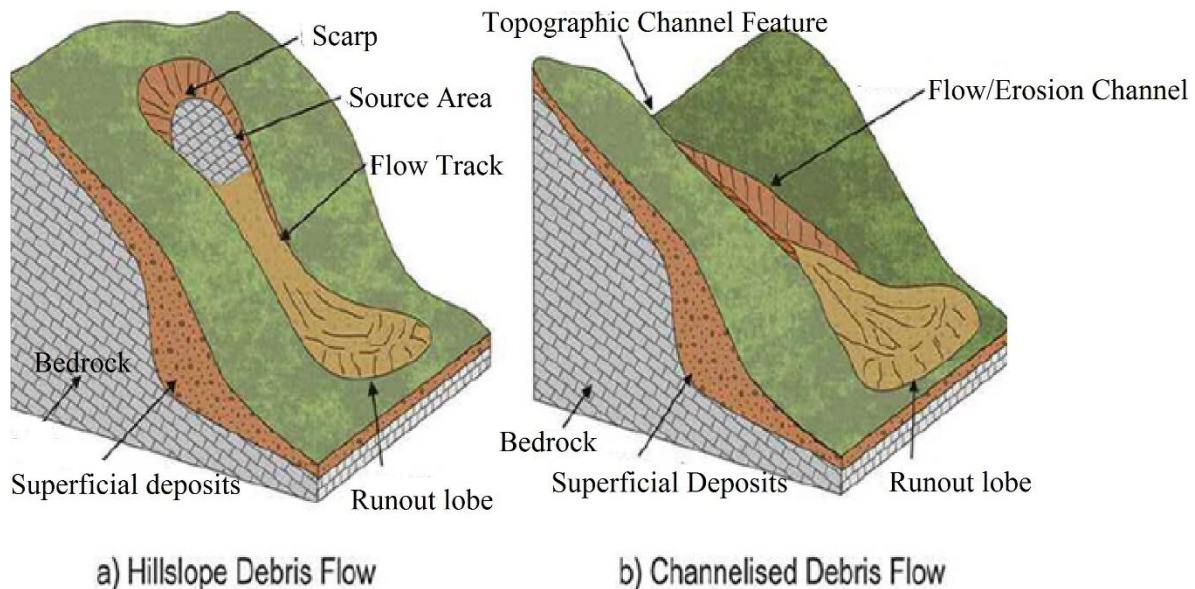
Figure 2-5 Illustration of Hillslope debris flow and Channelized debris flow (Nettleton et al., 2005)

There are five main phases of debris flow: initiation due to loosening of material from hillslope, transport of material to the channel system, storage of material within channel system, entrainment of the bed, deposition on the debris fan (Nettleton et al., 2005). The entire process from the initiation to the deposition of the debris flow is accompanied by potential energy converted into the kinetic energy and then it is consumed by the frictional resistance between the ground surface and the flowing mass (Takahashi, 2007e).

Calligaris and Zini (2012) explains three distinct zones of debris flow: source area, stream transport channel and the depositional area that have a fan morphology and Figure 2-6 illustrates these zones. The source of the debris flow has very steep slope greater than 15º, has enough supply of loose debris and contains enough moisture (Calligaris & Zini, 2012). Nettleton et al. (2005) mentions the slope of source area varying between 26º to 50º. The

parameter that determines the catchments or source geometry are perimeter of catchment, average length, elevation and average slope (Calligaris & Zini, 2012).

The transport zone is an intermediate zone, consisting of slope greater than 8º (Nettleton et al., 2005), where the debris flow is likely to increase its volume by entrainment before depositing in the deposition zone (Hussin, 2011). Debris flow in smaller basin has the capacity to transport huge amount of eroded bed because the smaller basins receives large amount of precipitation, mostly has hill sides with large slope and has high snow pack which can melt quickly in spring (Costa, 1984). The debris flow moves down as a mixture of wet concrete, with series of surges and these surges moves away even the big boulder (Costa, 1984). The surges are generated due to temporary damming of debris flow path (Costa, 1984). However, the experimental flow behavior showed that surges are generated due to mechanical instability and can exist even in absence of any obstruction within a flow path (Major, 1997). The surge head carries high concentration of large sediments (Iverson, 1997).

The deposition area consist of well-established debris fan or cone with thick deposits in proximal part while thinner deposits are seen in outlying part (Skilodimou & Bathrellos) . The slope of area where deposition of the debris flow starts varies in a wide range of $1°$ to $24°$ depending upon the topography, volume, and type of debris flow(Oldrich Hungr, McDougall, & Bovis, 2005). However, Hutter et al. (1994) mentions the slope angle of the deposition area as $3°$. But in overall the smaller debris flow can deposit in steeper angle while larger event rest on the mild slope (Oldrich Hungr et al., 2005). This zone includes the elements at risk (e.g. bridges, roads, houses, railways) being hit by debris flow deposits (Hussin, 2011).
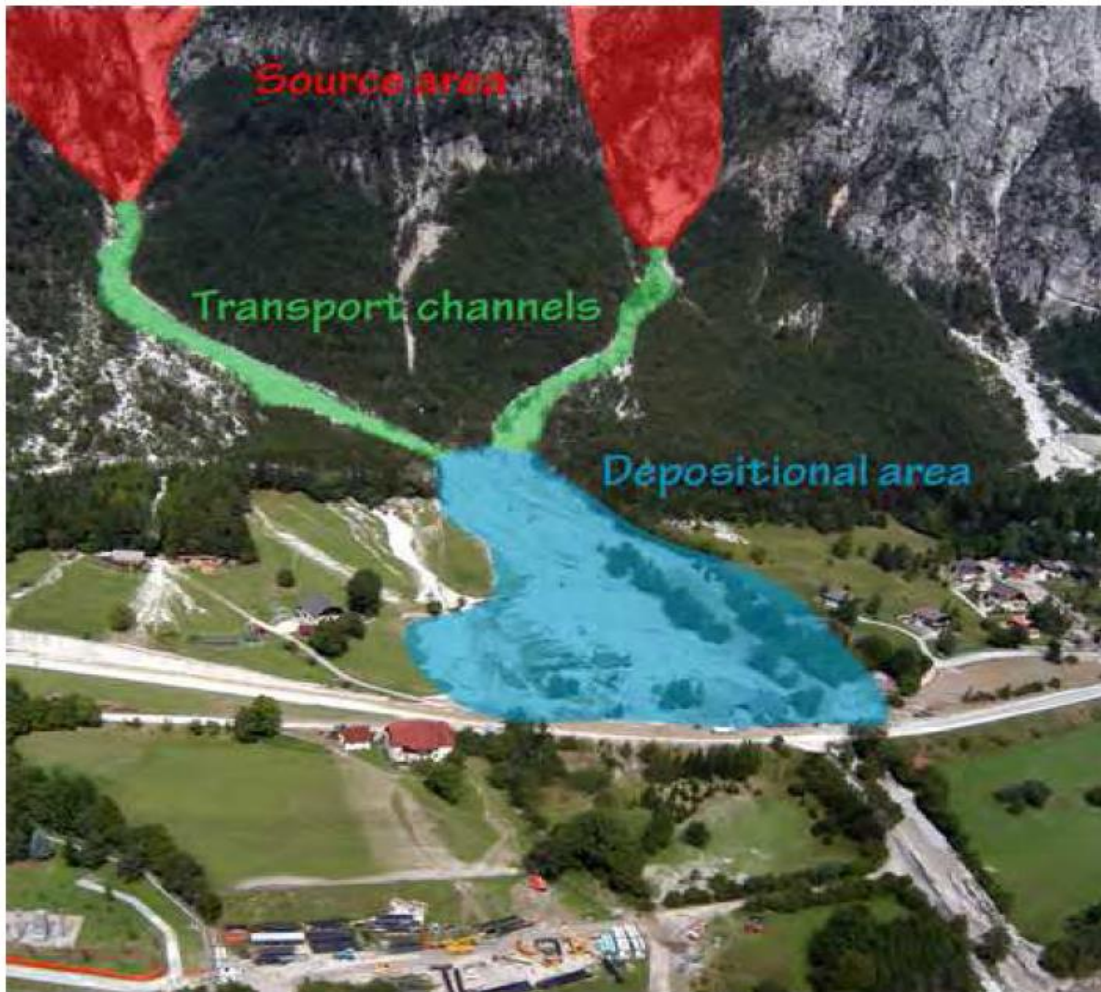
Figure 2-6 Identification of three main zones of debris flow phenomena (Calligaris & Zini, 2012)

1. Source area (red portion) 2. transport channel (green portion) 3. Depositional area (blue) (Calligaris & Zini, 2012)

Major (1997) describes the natural deposits as lobate shaped platforms having blunt margins, marginal banks and curved surface ridges and the water content of the source mass influences the depositional process and relatively thick deposits are seen for the unsaturated flow.Coussot and Meunier (1996) says that there is no particular grain sieving that appears within deposition area as debris flow material has high density and viscosity with strong shearing and mixing process during flow. However, the big boulders seem to be concentrated close to flow front (Coussot & Meunier, 1996). Fisher (1971) characterized the deposition of the debris flow as the inverse grading which has been accepted in the experiment by Major (1997) . The experimental work by Major, 1997 shows that there is an involvement of the horizontal source ward accumulation and progressive vertical grading during the process of deposition by a single

debris flow. According to Major (1997), for the less concentrated mixture a well sorted coarse material was seen depositing on the lee sides of surface edges whereas there was no significant difference seen for the high concentrated mixture in deposition at ridges and intervening channels. There was no distinct variation in particle size distribution seen longitudinally in deposition area but irregular variation was observed laterally, that denoted well-sorted coarse particle deposition due to front wave (Major, 1997).

Calligaris and Zini (2012) classifies the inverse grading of deposits into two types: one is distribution inverse grading and another is coarse tail grading. The former shows the increasing trend of the grain size from the base to the top of deposit with characteristic of poor matrix deposits and this flow pattern consists of high grain collision rate because of which the coarser grains are pushed upward by dispersive pressure and finer and pushed downward by kinetic sieving (Calligaris & Zini, 2012) . The coarser tail inversion grading has consistent boulder size increment on the base layer and the largest grains with non-uniform mixture of sediment are seen resting on the top layer (Calligaris & Zini, 2012). As explained by Nemec and Postma (1991), this setting of coarser boulder from the flow is due to the differential decrease of matrix strength caused due to shear strain (Calligaris & Zini, 2012).

The inverse grading is mostly developed during the high concentrated laminar flow , that have high density and strength and where the material rest in place just as internal shear stresses decreases below yield strength of the fluid (Fisher, 1971). This is because during high concentrated flow, the density of coarse particles and fine particles are very close and thus, the coarse particles are segregated on the top due to buoyant forces and dispersive pressures (Fisher, 1971). The dispersive pressure is generated due to grain collision and coarser material moves in suspension in the sediment mixture where shearing velocity gradient is smallest (R. Bagnold, 1968). According to Coussot and Meunier (1996), the critical value of concentration is defined beyond which sedimentation is insignificant and if the concentration of the flow is less than the critical value, coarser particle will fall and stay close to the bottom. The decrease in material strength due to reduction in the average solid fraction, will in turn reduce the ability to transport coarse solid particles in suspension (Coussot & Meunier, 1996).

The velocity of the debris flow varies from zero at the bottom to maximum at the surface layer and the average velocity lies in between bottom and top layer (Takahashi, 2007a). The consequence of which the floating coarser particles are transported forward in fast rate than the

average velocity of debris flow front and this leads to the accumulation of bolder in flow front (Takahashi, 2007a).

Figure 2-7 shows how the particles are distribute along the flow direction in debris flow. In Figure 2-7, it can be seen that the tail consists of the hyper-concentrated stream flow and the head consist of the boulders and the coarser particles are moving in suspension.
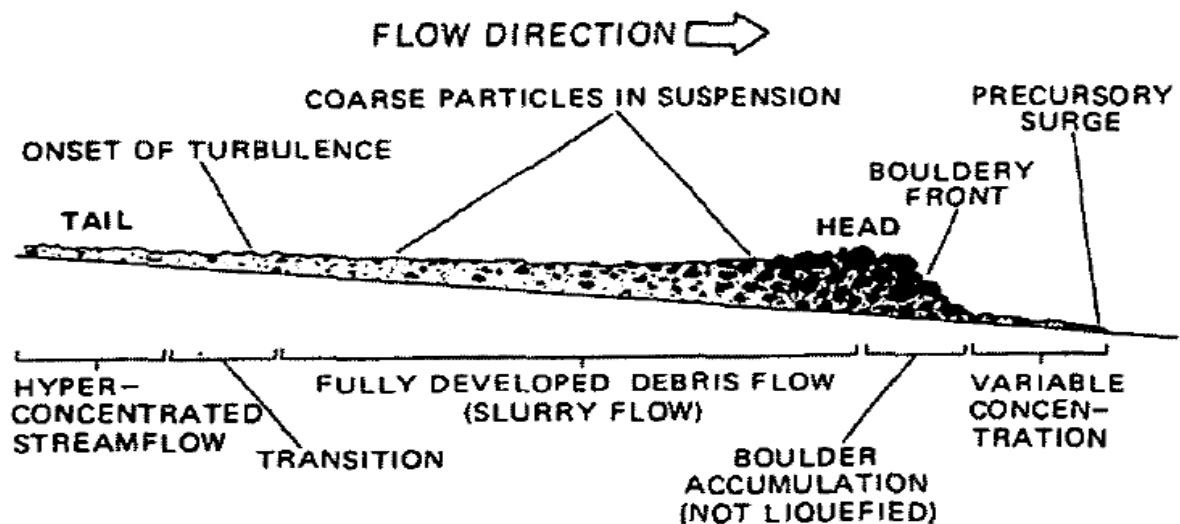
Figure 2-7 Particles and flow distribution of the debris flow along the flow direction (T. Pierson, 1986)

The phenomena such as: slides or collapses, bed erosion and transport, that goes together with debris flow will lead to increase in solid concentration due to the erosive nature of the flowing fluid and this process is known as entrainment (Coussot & Meunier, 1996). The debris flow moving on the erodible channel will erode the channel bed and increase the sediment concentration if it initially has too small mass of sediment, while it will deposit on the way and decrease its concentration if it contains too much mass of sediment (Takahashi, 2007e). So, the debris flow in erodible channel have equilibrium state of deposition and erosion (Takahashi, 2007e). However, it is seen that mostly the initiating volume of flow is small and the huge volume is transported to the deposition area due to the entrainment of the material along the channel and it is the efficiency of the entrainment process that regulates the volume of debris flow (Oldrich Hungr et al., 2005). Iverson et al. (2011) explains that the type of sediments bed that is entrapped on the way determines the change in momentum and speed. If the bed is wet then, the pore pressure increases which in turn increases the flow momentum and velocity by reducing the basal friction, while the entrainment from dry bed does the opposite and the momentum decline (Iverson et al., 2011) . This was demonstrated through the entrainment

experiment conducted by Iverson et al. (2011) with 95 m long and 2 m wide flume using 6 m^3 of debris flow containing 56% gravel, 37% sand and 7% mud sized grains and releasing suddenly from a head gate that flows over the bed of saturated sand gravel mixture. The experiment result showed that pore pressure was generated as wet bed erodes, and debris flow entrainment process can reduce the friction and increase the flow momentum. Friction reduction is not happening immediately beneath dilated flow fronts but occurs on the next front arriving after about 1s. However, the results of experiment done by Mangeney et al. (2010) presented that even for the dry granular flows moving over moderate slope of small thickness of erodible layer, the runout increased by 40% due to entrainment on the way. The entrainment process is influenced by sediment concentration of mixture, which then again influences the grain size distribution and the solid fraction of the flow mixture (Coussot & Meunier, 1996).

The main mechanism of entrainment process are: entrainment of the bed material due to the destabilization of the bed resulting from the basal drag forces, and entrainment of the weak unstable stream banks due to rapid undrained loading, impact loading and liquefaction of saturated flow (Oldrich Hungr et al., 2005).

Oldrich Hungr et al. (2005) denoted the estimation of the volume of debris flow as:

$$V = V_{intial} + \sum V_{point} + \sum_{i=1}^{n} Y_i L_i \qquad (2.3)$$

In Equation (2.3), $V_{initial}$ is the volume of initiating landslide, V_{point} is the volume of any point sources, L_i and Y_i are yield rate and length of n channel reaches. The entrainment process initiates if the channel slope is steeper than 11° (Takahashi, 2007a).

The particular mechanism of stopping of debris flow is not certain, however, one of the reason could be the reduction in pore pressure of fluid like mixture of water, fine slit or clay, which helps debris flow to gain its internal friction and this leads it to stop (Costa, 1984). Another mechanism given by Calligaris and Zini (2012) is the reduction in the internal kinetic energy below the level required to maintain the fluid to flow, mostly due to flattening or the reduction in slope of the channel through which debris flow is moving.

2.3   Physics of Debris flows

There are several theories explaining the occurrence of the debris flow depending on its type. According to Coussot and Meunier (1996), the fluid mechanics approach is more applicable to debris flow while the quasi-static cannot be applicable at all.

As mentioned by T. C. Pierson and Scott (1985) , for a Newtonian fluid, there is a linear relation between applied shear stress (τ) and shear strain rate (du/dy) which can be shown as in Equation (2.4)

$$\tau = \mu \, du/dy \tag{2.4}$$

In Equation (2.4) , μ is coefficient of viscosity of the fluid, u is velocity, y is depth.

T. C. Pierson and Scott (1985) explains the Newtonian or non- Newtonian rheological behavior of sediment- water mixtures are dependent on the concentration of sediment, type and grain size distribution. The non-Newtonian flow of open channels can be characterized as: the flow contains high concentration of the boulders in the flow front, the flow contains number of surges, the coarsest particles can be segregated in the surface and in the flow center (T. C. Pierson & Scott, 1985).

T. C. Pierson and Scott (1985) further explains that the mixture of the sediment water containing very less amount of silt and clay tends to maintain Newtonian behavior till concentrations as high as 50% by volumes which contains coarse particles of comparatively uniform size. When more amount of silt and /or clay is added into the mixture, the mixture gains the yield strength and the yield stress is dependent on the particle size distribution of mixture as it is generated due to the cohesive forces of fine grained suspensions (T. C. Pierson & Scott, 1985) . Non- Newtonian Bingham plastics model, given by Equation (2.5) , can be used to the material with finite shear strength (T. C. Pierson & Scott, 1985).

$$\tau = \tau_y + \mu_p \, du/dy \tag{2.5}$$

The other models for debris flow modeling are Herschel- Bulkley fluid and Dilatant fluid and their equation are given in Equation (2.6) and (2.7) (Takahashi, 2007d) .

Herschel- Bulkley fluid: $\tau = \tau_y + K_1(du/dy)^n, n \le 1$ (2.6)

Dilatant fluid $\tau = K_2(du/dy)^n, n > 1$ (2.7)

In Equation (2.5), (2.6) and (2.7), τ_y is the yield strength, μ_p is the plastic viscosity, du/dy is the rate of shear strain.

The velocity of the Bingham flow given by Oldrich Hungr (1995) can be denoted as in Equation (2.8)

$$v = \frac{H}{6\mu}\left(\frac{2T}{A} - 3\tau_r + \frac{\tau_r{}^3 A^2}{T^2}\right) \tag{2.8}$$

In Equation (2.8), v is the velocity of the flow, μ is the viscosity, T is the basal flow resistance, H is the flow height, A is the base area, τ_r is the constant yield stress of the flow. Equation (2.8) shows that when the yield stress of the flow increases, the velocity of the flow also increases.

Since, debris flow contains significant amount of fines and clay and behave differently to plain water, it will exhibit the non-Newtonian flow behavior (T. C. Pierson & Scott, 1985) . Depending on the relation between shear stress and velocity, one can choose any of existing non-Newtonian model for debris flow modeling (Takahashi, 2007d).

The relation between shear strain and shear stress for different fluid model is shown in Figure 2-8.
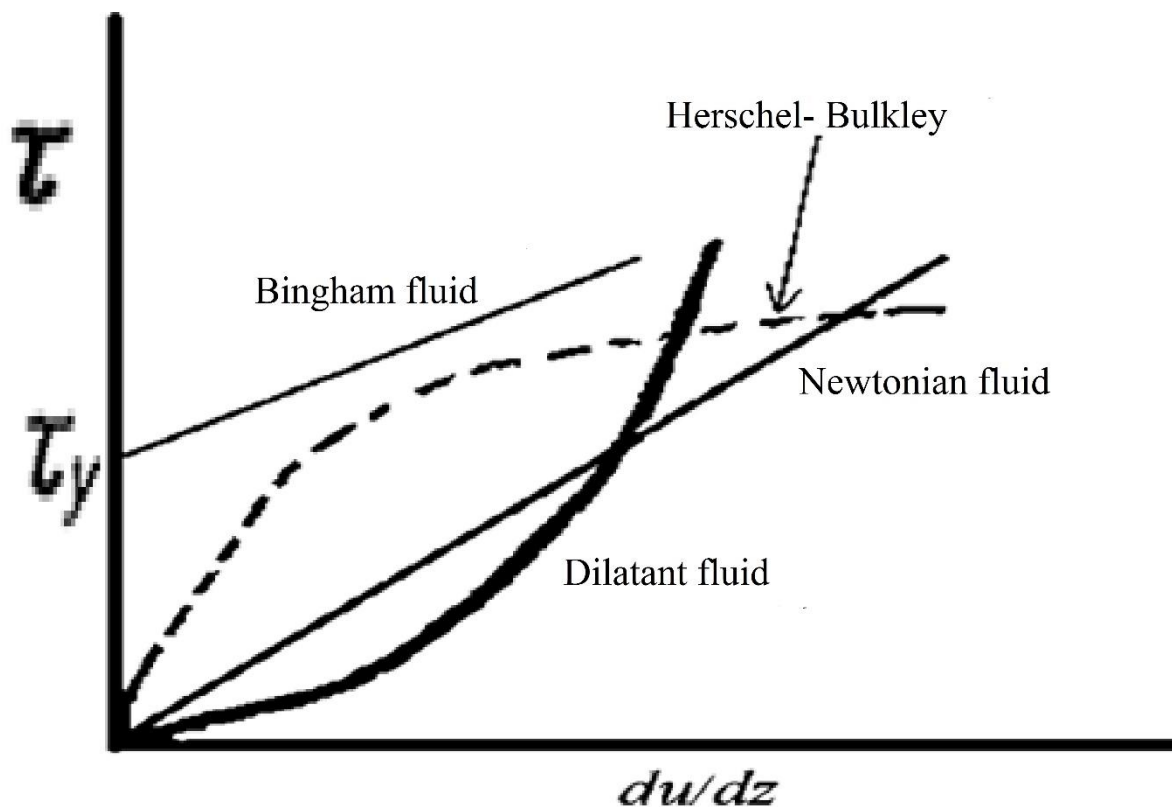

Figure 2-8 Relation of shear stress to strain for of different fluid model (Takahashi, 2007d)

Takahashi (2007d) explains that the Bingham fluid shows no deformation if the applied stress is less than the limiting strength and when the applied shear stress exceeds the threshold stress

limit called yield stress/ strength, it starts to deform in a manner as Newtonian fluid, Yield stress is the fundamental rheological property of debris flow material that can even result to the thick deposits on steep slopes (Coussot & Meunier, 1996). Takahashi (2007d) describes Herschel-Bulkley fluid as a fluid that deforms with an increase in the applied stress and this kind of flow behavior is shown by the water saturated clay mixture upon application of the stress larger than the yield strength. Upon this situation, the particles get disperse reducing their flow resistance and gets high runout. Dilatant fluid shows the behavior of reduced runout with an increase in applied stress because as the stress increases, the particle tendency to getting over each other increase and thus the runout decreases (Takahashi, 2007d) . The Hershel Bulkley model can be applied to muddy debris flow whereas for granular debris flow, no clear flow curve type can be used (Coussot & Meunier, 1996). Moreover, Christiansen (2013) signifies debris flow as approximately a Bingham fluid.

The plastic viscosity and yield stress varies significantly with variation in the concentration of sediment (Calligaris & Zini, 2012). The effect of change in sediment concentration by volume in yield stress of mixture with varying grain size is illustrated in Figure 2-9. From Figure 2-9 it can be observed that there is an increase in yield strength with an increase in the sediment concentration by volume while the increasing trend of the yield strength of the mixture is observed as it changes its state from water to hyper-concentrated flow then to debris flow as illustrated in Figure 2-10. Figure 2-10 explains that as the sediment concentration increases, the mixture of water and sediment changes its state from hyper-concentrated flow to debris flow and in this process, the shear strength of the flow increases such that the gravel can move in suspension as it reaches debris flow state.

The change of viscosity of the Bingham fluid with concentration is shown in Figure 2-11. From Figure 2-11 it is seen that the viscosity of the flow increases as the sediment concentration increases and thus the flow resistance increases.
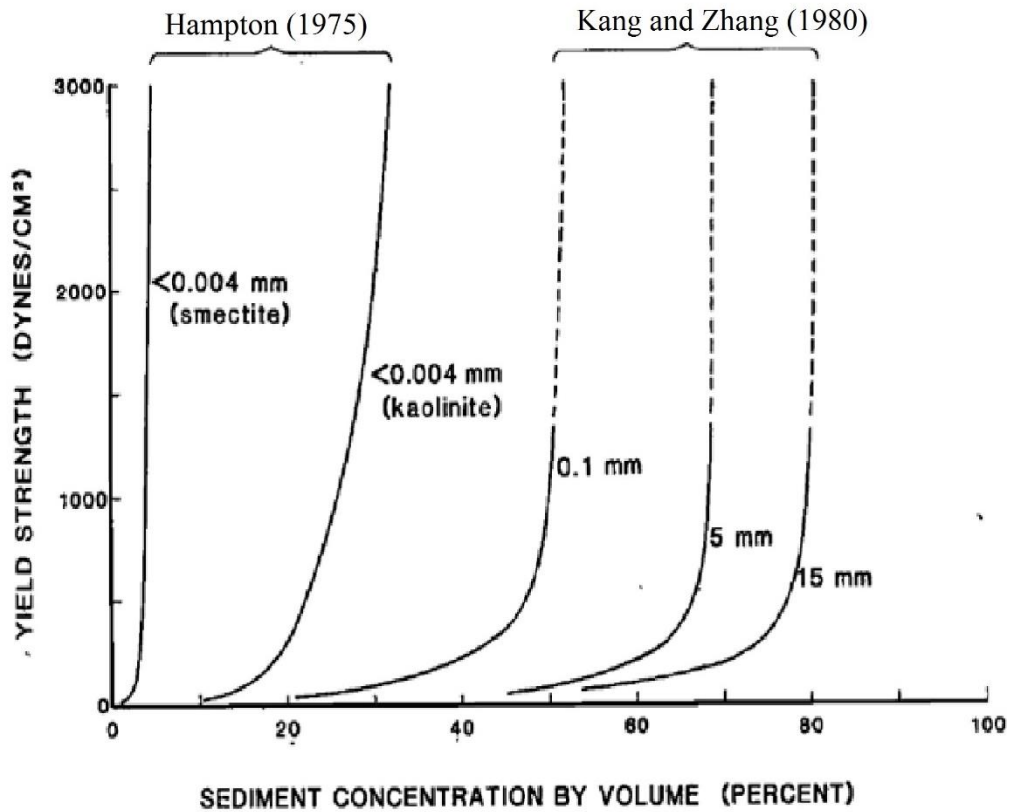
Figure 2-9 Variation in yield strength of different sediment- water mixtures of varying grain size with change in concentration by volume (T. C. Pierson & Scott, 1985)
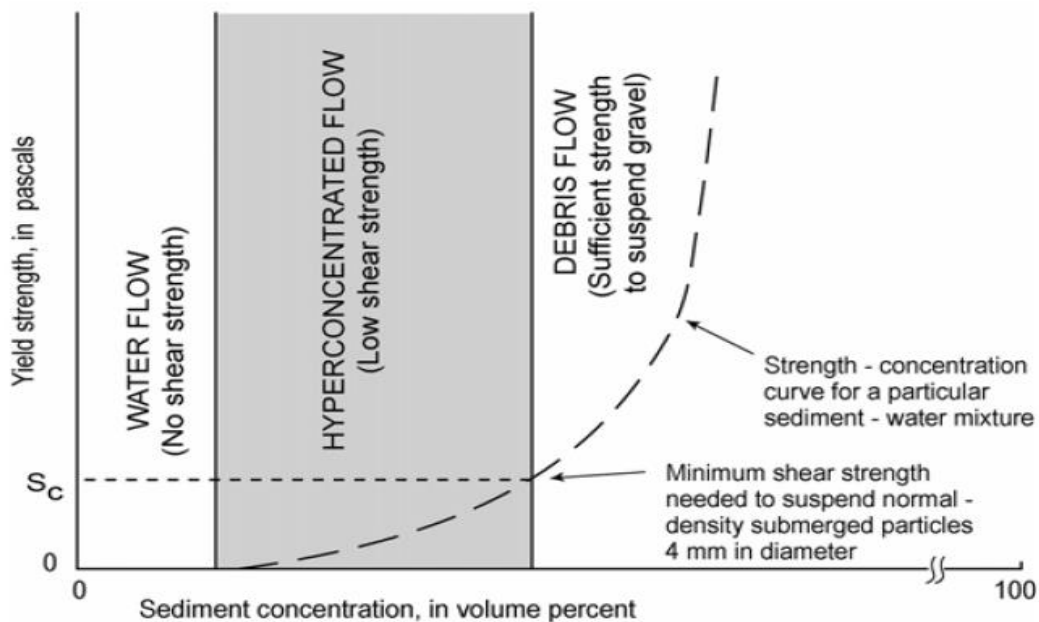
Figure 2-10 Variation of yield strength of sediment water mixture for different states depending on the concentration (T. C. Pierson, 2005)
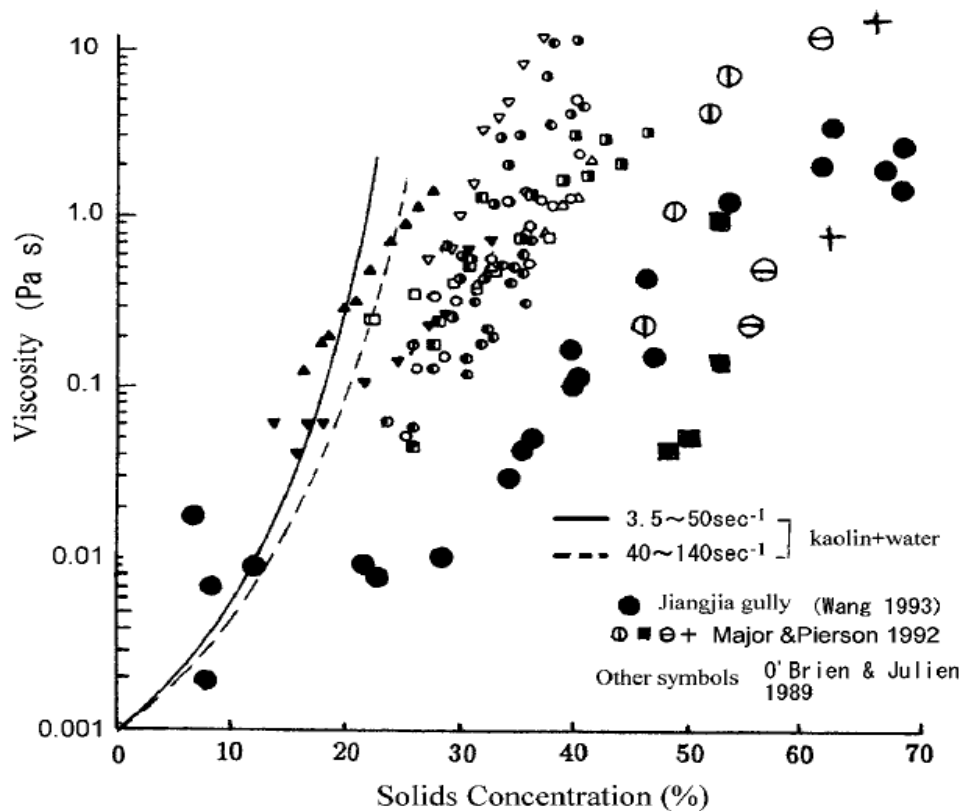
Figure 2-11 Change in viscosity of Bingham fluid as a function of concentration (Takahashi, 2007d)

Granular temperature (T) is a measure of the agitation of the debris flow that influences the kinetic sieving of the debris flow and is understood as twice the change in kinetic energy per unit mass of granular solids (Iverson, 1997). The mass with higher granular temperature acts like fluid (Iverson, 1997). Iverson (1997) has given the relation between velocity and granular temperature as Equation (2.9).

$$T = (V_s - \bar{v}_s)^2 \tag{2.9}$$

In Equation (2.9), V_s is the instantaneous grain velocity and $\bar{v}_s$ is the sum of mean velocity. So, as the velocity increases, the granular temperature increases.

Iverson (1997) explains the deposition just starts as the granular temperature of the coarse material moving ahead becomes zero and all the energy is dissipated. This forms a kind of dam or obstruction of the way to the material moving on the back which lead them to stop as well (Iverson, 1997) . If they still have enough momentum due to high pore pressure, then the coarser particles are pushed forward due to the pushing effect of the finer particles behind (Iverson, 1997).

2.4 Pore pressure

One of the factor that leads to reduce the shear strength of the soil mass is the change in intergranular forces due to water content and the rise in pore pressure, and this will give rise to buoyancy when the soil is saturated and reduces the effective intergranular pressure and friction (Varnes, 1978). The buoyancy acting on the particles during debris flow has distinct effect on large mobility evidenced by the flow even on gentle slope as flat as 3° (Takahashi, 2007e). It reduces the effective stresses of the soil and this reduction in effective stresses is the factor that governs the slope equilibrium condition of the hills (Calligaris & Zini, 2012).

The pore water pressure are usually generated by rainfall and has hydrostatic distribution. (Calligaris & Zini, 2012). It is effected by the rates and duration of the precipitation (Varnes, 1978). The pore pressure in soil rises as the infiltration rate from rainfall or melting snow exceed the rate of deep percolation of soil and due to the high pore pressure, the shear strength of the soil is reduced as the coherency of soil particle is loss (Costa, 1984). Moreover, the excess pore water pressure is generated as the volume reduces due to collapse of soil structure during liquefaction process of the landslide(Kyoji Sassa & hui Wang, 2005). The pore pressure at the base of surge heads is almost zero (Iverson, 1997).

The experiment by Kyoji Sassa, Fukuoka, Wang, and Wang (2007) describes that the high pore pressure is generated due to rapid loading on soil mass on surface and even small increment in the shear stress can cause shear failure of the soil mass on surface and the mass liquifies. Due to this liquefaction process, the debris flow moves as a viscous fluid and thus resistance depends upon viscosity of flow, not in sliding friction (Costa, 1984).

Pore pressure is one of the factor for high runout length, however, the debris flow still can have higher runout even if the pore pressure is zero provided that it has sufficient granular temperature (Iverson, 1997).

2.5 Debris flow modeling

2.5.1 Physical modeling

There are already existing relevant physical models for studying muddy debris flow dynamics and more progress is required concerning granular flows (Coussot & Meunier, 1996). The realistic debris flow can be simulated by using the mixture of only sand gravel then adding silt to see the effect of fine particles in flow (Major, 1997). The numerical models can be developed after establishing the material behavior (Coussot & Meunier, 1996). However, since, the natural debris flow contains granular materials and few amount of fine material which is less than 63μm, the small scale experiments is not effective enough to represent the natural process of depositional pattern and character of material of deposit and this demands high scale modeling method for debris flow (Major, 1997).

Crowe, Elger, Williams, and Roberson (2009a) describes the use of theory of the similitude to predict the actual flow scenario of fluid flow from model observation and this theory can be applied to debris flow as well (Coussot & Meunier, 1996) . According to Crowe et al. (2009a), the theory of similitude involves the application of Reynolds number or the Froude number to predict prototype performance from the model testing. The Reynolds number is the ratio of kinetic to viscous forces (Crowe et al., 2009a) and can be given as Equation (2.10)

$$Re = \frac{\rho V L}{\mu} \qquad (2.10)$$

In Equation (2.10), ρ is the density of the fluid, V is the velocity, L is the general length (pipe diameter) and μ is viscosity of the fluid. The low Reynolds number implies viscous flow i.e. laminar and high implies kinetic force dominancy i.e. turbulent flow.

The Froude number is defined as ratio of square root of inertial force to square root of gravitational force or the ratio of water velocity to wave velocity and is useful to define flow regime i.e. supercritical or subcritical flow (Chadwick, Morfett, & Borthwick, 2013). The Froude number can be expressed as Equation (2.11) .

$$Fr^2 = \frac{inertial\ force}{gravitational\ force} = \frac{\rho L^2 V^2}{\rho g L^3} = \frac{V^2}{gL} \qquad (2.11)$$

The Equation (2.12) can be written as Equation (2.12)

$$Fr = \frac{V}{\sqrt{gL}} = \frac{water\ velocity}{wave\ velocity} \qquad (2.12)$$

Froude number is important when gravitational forces influences the pattern of flow and is not significant when gravity only causes the hydrostatic pressure distribution like in closed pipe (Crowe et al., 2009a).

As described by Crowe et al. (2009a), there are two types of similitude: geometric similitude and the dynamic similitude. Geometric similitude implies that the model is the exact replica of the prototype. If 1: R is the scale of the model, all the linear dimensions of prototype is supposed to be scaled down in the ratio of 1:R to fit the model. So, if l, *w* and *c* are the specific linear dimensions associated with model (m) and prototype (p) then

$$\frac{l_m}{l_p} = \frac{w_m}{w_p} = \frac{c_m}{c_p} = \frac{1}{R} = L_r \qquad (2.13)$$

The area ratio and the volume ratio will be Lr^2 and Lr^3 respectively.

The dynamic similitude means that the forces acting in model and prototype should be in same ratio i.e. (*Fm/Fp* = constant) (Crowe et al., 2009a) . Equation (2.14) is generated from the ratio of the gravitational forces acting in the model and prototype.

$$\frac{V_m}{\sqrt{g_m * L_m}} = \frac{V_p}{\sqrt{g_p * L_p}} \qquad (2.14)$$

That means the Froude number of the model and prototype must be equal.

Similarly. the ratio of the viscous forces acting in the model and the prototype gives the condition that the Reynolds number of the model and prototype must be equal (Crowe et al., 2009a) .

2.5.2   Numerical modeling

Hutter et al. (1994) denotes that the numerical model of debris flow must include dilatancy, internal friction, cohesion, fluidization, and particle segregation. The internal friction and cohesion is important as they influence the shear stress of the debris flow and as these parameters reduces due to fluctuation of solid particles and motion of interstitial fluid, the pore volume will increase so that the material behaves like fluid (Hutter et al., 1994). The realistic model of debris flow should consider the inverse grading of the debris flow as well (Hutter et al., 1994) . The   pore pressure that influences the flow mechanics can be modeled by considering simple pore pressure distribution (Iverson, 1997). The calibration of numerical modeling can be done by back calculation of previous events (Oldrich Hungr, 1995).

The Continuum model, based on Lagrangian solution of equations of motion, has been developed for debris flow simulation and to analyze the runout for measuring degree of risk and design of intervention measures against the hazards like debris flow (Oldrich Hungr, 1995). The Newtonian or power law models, do not consider yield stress and thus is not capable of predicting flow stoppage. Therefore, the use of tools found in non-Newtonian fluid mechanism is recommended to model debris flow (Coussot & Meunier, 1996). Among existing non-Newtonian fluid continuum models, Bingham rheology is one of the most used basis for the existing well-developed models (Oldrich Hungr, 1995).

Among the existing numerical models for debris flow simulation, DAN (dynamic analysis is used to model an unsteady flow (Oldrich Hungr, 1995). FLO-2D, the two-dimensional numerical code, is used to simulate the debris flow along the given topographical area and it uses inflow hydrograph, plastic viscosity of material and yield stress as an input and is thus based on volume conservation (Calligaris & Zini, 2012). Similarly, DF-SIM, the tool based on the cellular automata theory, is helpful to characterize the behavior of debris flow with the parameters namely: solidification, dynamic friction angle and internal friction angle, critical height, and humidity (Calligaris & Zini, 2012). Debris is another simulation tool based on the analysis of two-dimensional model which is used to evaluate the magnitude of the deposition area and it requires a detail topography to obtain good result (Calligaris & Zini, 2012).

2.6   Energy transformation and impact force of debris flow

The debris flow motion involves the transformation of the bulk gravitational potential energy into irreversible bulk translational kinetic energy which is further converted as reversible grain vibration kinetic energy and fluid pressure energy and irreversible heat energy (Iverson, 1997). More the efficiency of the conversion, lesser the amount of irrecoverable heat energy produced and this results in farther runout before flow stops (Iverson, 1997). Once the flow stops the potential and the kinetic energy is zero and al the potential energy has been converted to heat energy ("Håndbok v139: Flom- og sørpeskred," 2014).

The Bernoulli equation applied between two points on the stream line is given as Equation (2.15) and energy equation is given as Equation (2.16) (Crowe, Elger, Williams, & Roberson, 2009b)

$$\frac{V_1{}^2}{2} + \frac{P_1}{\gamma} + z_1 = \frac{V_2{}^2}{2} + \frac{P_2}{\gamma} + z_2 \qquad (2.15)$$

$$\alpha_1 \frac{V_1^{\,2}}{2} + \frac{P_1}{\gamma} + z_1 = \alpha_2 \frac{V_2^{\,2}}{2} + \frac{P_2}{\gamma} + z_2 + h_L \tag{2.16}$$

In Equation (2.15) and (2.16), V_1 and V_2 are velocity at point 1 and 2 respectively, P_1 and P_2 are pressure at point 1 and 2, z_1 and z_2 are elevation head at point 1 and 2 respectively, α_1 and α_2 are kinetic energy correction factor at point 1 and 2, h_L is the energy loss in form of heat energy.

The energy at the point along the flow path of debris flow is given as the sum of potential energy, kinetic energy, elevation head and heat loss as illustrated in Figure 2-12. The other energy head except head loss is measurable and are given in Equation (2.17), (2.18) and (2.19) ("Håndbok v139: Flom- og sørpeskred," 2014).

Elevation head: $\qquad\qquad\qquad H_z = z \qquad\qquad\qquad\qquad$ (2.17)

z is the elevation at given point along the debris flow path

Pressure energy: $\qquad\qquad\qquad H_p = \dfrac{\rho g h}{\rho g} = h \qquad\qquad\qquad$ (2.18)

h is the flow height of the debris flow

Kinetic energy: $\qquad\qquad\qquad H_k = \dfrac{V^2}{2g} \qquad\qquad\qquad\qquad$ (2.19)

The total energy is given as He= Hz+Hp+Hk. In Figure 2-12, the difference in energy between point 1 and 2 i.e. He_1-He_2 is the energy loss at heat energy at point 2.
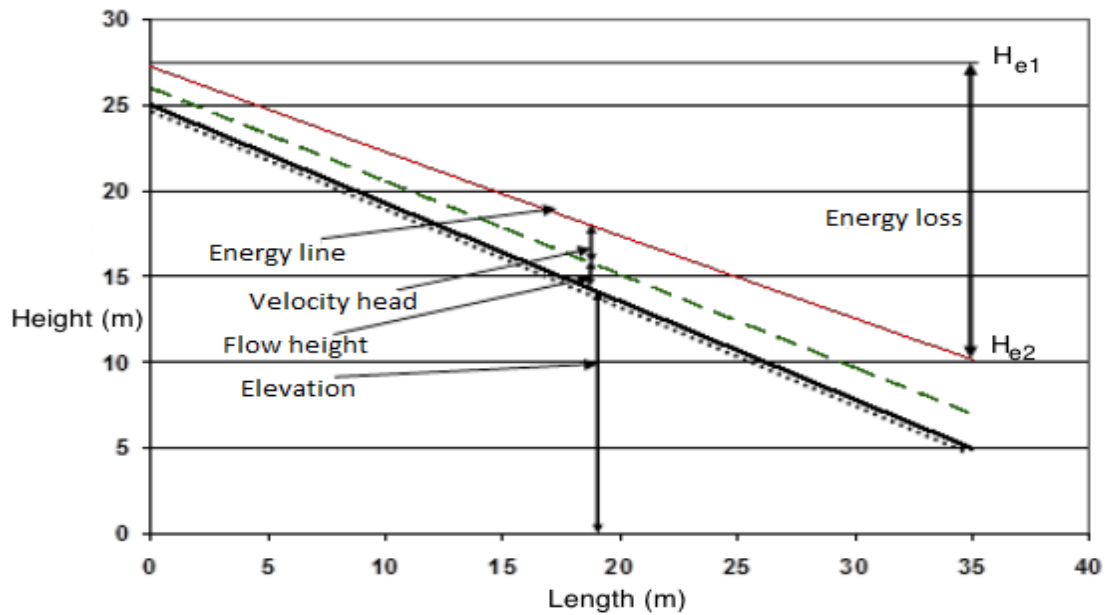
Figure 2-12 Energy line along the debris flow path ("Håndbok v139: Flom- og sørpeskred," 2014) translated by Laache (2016)

The loss of the energy as eddy or heat energy is due to friction between flowing mass and the terrain, due to grain collision and due to the hydraulic jump of turbulent surge waves (Takahashi, 2007e). The hydraulic jump occurs as supercritical flow meets subcritical flow (Chadwick et al., 2013). The flow is supercritical as the Froude number is greater than 1 and subcritical as Froude number is less than 1 (Chadwick et al., 2013). The equation of hydraulic jump given by Chadwick et al. (2013) is expressed as Equation (2.20).

$$\frac{y_2}{y_1} = \frac{1}{2}\left(\sqrt{1 + 8F_1{}^2} - 1\right) \tag{2.20}$$

In Equation (2.20) y_1, $F_1 = \frac{V_1{}^2}{\sqrt{gy_1}}$ and V_1 is the flow height, Froude number, velocity of flow in the supercritical regime respectively. "y_2" is the flow height in subcritical regime.

Equation (2.20) shows that the flow height in the subcritical regime increases as the Froude number increases in supercritical regime i.e. when the velocity of flow increases in supercritical regime.

There are several formulations existing for estimating the impact of the debris flow. Since debris flow impact is related to either hydrostatic pressure or kinetics flow height, the three group of relation can be used namely: hydrostatic, hydrodynamic and mixed models for its estimation (Vagnon & Segalini, 2016).

The debris flow material's composition and volume are the main governing factor for its movement and impact energy (Boniello et al., 2010). Vagnon and Segalini (2016) has laid down the formulas for the maximum impact thrust of debris flow for the three models (Equation (2.21), (2.23), (2.25))

The equation for the hydrostatic model is:

$$F_{peak} = k.\rho_m.g.h_f.A \qquad (2.21)$$

In Equation (2.21), F_{peak} is the maximum impact thrust in N, k is an empirical coefficient, ρ_m is the mean density of the debris impacting fluid in kgm^{-3}, g is gravity in ms^{-2}, h_f is the flow height in m and A is the impact surface in m^2. The coefficient k varies from 2.5 to 11 (Vagnon & Segalini, 2016).

ρm can be given as:

$$\rho_m = \frac{mass\ of\ sediment + mass\ of\ water}{total\ volume} \qquad \text{(Sandven et al., 2014)} \qquad (2.22)$$

The equation for the hydrodynamic model is:

$$F_{peak} = \alpha.\rho_m.v_f^2.A \qquad (2.23)$$

In Equation (2.23), α is a dynamic coefficient and v_f is the flow velocity m/s. The value of α is given as 1.5 (O Hungr, Morgan, & Kellerhals, 1984). Zhang (1993) suggested α value in between 3 to 5. Bugnion, McArdell, Bartelt, and Wendeler (2012) has given the α value between 0.4 to 0.8 and Canelli, Ferrero, Migliazza, and Segalini (2012) suggested in between 1.5 to 5.

Another hydrodynamic model suggested by Huebl and Holzinger (2003) is given as Equation (2.24).

$$F_{peak} = 5.\rho_m.v_f^{0.8}.(g.h_f)^{0.6}.A \qquad (2.24)$$

The mixed model given by Vagnon and Segalini (2016) is given as (2.25)

$$F_{peak} = \frac{1}{2}.\rho_m.g.h_f.A + \rho_m.v_f^2.A \qquad (2.25)$$

The parameter ρ_m, v_f, A, h_f, in Equation (2.24) and (2.25) have same meaning as in Equation (2.21) and (2.23)

3 THE PHYSICAL MODELING AND EXPERIMENTAL SETUP

This chapter describes the physical model and its setup, the test materials, the experimental plan and the procedures.

3.1 Physical model for debris flow experiment

The test has been carried out in the debris flow model, found in Hydraulics laboratory at NTNU in the department of Civil and Environmental Engineering. The model is a 1:20 down-scaled representation of a real debris flow topography. The model does not represent any specific debris flow of any specific location and it is just a representation of the common debris flow event. However, it is a model suitable to study the behavior and effect of debris flow phenomena in general.

As described by Laache (2016), the testing on the model was first carried out by Heller and Jenssen (2009) for studying the effect of deflection structures to channel debris flow under a bridge. Figure 3-1 shows the model that has been used for the study by Heller and Jenssen (2009) . The runout table was added in the model in 2012 to study the effectiveness of check dams, silt dams and baffles by Fiskum (2012). In 2013, the study of the effectiveness of deflection structures and channels was done in the same model by Christiansen (2013). She expanded the runout table more for her study. In 2016, the same model has been used by Laache (2016) for conducting the experiment with debris flow breaker and to investigate their effectiveness (Figure 3-2).

The same model has been used without any modification for all the test with debris slide and the debris flow. Additionally, for measuring the impact force of debris flow, the cylinder with a sensor has been placed in the lower slope. The grid lines in the runout table and the lines in the slope was faded. So, the painting of those grid lines had been done before beginning the tests.

The model consists of two consecutive slopes of 23º and 13.8º whereas the runout table is sloped with a small angle of 1.6º (Figure 3-4). The runout table is 360 cm long. Each grid in the run-out table is of 20cm x 20 cm. A line runs from left edge to right edge, spaced in 10 cm, along the channel bed having slope of 13.8º. Figure 3-4 shows the two-dimensional and three-dimensional view of the model with cylinder. The dimensions are adapted from Christiansen (2013). The model with the cylinder on the flow path has been shown in Figure 3-3.
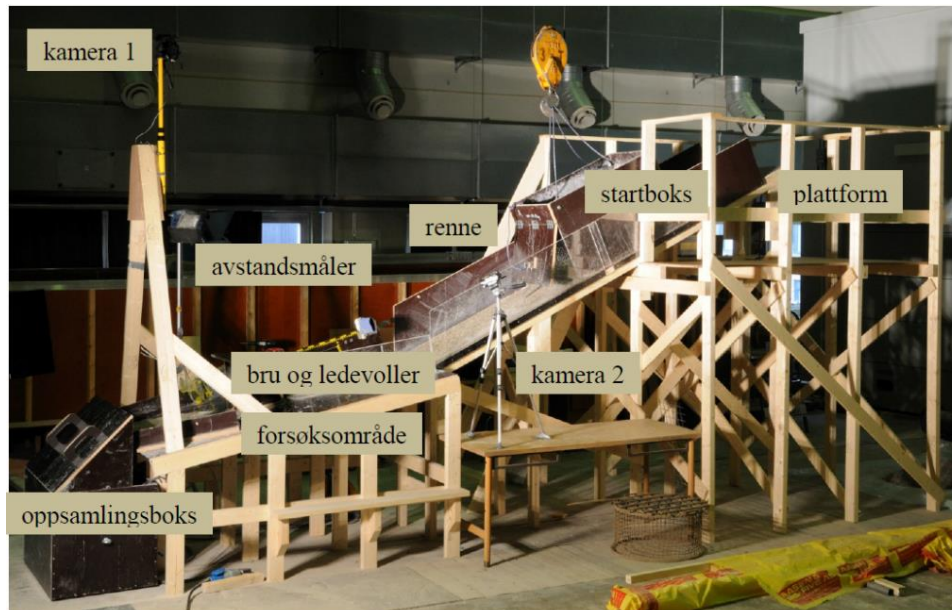
Figure 3-1 Model used by Heller to study the effect of the channeling debris flow under a bridge using deflection structures (Heller & Jenssen, 2009)
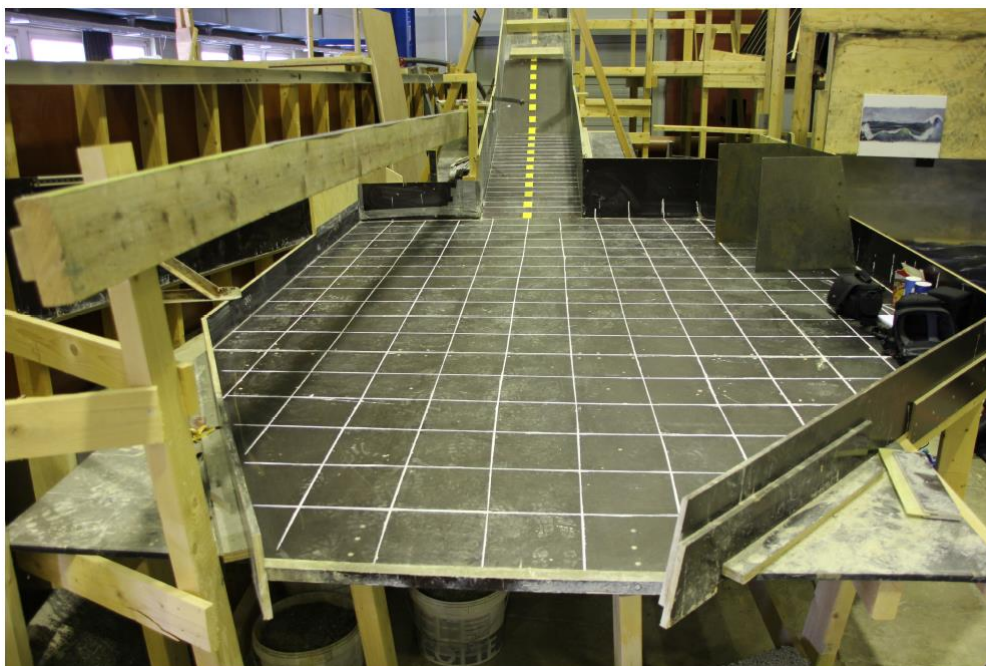

Figure 3-2 The model used by the Emile for her study in effectiveness of the debris flow breaker (Laache, 2016)
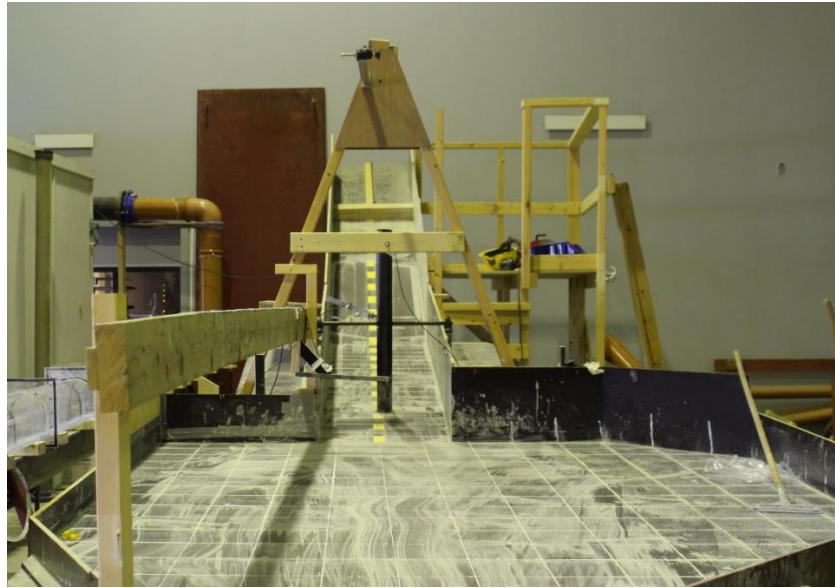
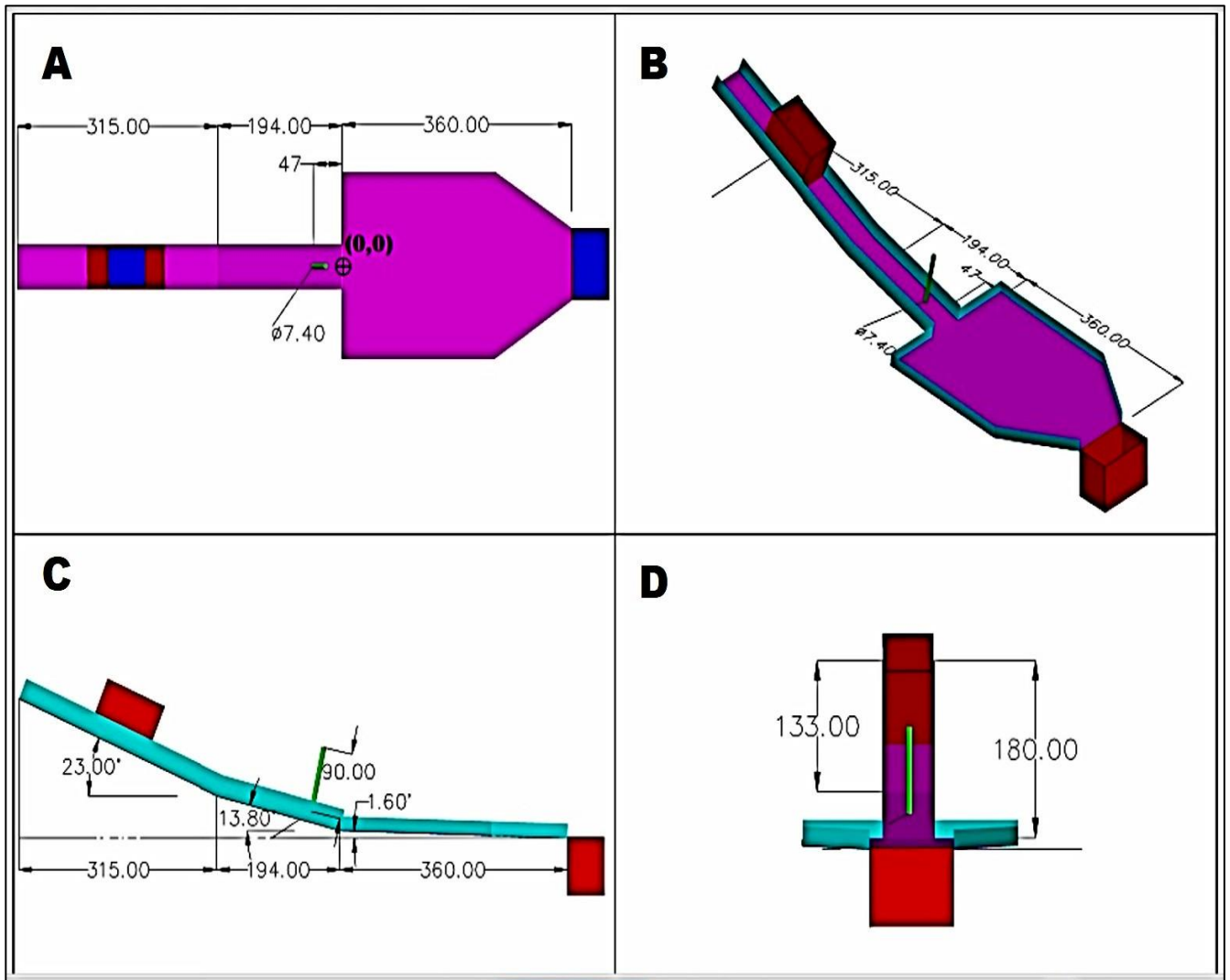Figure 3-3 The debris flow model with the cylinder to measure impact force

Figure 3-4 Section views and perspective view of the model with cylinder

In Figure 3-4, "A" is the plan view of the model, "B" is the 3D perspective view of the model, "C" is the side view of the model and "D" is the front view of the model. All dimensions are in centimeter in Figure 3-4.

The point in the figure denoted by (0,0) in "A" denotes the point from which all the debris flow runout has been measured. In the graphs of velocity and energy line, the positive sign is used to represent the length on right from the point (0,0) i.e. toward the deposition area and negative sign is used to denote the length on left side from point (0,0) i.e. towards the sloppy channel.

3.2 Model Laws

The physical model for the study involves the down-scaling of the full-scale system i.e. prototype to a subscale model. The results obtained from model are later scaled up to make necessary interpretation for the prototype. It needs an identification of the dimensionless groups to find scale factor between the model and prototype data which was carried out by dimensional analysis (Crowe et al., 2009a).

Among the two criteria of dynamic similitude, the Froude number criteria is used for modeling of debris flow (Coussot & Meunier, 1996) . The Froude number has been used by Fiskum (2012), Christiansen (2013) and (Laache, 2016) while generating the results from the model and compare with the real phenomena. In the case of debris flow, the Froude number is given as Equation (3.1).

$$Fr = \frac{V}{\sqrt{gh}}$$
(3.1)

In Equation (3.1), v = velocity of the debris flow (m/s)

g= acceleration due to gravity (9.81 m/s^2)

h= flow height of debris flow (m)

Practically, the flow height of the debris flow is approximately in the range of 1 m to 3 m (Laache, 2016) and the velocity range is 0.5-20 m/s (Costa, 1984). Using the maximum and minimum values of flow height and velocity, the range of Froude number (Fr) of the debris flow is found as 0.16- 3.69.

The same the similitude criteria for fluid flow modeling (Equation (3.2))as mentioned in Crowe et al. (2009a) is used for debris flow simulation .

$$Fr_{model} = Fr_{nature} \qquad (3.2)$$

If Lr is the ratio of the linear dimension of the model and the prototype, then we have

$$\frac{h_m}{h_p} = Lr \qquad (3.3)$$

$$h_m = Lr * h_p \qquad (3.4)$$

We have from Equation 2.14

$$\frac{V_m}{\sqrt{g_m * h_m}} = \frac{V_p}{\sqrt{g_p * h_p}} \qquad (3.5)$$

From equation
(3.3) and (3.5)
$$\frac{h_p}{h_m} = \frac{v_p^2}{v_m^2} = \frac{1}{Lr} \qquad (3.6)$$

Therefore, $$v_m = v_p\sqrt{Lr} \qquad (3.7)$$

The scale of the model used for the experiment of this thesis is 1:20 i.e. Lr= 0.05.

The corresponding range of the flow height and velocity of the debris flow of model are:

hm= 1*0.05 m= 0.05 m= 50 mm to hm= 3*0.05 m =0.15 m= 150 mm

v_m= $0.5 * \sqrt{0.05}$ m/s = 0.11 m/s to v_m = $20 * \sqrt{0.05}$ = 4.47 m/s

The range of the flow height of the debris flow is obtained as 50 mm to 150 mm and velocity ranges from 0.11 m/s to 4.47 m/s.

Similarly, Crowe et al. (2009a) explains that to maintain the dynamic similitude of the model and prototype of the fluid flow, the ratio of the forces that is exerted on masses of model and prototype must be constant and thus gives the ratio of the gravitational force of the flow of the fluid model (F_{gm}) and natural flow (F_{gp}) as Equation (3.8).

$$\frac{F_{gm}}{F_{gp}} = \frac{M_m * a_m}{M_p * a_p} = \frac{\rho_m * L_m^3 * a_m}{\rho_p * L_p^3 * a_p} \qquad (3.8)$$

In Equation (3.8), a_m and a_p represents acceleration due to gravity and they are equal. M_m and M_p are mass of fluid flow in model and in prototype i.e. in nature respectively. Assuming that the density of the material used in the model (ρ_m) tends to be equal to density of the flow mixture in nature (ρ_p), Equation (3.9) is obtained as the ratio of force acted by fluid flow in model to the force acted by natural fluid flow. Applying this condition on the debris flow event,

Equation (3.9) is obtained as the ratio between force exerted by debris flow in model to the force exerted by natural debris flow event. Equation (3.9) reveals that the force acted by natural debris flow event is 8000 times the force acted by debris flow in the model used for this thesis.

$$\frac{F_m}{F_p} = \left(\frac{L_m}{L_p}\right)^3 = \left(\frac{1}{20}\right)^3 = 1.25 * 10^{-4} \quad\quad (3.9)$$

3.3 Test materials

Since the natural debris flow phenomena include the mixture of material ranging from fine silt, sand, clay to fine and coarse gravels, it is uncertain about the exact character and the grain size distribution of debris flow material that can be used in test with physical model. However, the density of the flow must be in the range of 1-1.5 g/cm^3 (Takahashi, 2007e). As mentioned by Laache (2016), both Fiskum (2012) and Christiansen (2013) tried to conduct test with different material and different solid -water combination but still they had faced difficulty in releasing the debris flow material out of the box.

For the test in this thesis, the debris slide test has been conducted using two different materials: one with more coarse-grained soil and another with more fine-grained soil. The sieve analysis has been done using the criteria given by (*Håndbok 014: Laboratorieundersøkelser*). The coarser material used is the same material used by Laache (2016). However, there is some variation in the grain size distribution graph between the material used previously by Laache (2016) and the material used for the test in this thesis. This may be because the sample taken for sieve analysis is segregated or not mixed well. The material left from the test of Laache (2016) was not enough. So, another additional material was prepared by mixing 25% 4-8 mm material from Lauvåsen and 75% 0-4 mm material from Steinkjer, as done by Laache (2016).

The Grain size distribution (GSD) of the coarse material and fine material used for tests in this thesis is shown in Figure 3-5. The coefficient of uniformity is given as $"Cu" = \frac{d\_60}{d\_10}$ (Sandven et al., 2014). The "Cu" of the fine material and coarse material 21.3 and 25.5 respectively. Since the value of "Cu" is greater than 15, they are all well graded (Sandven et al., 2014).

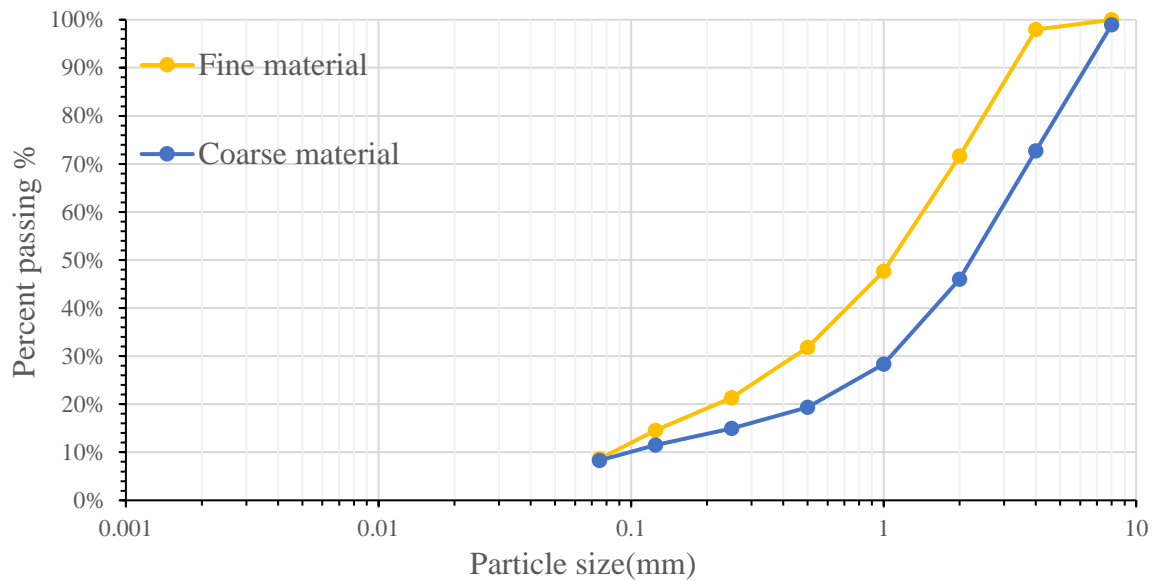## Grain size distribution of the different material

Figure 3-5 Grain size distribution curves of fine material and coarse material

The result of pycnometer test gives the grain size density of the fine material as 2.72 gm/cm^3. The grain size density of coarse material is 2.71 gm/cm^3 (Laache, 2016) .

To see the behavior of the fine and coarse debris flow material and the ease in mixing, three debris flow tests for each material were conducted. In all the test, mixture of 80 kg of debris flow material and 20 kg of water was let to flow. The fine material was found to be more difficult to mix and to release from the box in comparison to the coarse material because of which more material was remained inside the box in case of test using fine material. Figure 3-6 and Figure 3-7 shows the material left inside the box after test with fine material and coarse material respectively. In comparison, to test with coarse material, there was much frozen mass seen after the test with the fine material, as presented in Figure 3-8 and Figure 3-9. This may be because of the cohesive force between particles of fine material, due to the presence of fine silt or small amount of clay. Therefore, further tests were decided to be conducted using the coarser material.

Figure 3-6 Material remained in the box with the test using 80 kg of fine material and 20 kg of material
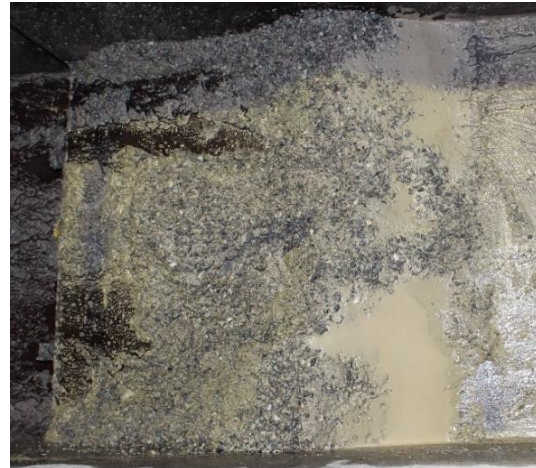

Figure 3-7 Material remained in the box with the test using 80 kg of coarse material and 20 kg of material

Figure 3-8 Frozen material as seen during the flow with the fine material

Figure 3-9 Flow with the coarse material without any frozen material

3.4 Test plans

The list of the tests that have been conducted are shown in Table 3-1 . The first number in the name denotes the mass of debris flow material (kg) and the second number denotes mass of water in kilogram (kg).

Table 3-1 List of the tests conducted and their specification

Test no.	Test set	Name	Material type	Mass of debris flow material (kg)	Mass of water (kg)	Concentration (%)
1	1	80 Coarse	Coarse	80	-	100
2	2	120 Coarse	Coarse	120	-	100
3	3	160 Coarse	Coarse	160	-	100
4	4	80+20	Coarse	80	20	60
5						
6						
7	5	80 Fine	Fine	80	-	100
8	6	120 Fine	Fine	120	-	100
9	7	160 Fine	Fine	160	-	100
10	8	80	Fine	80	20	60
11						
12						
13	9	80+30	Coarse	80	30	50
14						
15						
16	10	40+10	Coarse	40	10	60
17						
18						
19	11	40+15	Coarse	40	15	50
20						
21						
25						
22	12	40+12	Coarse	40	12	55
23						
24						
26	14	40+22	Coarse	40	22	40
27	15	50+12	Coarse	50	12	60
28						

29						
30	16	50+15	Coarse	50	15	55
31						
32						
33	17	50+18	Coarse	50	18	50
34						
35	18	45+11	Coarse	45	11	60
36						
37						
38	19	45+13.5	Coarse	45	13.5	55
39						
40						
41	20	45+16.5	Coarse	45	16.5	50
42						
43						
44	21	45+25	Coarse	45	25	40
45	22	45+11 (f)	Coarse	45	11	60
46						

Remarks: 45+11(f) are the tests with force measurements

Here, "test number" denotes the number in sequential order in which the tests have been conducted. "Test set" is the set of test for a given condition. "Name" is the name given to that very test. "Type of material" says if the material is fine or coarse material. "Mass of debris flow material and water" is the sediment and water mass respectively which has been used to prepare a sample of given combination of mixture. "Concentration" is the volumetric sediment concentration of mixture that was intended to be maintained at the beginning of the test.

The main objective was to obtain the plot of runout, maximum surge height, deposition height, grain size distribution as a function of sediment concentration and volume of mixture. For this, at first, the test was conducted with coarse material and fine material to see their respective behavior and to select the best material for the further testing. The debris slide tests with 80 kg, 120 kg, and 160 kg of the coarse and fine material have been conducted without adding any water to mixture. The material used for debris slide tests is perhaps not completely dry because of its exposure to humid environment in the hydraulics laboratory.

As discussed earlier, the coarse material proved to be better in terms of mixing and with no frozen mass for debris flow tests. So, further test was conducted using coarse material. Several trial tests had to be conducted to decide the final masses of material and sediment concentration

of mixture for further test. The debris flow tests with more volume (mass) of debris flow material and/or with lower concentration, tended to flow out of runout table. Therefore, it was decided to conduct tests with smaller mass of debris flow material. The mass of debris flow material are 40 kg, 45 kg and 50 kg and for each of these masses, the tests were conducted with three concentrations: 50%, 55% and 60%. To see the behavior of hyper-concentrated flow, the tests with 40% concentration have been conducted, although the runout for all these tests went out of table.

The installation of the cylinder for the force measurement was done at the late stage. So, only two tests have been conducted to measure the force.

The investigation of the effect of volume increment and concentration increment was planned to be done on basis of runout of the flow, velocity, energy head, flow height, deposition height and grain size distribution in deposition area. The aim was also to measure the impact force. Velocity was obtained by taking the video along the flow stream. For this, three cameras were used: one to take the overview, one to take video in lower slope and one to take video in the deposition area. Two ultrasound sensors were used to record the flow height on upstream (on the lower slope) and to the downstream (on the deposition area). The impact force was measured by placing a cylinder with a sensor at the end of lower slope. The specification of equipment and their usage is given in Table 3-2. The placement of the equipment is shown in Figure 3-10

Table 3-2 List of the equipment with their specification and usage

Equipment	Specification	Usage
Video Camera 1	Captures 25 fps	Films the whole overview of the model
Video Camera 2	Captures 50 fps	Films the flow along the lower slope of the model
Video Camera 3	Captures 25 fps	Films the flow along the deposition area of the model
Ultrasonic sensor 1	Records 50 flow height dps	Measures flow height on the lower slope
Ultrasonic sensor 2	Records 50 flow height dps	Measures flow height on the deposition area
Cylinder with sensor	Records 50 force dps	Measures impact force hits the cylinder

In table Table 3-2, "fps" is frame per second and "dps" is data per second.
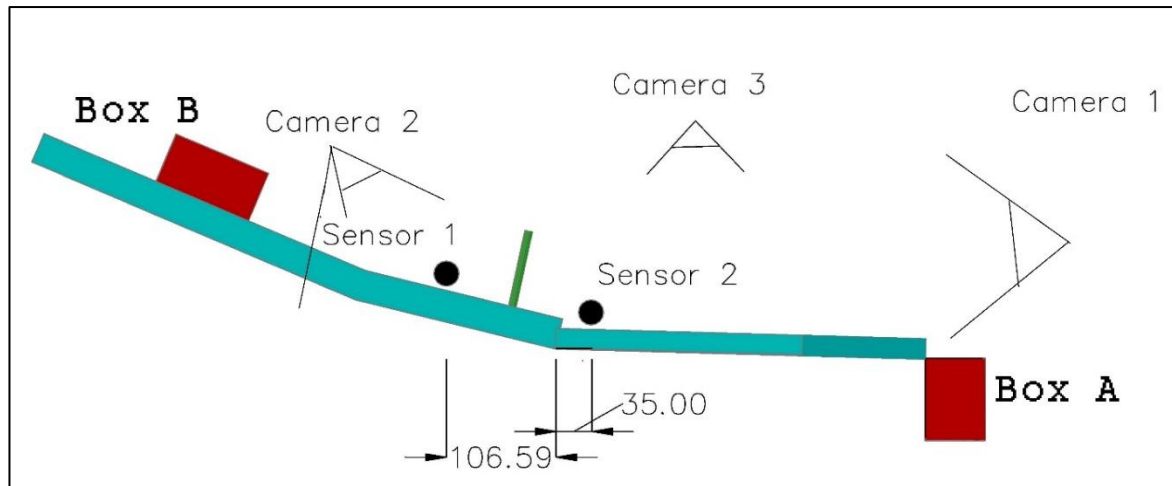
Figure 3-10 Demonstration of the placement of the cameras and sensors

In Figure 3-10 ,the camera "1" rests on the camera stand in front of the model. Camera "3" is molded on the top and camera "2" rests on the camera stand on the side bench. The cylinder with the sensor stands perpendicular to the slope. The ultrasound sensor "1" just starts as the flow front reaches to it and the ultrasound sensor "2" and the sensor in cylinder starts recording just as sensor "1" gets activated.

There are two boxes "A" and "B": "A" to collect the material after the debris flow occurs and "B" to release the mixture of debris flow and vice versa.

In case of tests with debris slide, only single camera to take the overview was used.

3.5   Procedures for debris flow test

There are certain procedures that have been followed to conduct the tests, which goes on the repetitive cycle. Overall procedure in summary is: first preparing the samples for debris flow tests, then setting up the equipment, then conducting the test in hydraulic laboratory, then taking necessary measurements and samples for water content measurement and sieve analysis and finally testing the collected samples in the geotechnical laboratory. The test procedures can be divided into three parts. First, the procedure required to prepare the mixture, followed by procedure for the test conduction in physical model and finally procedure for testing the sample collected after the test.

3.5.1   Preparation of the debris flow mixture

Debris flow samples of different total volume, using 50 kg, 45 kg and 40 kg of debris flow material, had to be prepared with 60% concentration, 55% concentration, 50% concentration and 40% concentration for each mass. The best alternative for this was to get a fixed mass of

the debris flow material and to increase the water content as required to reduce the concentration. In general, following procedure has been carried out to prepare a sample.

1. The weight of water for given concentration of sediment by volume (concentration) is calculated.

   Neglecting the void volume, the concentration is given by Equation (3.10).

   $$Cv = \frac{Volume\ of\ the\ dry\ solids\ (V_S)}{Volume\ of\ dry\ solids(V_S)+Volume\ of\ the\ liquid\ phase(V_w)} \quad \text{("Solids} \tag{3.10}$$
   and Slurries - Definition of Terms,")

   Here, the dry solids are debris flow material and liquid phase is water. For a given concentration, the volume of water can be found as

   The volume of the solid (V_S) can be found as:
   $$V_S = \frac{M_S}{\rho_S} \tag{3.11}$$

   The volume of water (V_W) can be found as:
   $$V_W = \frac{V_S}{C_v} - V_S \tag{3.12}$$

   Similarly, mass of the water (M_W) can be found as:
   $$M_W = V_W * \rho_W \tag{3.13}$$

   In Equation (3.11), M_S and ρ_S are the mass and density of solid material. Using Equation (3.11) and (3.12), the volume of water (V_W) can be found for given mass of debris flow material and given concentration and Equation (3.13) gives weight of water.

2. A sheet with an elaboration of the different weight of the debris flow material and weight of water for the given concentrations is prepared.

3. The sample is prepared by mixing water and solid for given concentration referring to the sheet prepared previously.

3.5.2 Conduction of debris flow test

There are sets of procedures that is applied in all the test and goes in cyclic order. The procedures can be divided into two sub-group before starting the test and after the test ends.

Before starting the test following procedures are followed.

1. The model is cleaned making sure that no water and sediment are left, mainly below the area where box is resting at the top.

2. For very first test, the box is weighted, and material and water is added as required. For the repeated tests of given test condition, material and water is added as required to maintain the required condition.

3. With the help of crane, the releasing box "B" is lifted to the position at top of model.

4. The second collecting box "A" is put in front of the model.

5. The note with the test number and specification in brief is written.

6. The position of the cameras is set.

7. The note is put in front of each camera to know which test is being conducted. After that, the recording of camera is started.

8. Auto recording bottom in labview program is clicked and the time is set as 10 seconds. This means that the sensor will automatically start as flow front reaches sensor "1" and ends automatically after 10 seconds.

9. The debris flow mixture is pushed at the front.

10. The mixing of the debris flow mixture is started from the side using the hand mixture. The last mixing is done in the middle section for around 15 seconds.

11. The gate is opened at once just after the last mixing is done in the middle.

After the test ends following procedures are followed.

1. The cameras recording is stopped.

2. In the labview program, the name of file is specified and the file is saved.

3. The note with name of the test is put in front of the camera that is used for capturing pictures and a picture of note is taken to identify the test later.

4. The pictures are taken showing material left inside box, pattern of flow, run out distance, pattern of deposit, any freezing material on the flow path, deposit height.

5. With the help of crane, the releasing box is lifted down on weighing machine and weight the box with material left.

6. The number of the test with proper labels on the plastic bag is written.

7. The sample from the box in the plastic bag for water content measurement is taken. It is made sure that plastic bag is closed tightly so that no water vapor can go out of it.

8. All the material left inside releasing box is placed into the collecting box.

9. The soil sample at the beginning of the deposition area and end of deposition area is taken for the sieve analysis.

10. The soil sample at the middle of deposition area for the sieve analysis is taken for sieve analysis (only for test 35,35,37)

11. The debris flow mixture in model is pushed to the collecting box to collect all the water and sediments.

12. The mass of mixture in the collecting box is measured and the amount of material and water is added as required for next test.

Figure 3-11 shows the sample collected for the water content and Figure 3-12 shows the area namely: beginning, middle and end of deposition area, from which sample that has been collected for sieve analysis.

The process of taking down the box to weigh the material left, collecting samples and cleaning took approximately 30 minutes in each test. The cleaning was more time consuming when there was cylinder placed on the way.

Figure 3-12 The area from where the samples for sieve analysis has been collected

Figure 3-11 Samples collected to measure water content of the material left inside the box after test

3.5.3 Water content test and sieve analysis of the samples collected

The samples for water content calculation and sieve analysis have been collected after each debris flow test conducted with the physical model. Therefore, after the test in hydraulics laboratory, the water content calculation of material left inside the releasing box and sieve analysis of samples from depositional area (Figure 3-12), have been done in Geotechnics laboratory at NTNU. The actual sediment concentrations have been calculated based on the water content and the mass of the material left inside the box and the procedures are as follow.

For water content measurement and calculation of actual volume and concentration

1. The plastic bag (M_p) where the sample from the box is to be placed is weighted.

2. The sample with plastic bag (M_{sp}) is weighted.

3. The weight of the wet sample (M_{sw}) is calculated as given in Equation (3.14):

$$M_{sw} = M_{sp} - M_p \qquad (3.14)$$

4. The weight of the bowl where the sample is to be placed (M_b) is measured.

5. The sample is placed in the bowl. All the material left is carefully taken out in the labeled bowl with the help of water.

6. The sample is kept in the oven for 24 hours.

7. The sample is taken out from the oven and the weight of the dry sample with the bowl (M_{sb}) is measured.

8. The actual weight of the dry sample (M_{ds}) is calculated as:

$$M_{ds} = M_{sb} - M_b \qquad (3.15)$$

9. The weight of water contained in the sample is calculated as:

$$M_{ws} = M_{sw} - M_{ds} \qquad (3.16)$$

10. The water content is calculated as:

$$w = \frac{M_{ws}}{M_{ds}} \qquad (3.17)$$

11. The mass of the material left inside the box (M_{lb}) is calculated by deducting the mass of the box from the total measured weight.

12. The mass of the dry solid material left in the box (M_{sbox}) is calculate using Equation (3.18). If M_{wbox} is weight of water in material left inside the box, then the mass of the dry solid material left inside the box (M_{sbox}) is calculated as:

$$M_{lb} = M_{sbox} + M_{wbox}$$

$$M_{lb} = M_{sbox} + w * M_{sbox}$$

$$M_{sbox} = \frac{M_{lb}}{(1 + w)} \qquad (3.18)$$

13. The mass of the water left inside the box is calculated as:

$$M_{wbox} = M_{lb} - M_{sbox} \qquad (3.19)$$

14. The actual mass of the solid material (M_S) and actual mass of the water (M_W) contributing to the debris flow is calculated by deducting the mass of solid material and water left inside the box.

15. The actual concentration is finally found using Equation (3.10)

For sieve analysis of the sample from different depositional area

1. The sample is placed out of plastic bag in a labeled bowl and all the material is taken out with the help of water.
2. The sample is kept in over for 24 hours to dry.
3. The sample is taken out and placed in another bowl.
4. The sieve analysis is carried out based on *Håndbok 014: Laboratorieundersøkelser* 2005).

3.6 Procedures for debris slide tests

The procedure for debris slides are:

1. The weight of the releasing box is measured and the material is added as required.
2. The releasing box is lifted with the help of crane till the top.
3. The note is made with the test name and it is placed in front of the camera which takes the over view. The camera is started.
4. The debris slide is released by opening the gate.
5. The runout is measured and the picture showing the runout, pattern of deposition is taken.
6. The material is collected in the releasing box again.
7. The required material is added to conduct the next test.

4 RESULTS AND ANALYSIS

The results of the 46 tests that have been conducted on the debris flow physical model is presented here. The result section includes the results of actual concentration and density, the velocity of the debris flow front, flow height and deposition height, runout distance of the debris flow front. The analysis of the results is presented as energy lines, impact force and GSD curves of the material deposited at the beginning, middle and end of the deposition area. This chapter does not include any discussion of the results.

4.1 Actual concentration and Actual density

Some materials are left inside the box in every test. The amount of material left inside the box depends upon the mixing technique and is uncertain. However, it is seen that amount of material left inside the box is more for the high concentrated flow in comparison to lower concentrated flow. Due to the material left inside the box, each test has different actual concentration. Thus, every individual test is a unique test and has unique flow parameters. The variation of actual concentration of the debris flow mixture depends upon the weight and the water content of the material left inside the box. The water content is different in all samples of material left in the box and it ranges from 11% to 17%. The amount of material left inside the box and water content for all test are given in APPENDIX A.
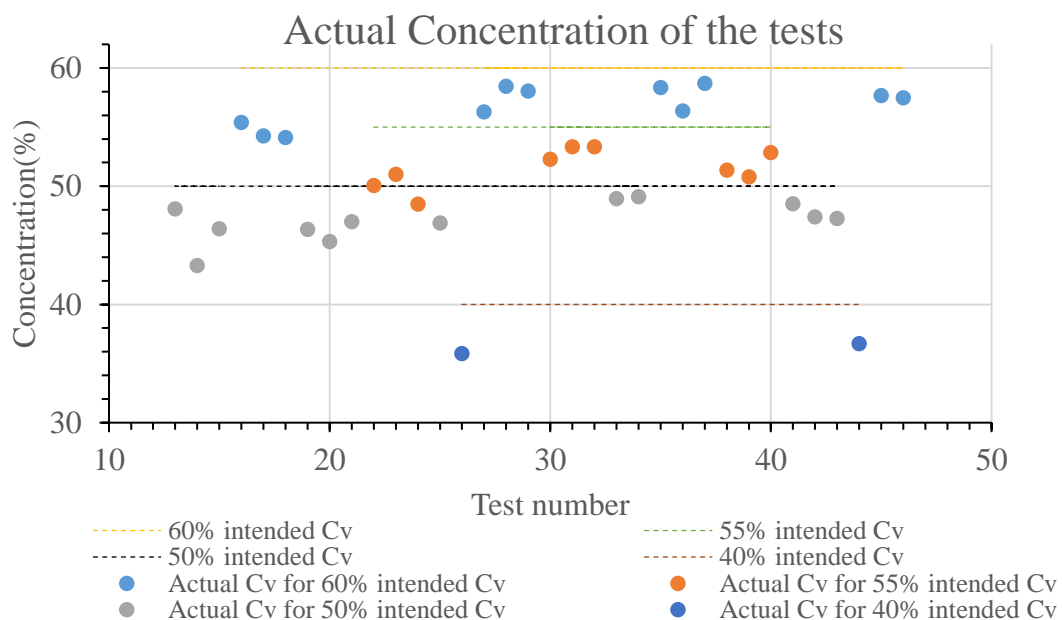
Figure 4-1 Illustration of deviation of actual concentration from intended concentration for the tests conducted

Figure 4-1 shows that, the actual concentration seems to be in the range of 58% for the 60% intended concentration. The concentration varied most for tests 16,17,18 which have been conducted using 40 kg of solid material. The concentration for these tests is around 54%. For 55% intended concentration, the actual concentration seems to be in the range of 50-53%. The actual concentration for the 50% of intended concentration seems to be ranging in between 45% to 49%. Even in the tests conducted with 55% concentration and 50% concentration, the variation is mostly seen for the mixture with 40 kg of debris flow material. For 40% intended concentration, the actual concentration tends to be around 35%.

So, the actual concentration varies from intended concentration somewhat from 1% to as high as 5% in the debris flow tests. This variation is mostly seen for the test with 40 kg of debris flow material. This may be because the material weight is small and the material left inside the box makes much difference in this case.
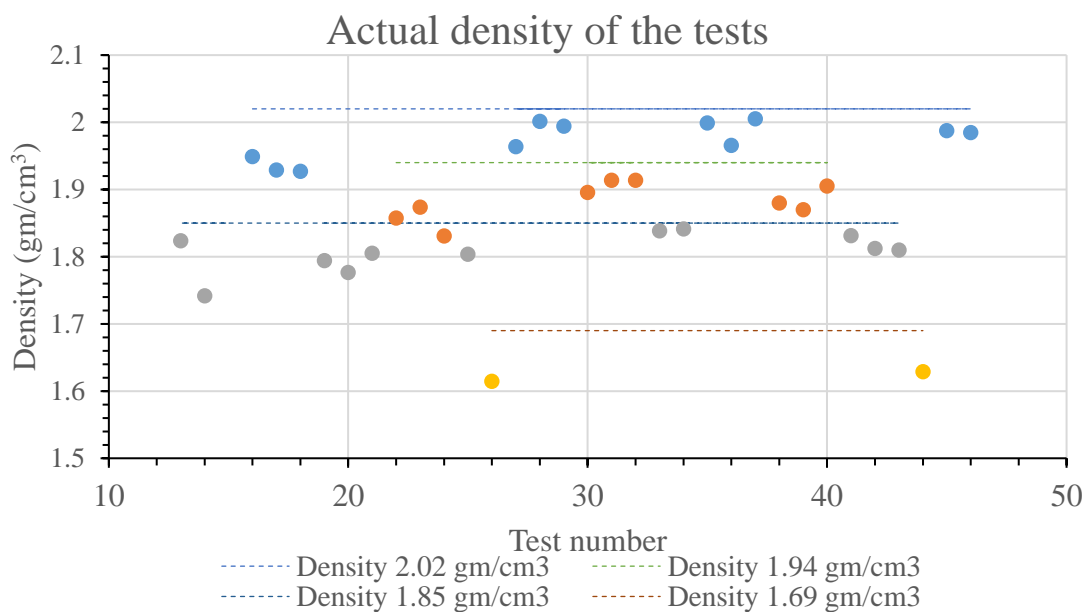
Figure 4-2 Illustration of deviation of actual density of the tests from intended density

Figure 4-2 illustrates that the deviation of the actual density from intended one. This is caused due to the variation in the actual concentration. The variation in actual density is seen much for the tests with 40 kg of material which is the direct result of the more variation in its concentration. Even though there is a variation in actual density from intended one, still the density satisfies the density of natural debris flow event.

4.2 Velocity

As explained in section 3.4 , the camera has been used to film the video along the debris flow path. The velocity of flow front has then been manually calculated by video image analysis. Since the camera frame could not capture the whole area of the debris flow path, the velocities have been calculated just in the middle section of the flow path. In the velocity plots, the dotted lines indicate the missing data.

The velocity has been obtained by following the debris flow front that travels ahead instantaneously as the debris flow mixture is released. The debris flow front moving ahead did not consist of the any frozen mass. Thus, the frozen mass did not create any effect in the velocity calculation. The debris flow front traveling ahead doesn't follow the center of the flow line in most of the cases and varies in all the tests. Moreover, the shape of flow front changes as it flows down, which creates difficulty in following that specific flow front throughout the velocity calculation of the given test. This makes it difficult to calculate the velocity accurately.

Figure 4-3 and Figure 4-4 shows that how differently the debris flow front is moving with time. The flow front is on the right side of the center line in time 1.868 s (Figure 4-3)where as it is on the left side of the center line in time 2.107 s (Figure 4-4).

Figure 4-3 Debris flow front for test 4 at time 1.868s
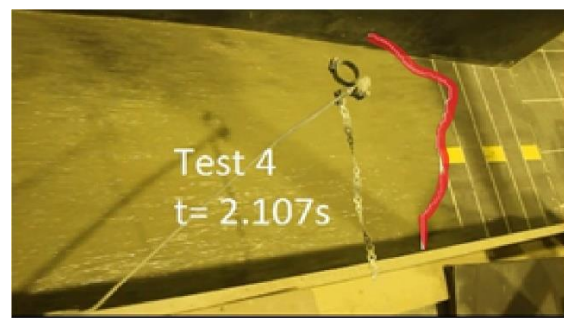
Figure 4-4 Debris flow front for test 4 at time 2.107s

Since, the velocities had to be calculated manually from the films, the velocity have been obtained only for those test sets which has lower standard deviation of concentration. Due to the variation in the actual concentration of the mixture, every individual test is a unique test. However, for simplicity in analyzing the data, the average of the velocities for given test condition have been used for study and comparison. The velocity plot for the individual test are given in APPENDIX B.

The velocities have been calculated for all together 23 tests of 8 test sets: 40+10, 80+20, 45+11(f) with 60% concentration; 50+15 with 55% concentration; 40+15, 45+16.5, 50+18, 80+30 with 50% concentration. The concentration, mass of debris flow material and mass of water denoted here are intended values. Since the velocity are calculated manually, there is difference in the velocity of the front among the tests of test set for any given condition. This difference may have caused due to the use of camera with low frame per second which may have led to inaccuracy in velocity calculation.

The average of the velocity of flow front for the test sets are shown in Figure 4-5, Figure 4-6, Figure 4-7 and Figure 4-8.
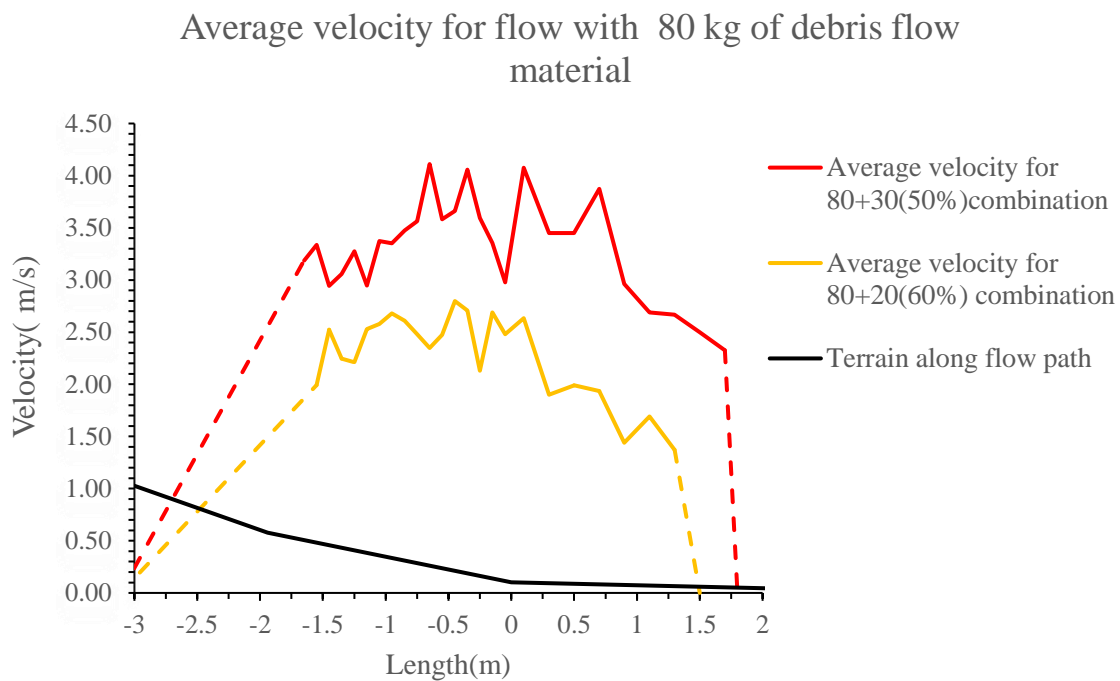
Figure 4-5 Debris flow front velocity of the flow with 80 kg of debris flow material with 60% concentration and 50% concentration
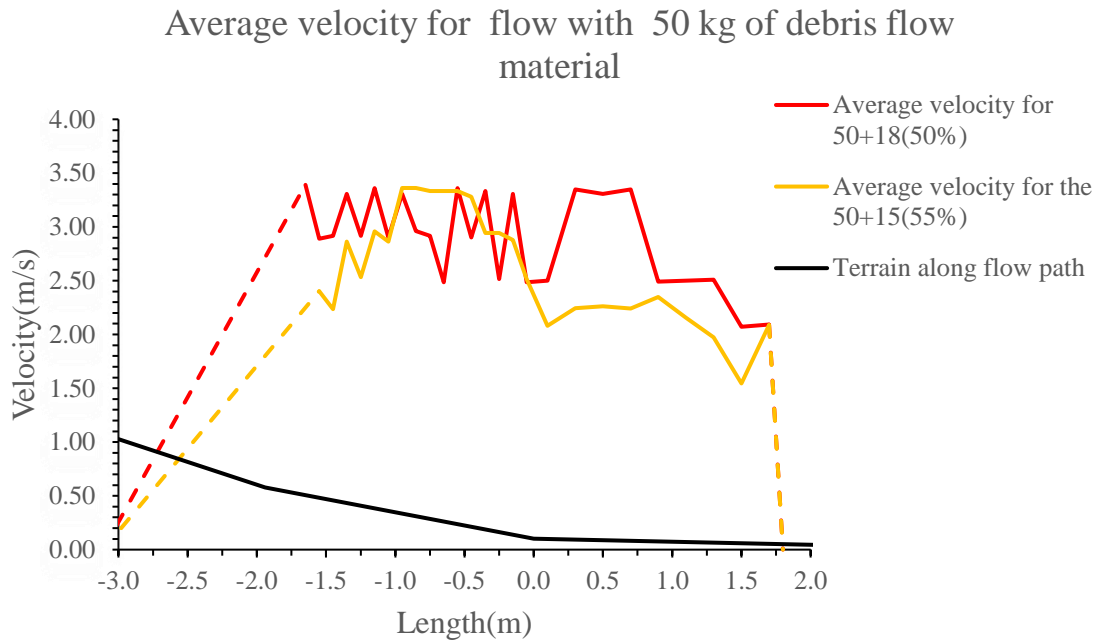
Figure 4-6 Debris flow front velocity of the flow with 50 kg of debris flow material with 55% concentration and 50% concentration
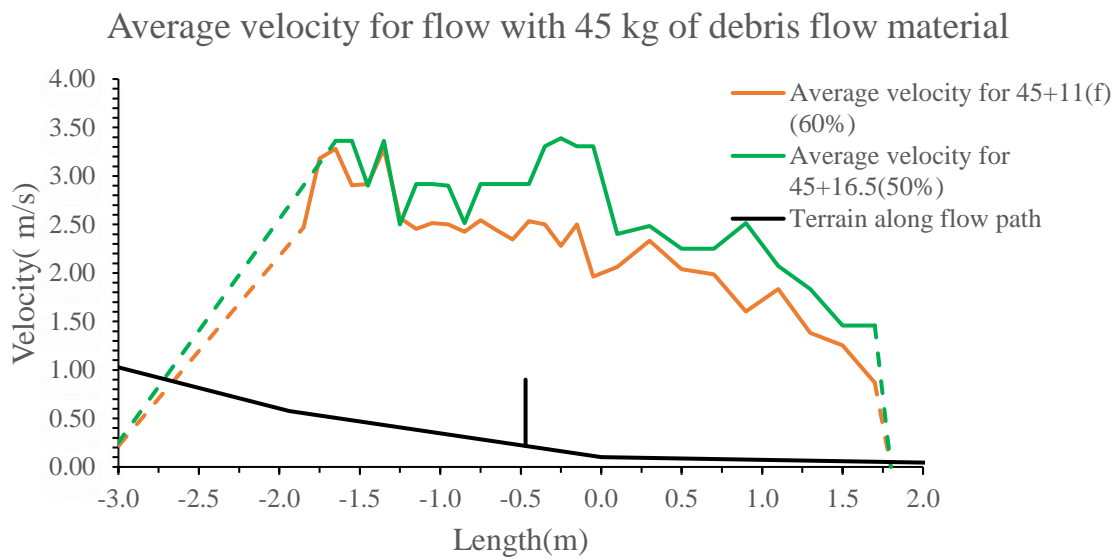
Figure 4-7 Debris flow front velocity of the flow with 45 kg of debris flow material with 60% concentration and 50% concentration
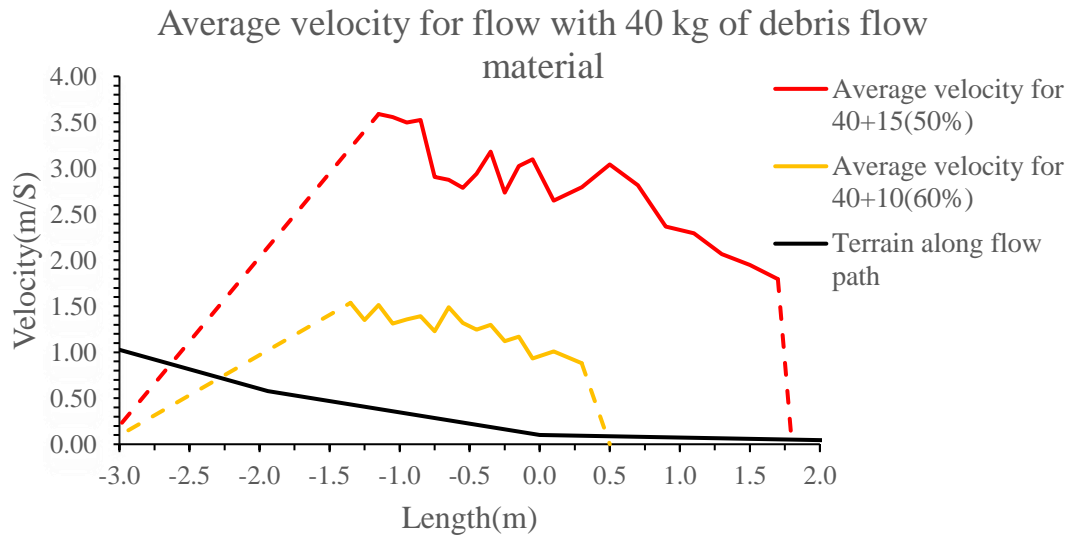
Figure 4-8 Debris flow front velocity of the flow with 40 kg of debris flow material with 60% concentration and 50% concentration

4.3 Runout

The origin for the runout measurements has been taken at the beginning of the deposition area for the debris flow test(Figure 3-4 and Figure 4-9) and at the gate opening for the debris slide test (Figure 4-9)
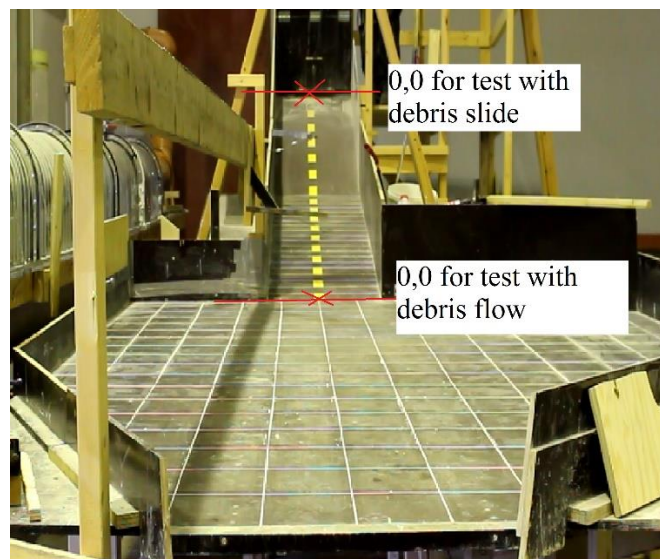
Figure 4-9 The origin for the runout measurement for the test with debris flow and debris slide

The runout length of the debris slide has been taken at the point till which the slide front reaches (Figure 4-10). Some small amount of the material, specially the coarse grain, travels far which is neglected with the assumption that those material traveling will have very less hazards in natural debris slide event.

The runout of the debris flow has been taken until the point where the debris flow front stops (Figure 4-11). The water, along with fine sediment particles, flows ahead even after debris flow front stops. But they are not considered in the runout length measurement, with an assumption that unlike the debris flow front that can cause significant damage to human life and properties, these water with fine sediment have very less damaging effect during the actual debris flow event.

Figure 4-10 Indication of the point for runout length measurement for the debris slide
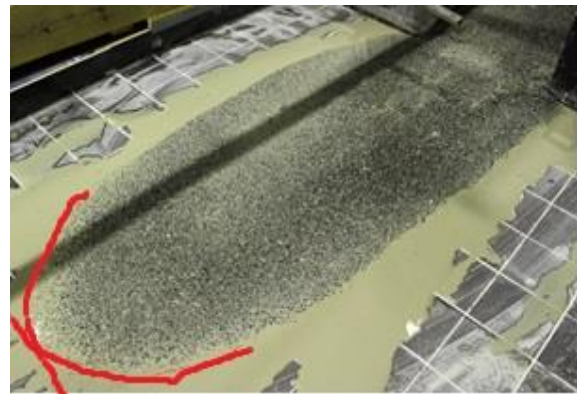
Figure 4-11 Indication of the point for runout length measurement for the debris flow

The pictures were taken after each test to study the change or difference in the runout pattern, deposition pattern and the runout distance. The pictures of the runout for all test are shown in APPENDIX F.

Graphical presentation of the runout length for the tests with debris flow is given in Figure 4-12 and for the debris slide is given in Figure 4-13. The runout data is missing for those test whose runout went out of the runout table.

There was some material left inside the box for the dry test as well. However, the weight of the material left has not been measured so the intended weight has been used for plotting the graphs for debris slide.
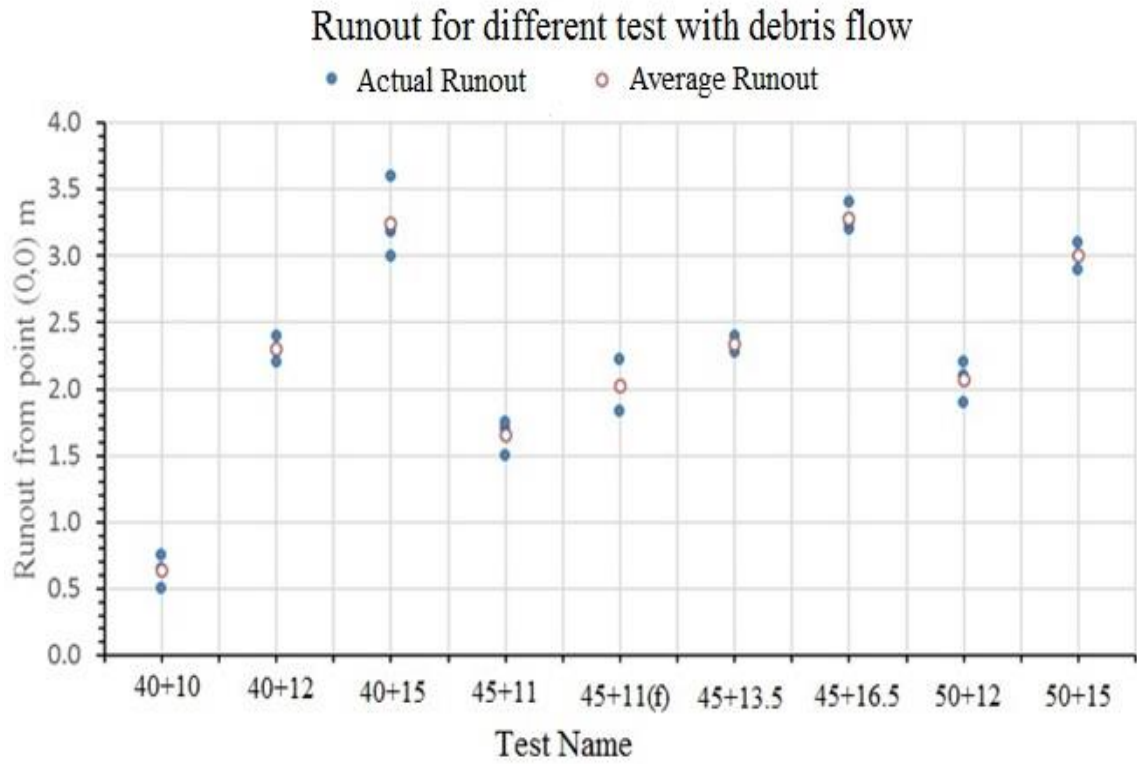
Figure 4-12 Average and Actual runout for different test set with debris flow
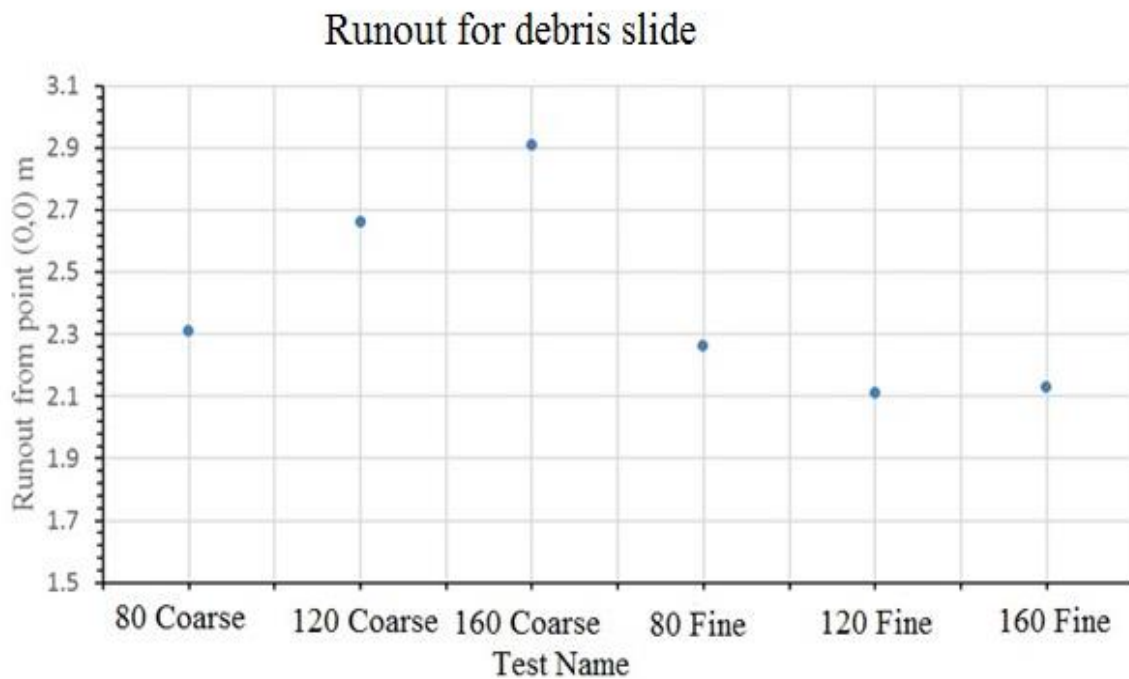
Figure 4-13 Runout for debris slide with coarse and fine material

4.4 Flow height

The flow height data could not be obtained for all the test as the sensors were not available during the earlier period of test conduction. The flow height data are only available for all together 25 tests. The flow height graphs are plotted for the flow height at a point in upstream (lower slope) and downstream (deposition area) where the sensor "1" and sensor "2" are placed respectively (Figure 3-10). The results obtained from flow height data have been categorized as: Maximum flow height in upstream, Maximum flow height in downstream and Deposition height in downstream.

The maximum flow height in the upstream and downstream refers to the peak flow height at respective points during the interval of debris flow event while the deposition height in downstream means the deposition height in the deposition area after the flow ends. Figure 4-14 shows the points which has been taken to obtain the results from flow height curve.
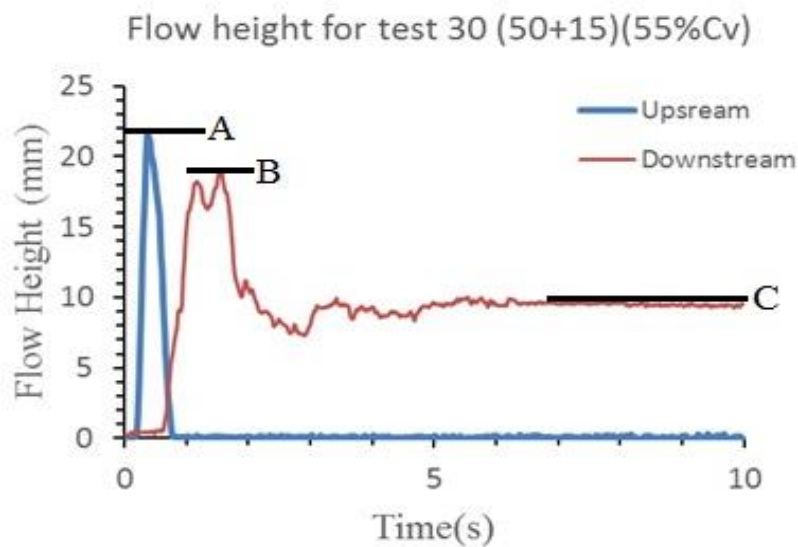
Figure 4-14 Flow height at upstream and downstream for test 30

Here, "A" is the point of maximum flow height at upstream; "B" is the point of maximum flow height at downstream and "C" is the deposition height downstream

Maximum flow height upstream for different test set
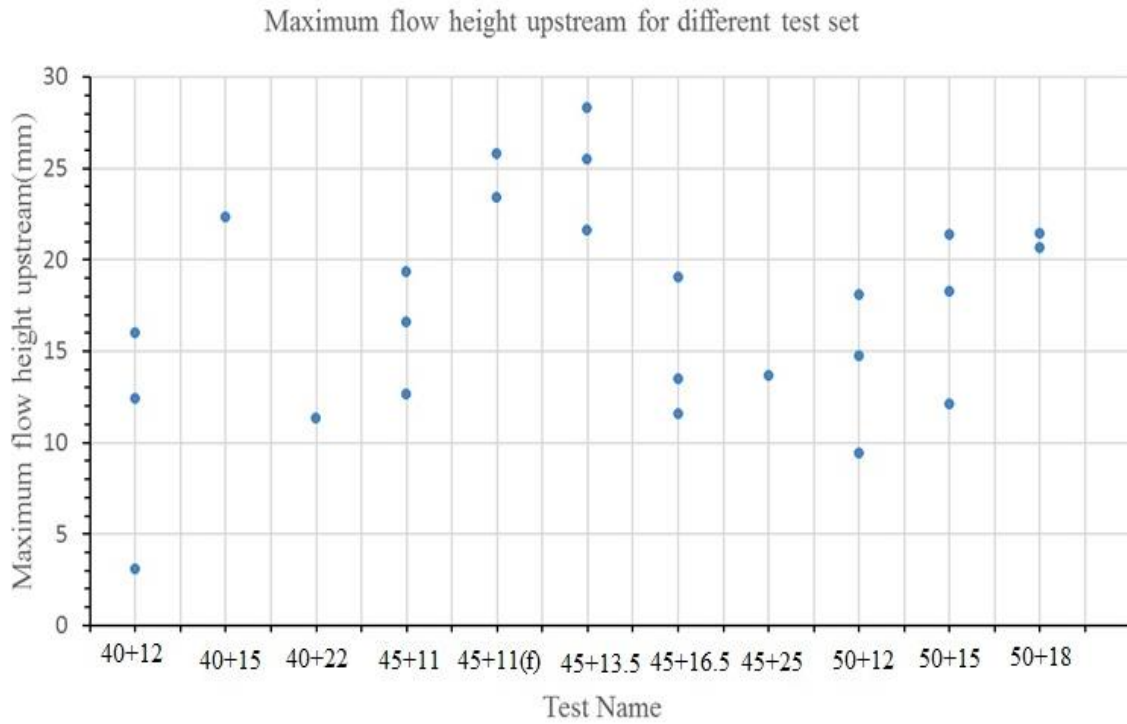
Figure 4-15 Maximum flow height upstream for test sets with debris flow

Maximum flow height downstream for different test set
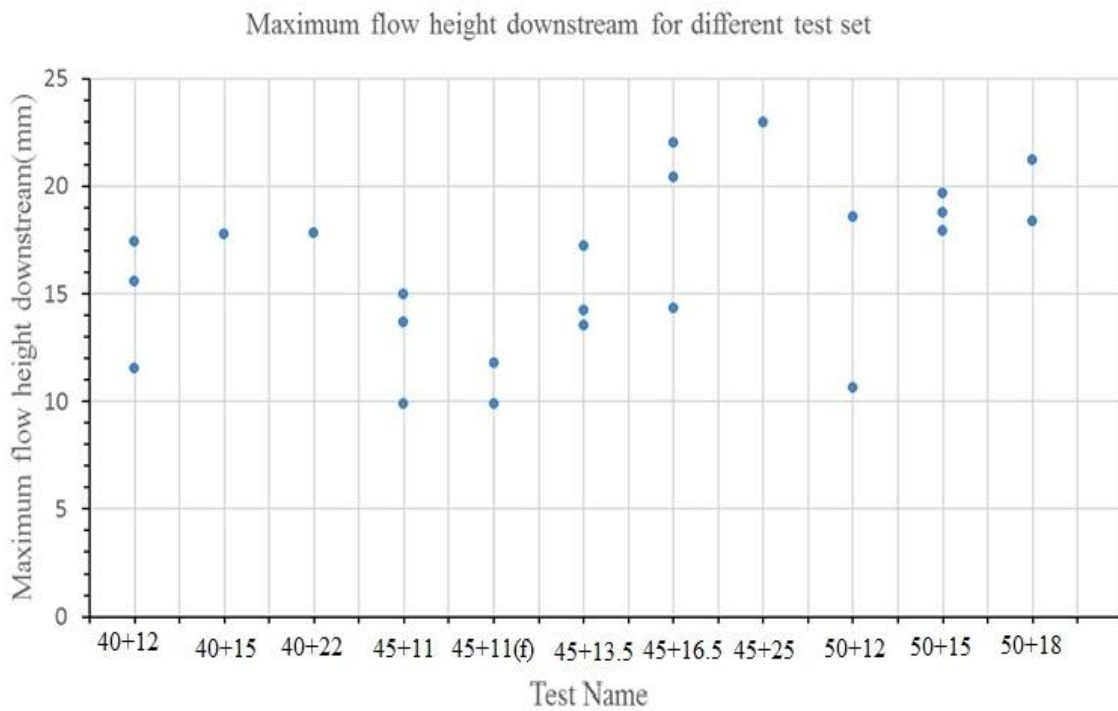
Figure 4-16 Maximum flow height downstream for test sets with debris flow
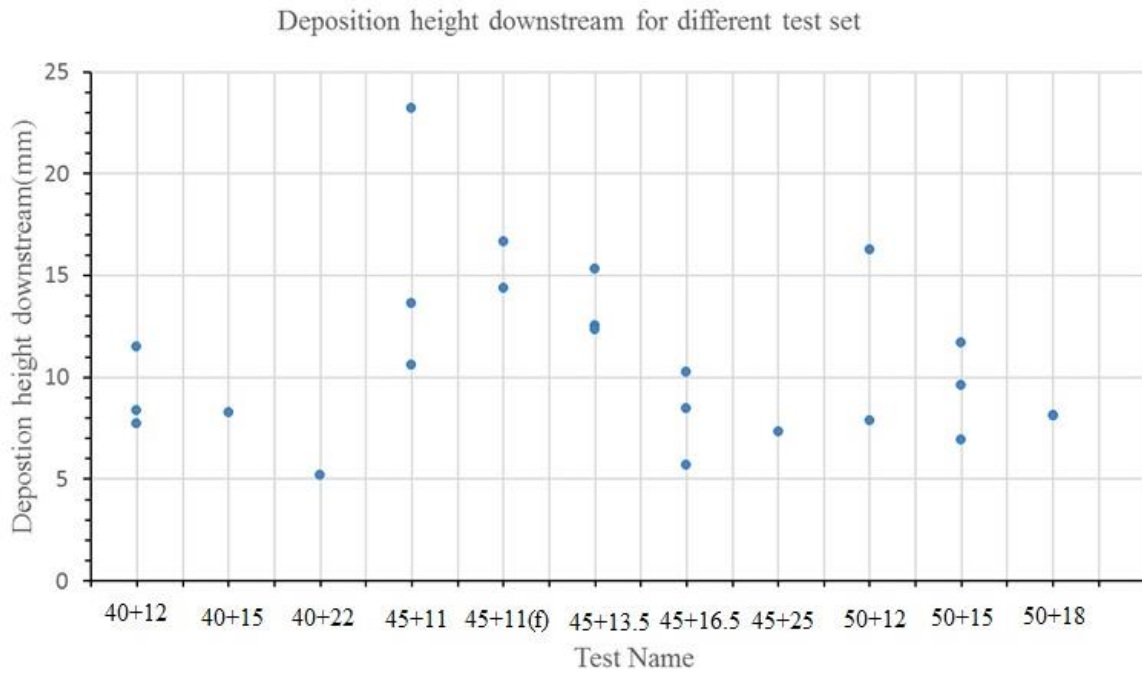
Figure 4-17 Deposition height at downstream for test sets with debris flow

The maximum flow height upstream, the maximum flow height downstream and deposition height of the tests for test sets are graphically presented in Figure 4-15, Figure 4-16 and Figure 4-17 respectively.

The flow height graph for the test with available flow height data are given in APPENDIX C.

4.5   Grain size distribution curve

To study the GSD variation due to change in concentration and total volume, the sample for sieve analysis has been taken at the beginning of the deposition area and at the end of the deposition area starting from test 13 till test 44. To see how the GSD varies along the runout length, the additional sample had been taken in the middle section of the deposition area for three tests 35,36,37. The area from where the samples are collected is shown in Figure 3-12. The sieve analysis has been done for all collected samples.

Even though every test is unique as discussed earlier, for each test sets, the average of the GSD curve has been obtained for the samples collected at the beginning and end of deposition area and these are shown in Figure 4-18. The average of GSD curve has been obtained to make a study and interpretation simpler. The GSD curve of individual plot is given in APPENDIX E.
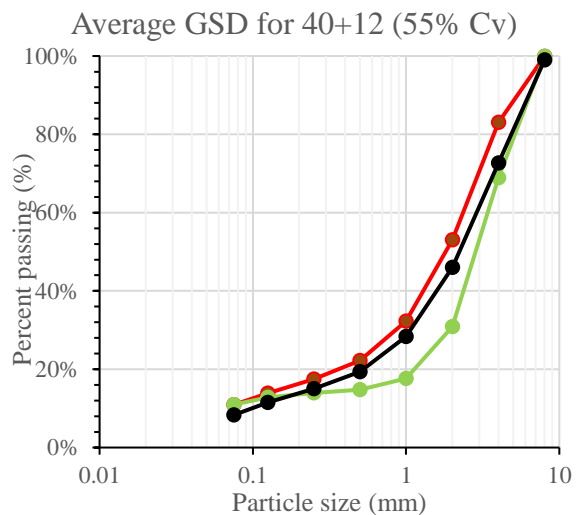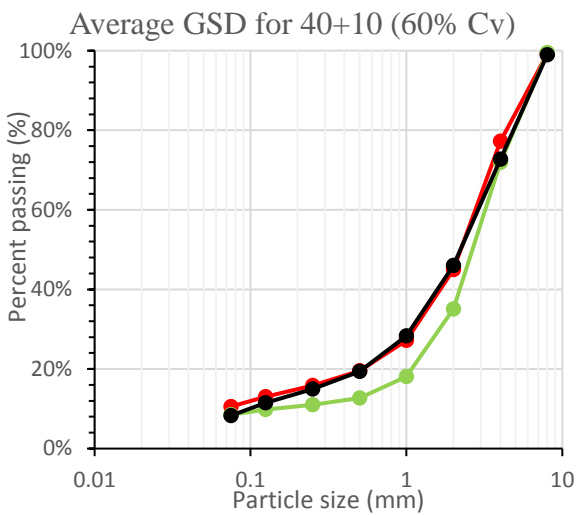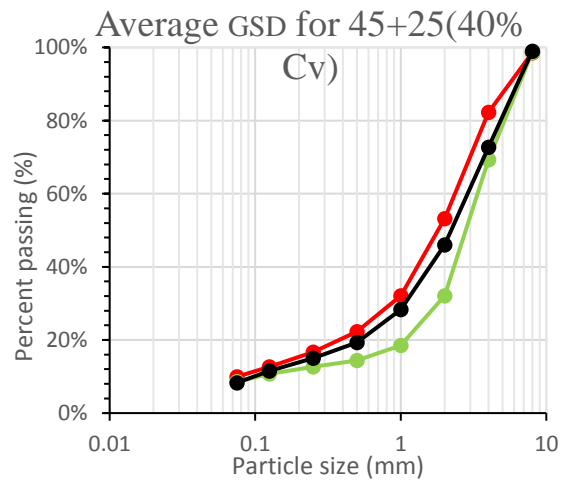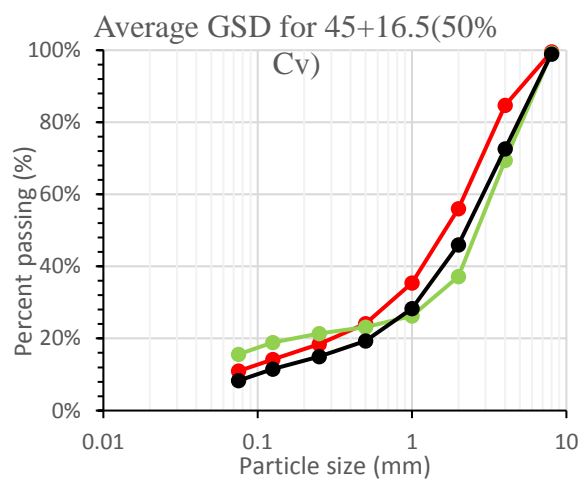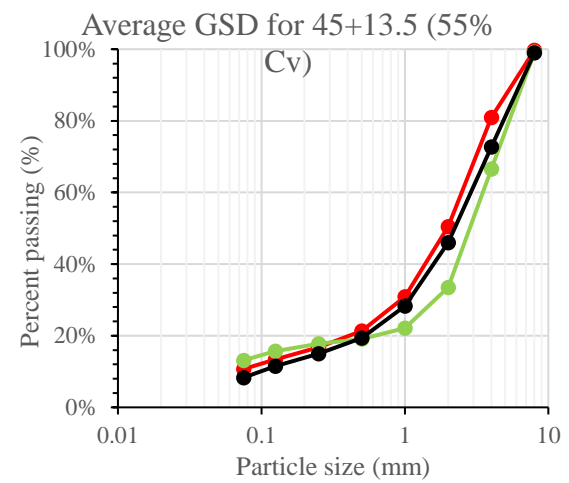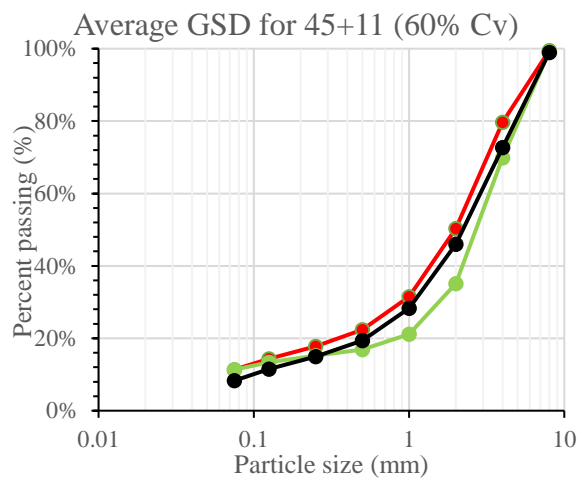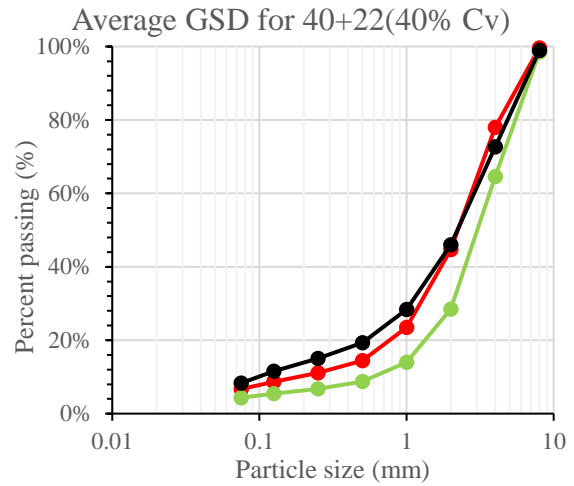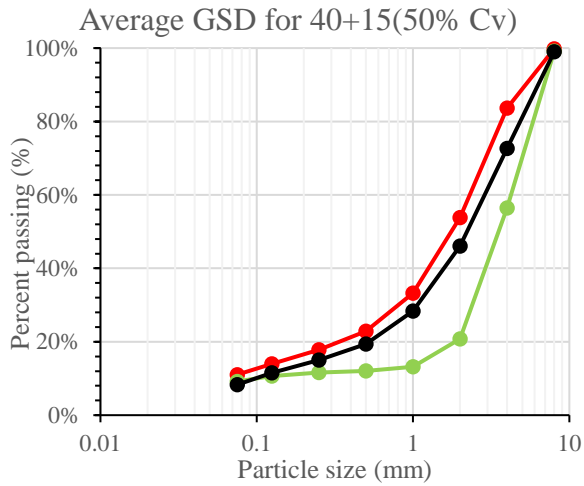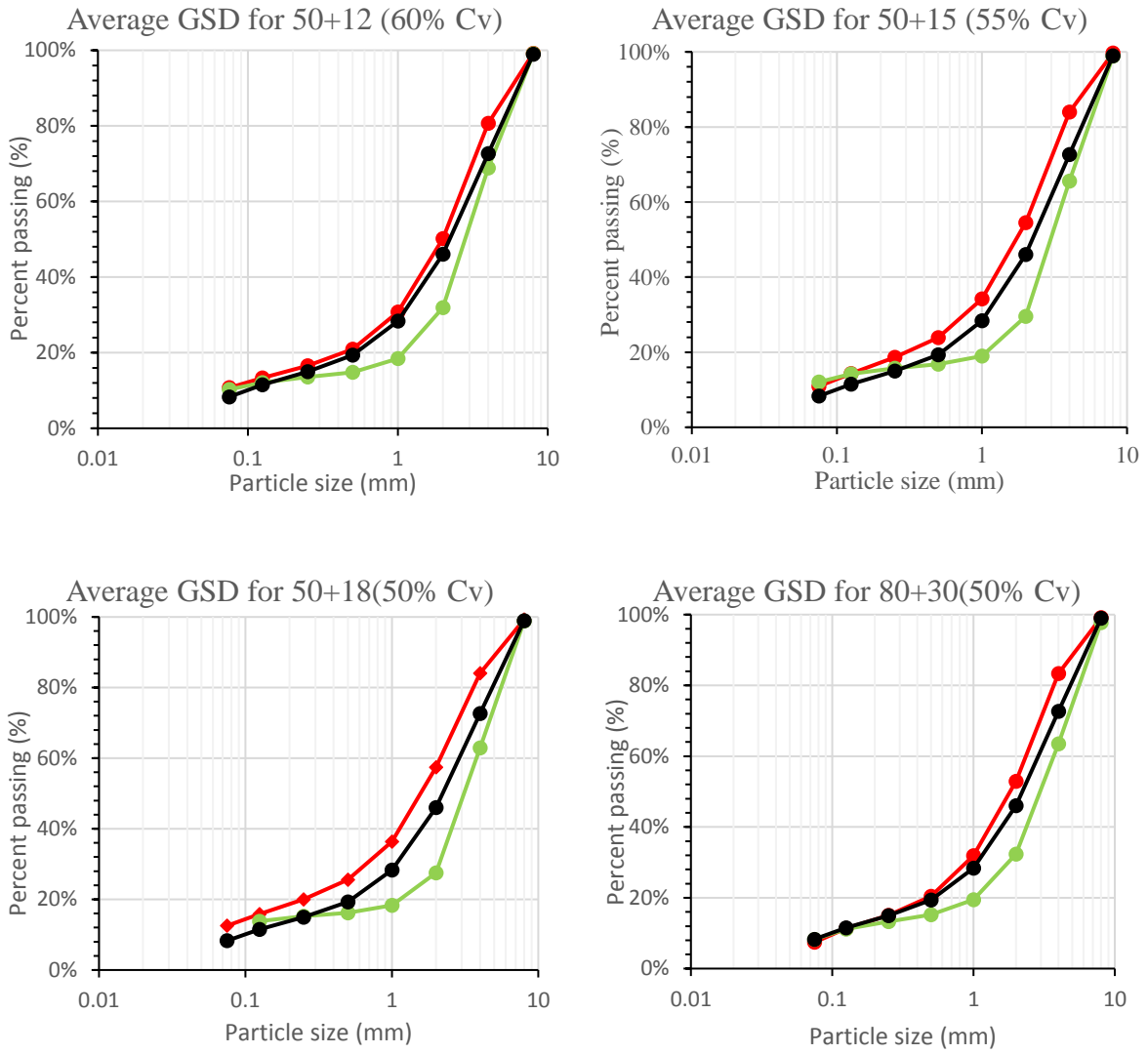
Figure 4-18 Average GSD for the deposition at upstream and downstream of deposition area

4.6   Energy lines

The energy lines have been calculated only for the tests of which the velocity has been calculated. The energy line are shown in Figure 4-19, Figure 4-20, Figure 4-21 and Figure 4-22.

Although the flow height i.e. pressure head contributes to the energy head of the debris flow, as the data of the flow height along the flow path is missing, the velocity head and elevation head is only used for calculating the energy line and their interpretation. It is assumed that the pressure head contributed by flow height is very small in comparison to velocity head and make very little difference in the analysis of the result. Thus, it can be neglected in the interpretation of energy line.
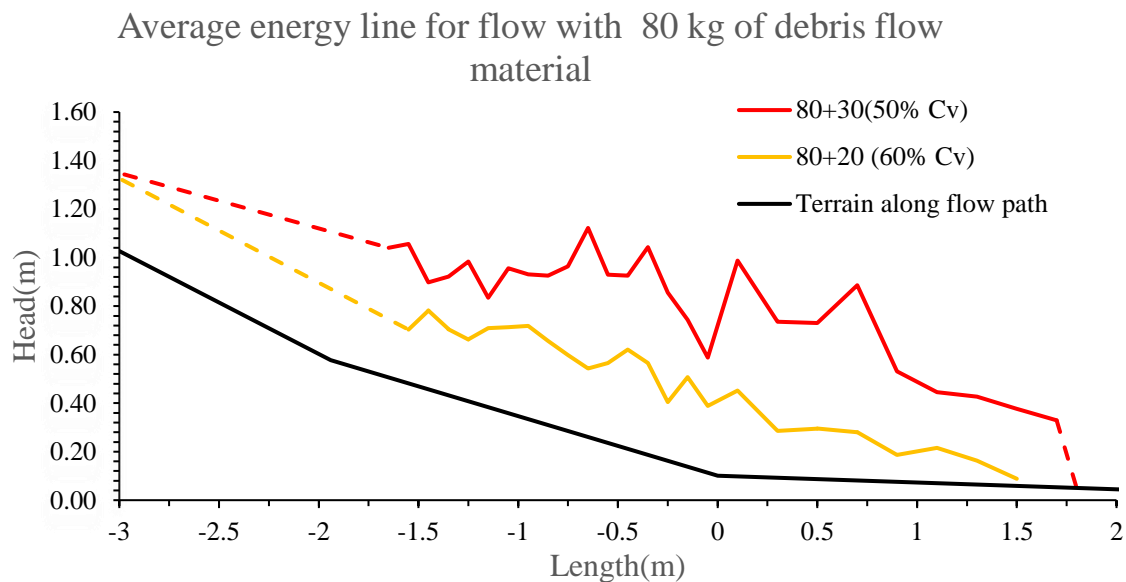
Figure 4-19 Energy line for the debris flow with 80 kg of debris flow material with 60% and 50% concentration

Figure 4-20 Energy line for the debris flow with 50 kg of debris flow material with 55% and 50% concentration

Figure 4-21 Energy line for the debris flow with 45 kg of debris flow material with 60% and 50% concentration

Average energy line for flow with 40 kg of debris flow material
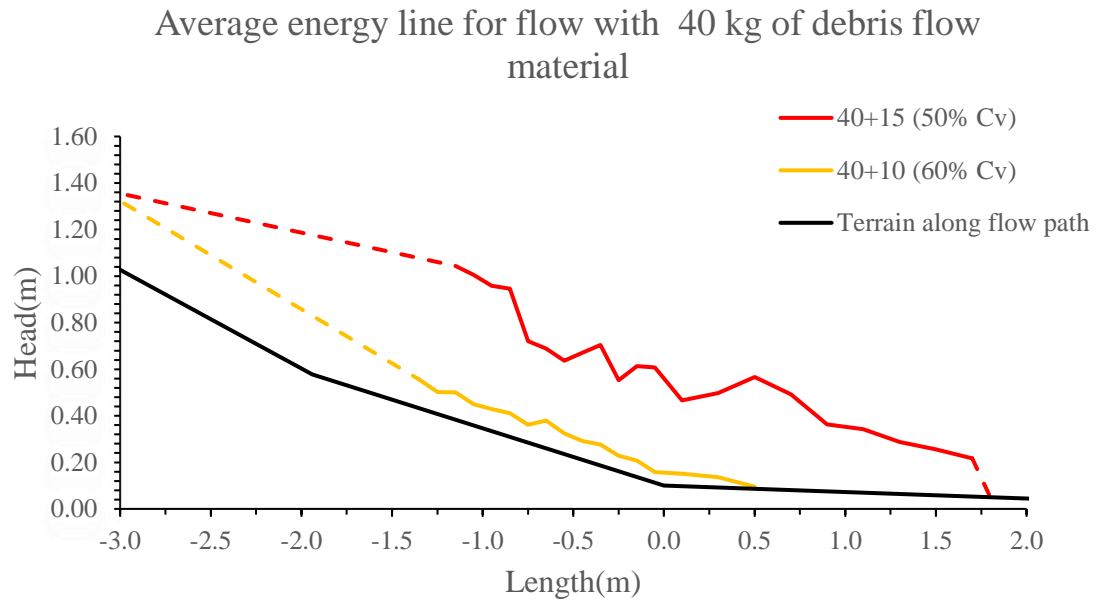
Figure 4-22 Energy line for the debris flow with 40 kg of debris flow material with 60% and 50% concentration

The gradient of the linear trend line of the energy line is given in Table 4-1. The energy line for all the test are shown in APPENDIX D.

Table 4-1 The gradient of linear trend line of the energy line

Test name	Intended concentration (%)	Gradient of linear trend line
40+10	60	0.29
40+15	50	0.27
45+11(f)	60	0.27
45+16.5	50	0.32
50+15	55	0.27
50+18	50	0.25
80+20	60	0.22
80+30	50	0.23

4.7 Impact Force

The force measurement has been done for only two tests: test 45 and test 46 with the mixture of 45 kg of debris flow material and 11 kg of the water. The peak force measured for two tests are 10.01 N and 9.74 N respectively. Figure 4-23 shows the plot of the force for test 45 and test 46 during the flow interval.
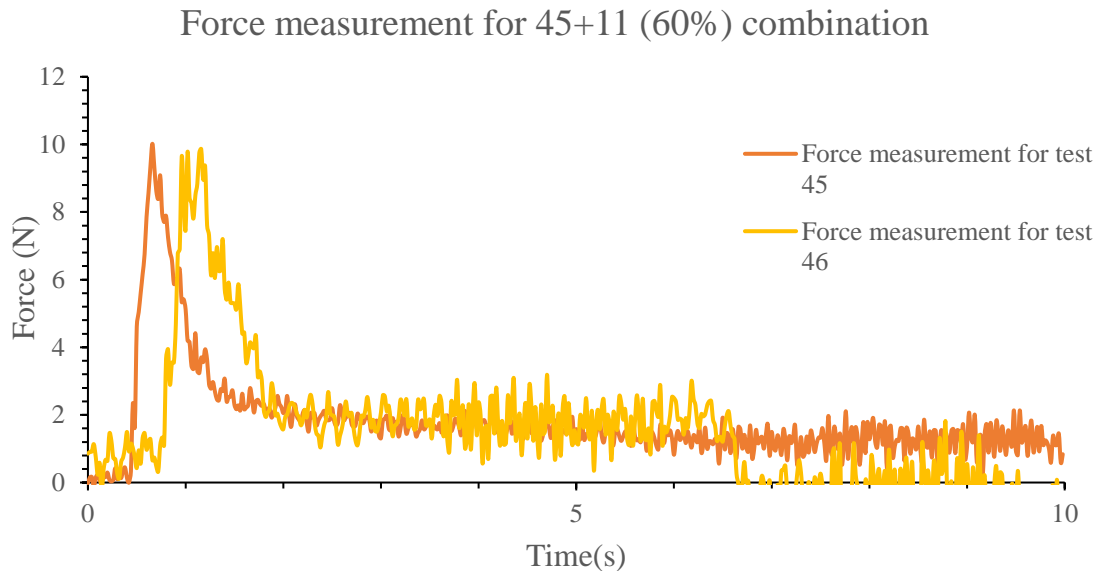
Figure 4-23 Force measurement for test 45 and test 46

This force measurements have been compared using the analytical method presented by Vagnon and Segalini (2016). The maximum flow height in the upstream for the test 45 and 46 is 0.023 m and 0.026 m respectively. The velocity of the flow front at upstream is 2.5 m/s and 2.2 m/s for test 45 and 46 respectively. The density of the debris flow mixture is 1.99 gm/cm^3 and 1.98 gm/cm^3. The diameter of the cylinder is 0.08 m. Therefore, the impact area is $0.08*0.023 = 1.84*10^{-3}$ m^2 for test 45 and $0.08*0.026 = 2.08*10^{-3}$ m^2 for test 46.

The equation in relation to hydro-static method is given as: $F_{peak} = k. \rho_m.g. h_f. A$

The terms are explained in Section 2.6. The back calculation gives the k value as 12 and 9.37 for test 45 and 46 respectively.

Using equation related to hydrodynamic model which is given as: $F_{peak} = \alpha \rho_m v_f^2. A$, the back calculated α value is obtained as 0.45 and 0.49 for test 45 and 46 respectively.

Using another hydrodynamic relation: $F_{peak} = 5 \rho_m v_f^{0.8}. (g.h_f)^{0.6}. A$, the F_{peak} is obtained as 15.6 N and 17.48 N for test 45 and test 46 respectively.

Using mixed model relation given as: $F_{peak} = 0.5 * \rho_m * g * h_f * A + \rho_{m*} v * A$, the F_{peak} is obtained as 9.56 N and 9.82N for test 45 and test 46 respectively.

5 DISCUSSION OF THE RESULTS

The discussion of the results and analysis, based on the objective of the thesis, is presented in this chapter. The discussion has been divided into six sub-chapters: velocity and energy line of the debris flow, runout distance of debris flow and debris slide, flow height of debris flow, deposition height and pattern of debris flow, GSD of the debris flow and impact force of the debris flow.

5.1 Velocity and Energy line

The expected velocity range for the down- scaled model in 1:20 ratio, is obtained in Section 3.2, as 0.11 m/s to 4.47 m/s. The velocity graph in Figure 5-4 shows that minimum velocity of the debris flow front is 0.88 m/s for the test 40+10 (60% Concentration) and the velocity graph in Figure 5-5 shows that maximum velocity of the debris flow front is 4.11 m/s for the test 80+30 (50% Concentration). This verifies the velocity of the debris flow lies within the acceptable range and the results obtained can be used for understanding the natural debris flow event.

As illustrated in Figure 4-3 and Figure 4-4, the debris flow front is changing its shape with time. This shows that the whole flow front is not moving with the same velocity. The change in flow front was mostly seen in case of the flow with high velocity. In the test with low velocity, the flow front which is ahead is seen to follow the center of the flow path throughout the duration of test as shown in Figure 5-1 and Figure 5-2. There is almost no change in the flow front shape and they almost have a curve pattern with very less curvature. So, it can be said that for the flow with the lower velocity, the debris flow front velocity varies insignificantly unlike with the flow with high velocity.
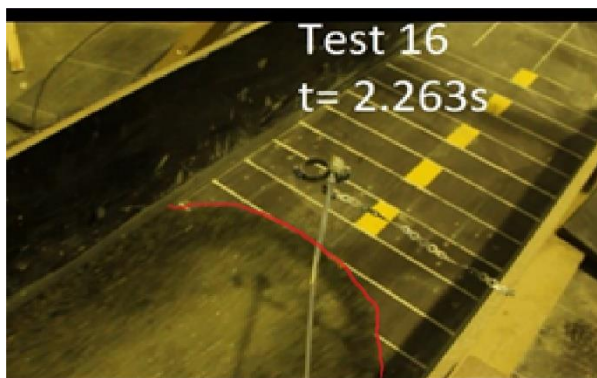
Figure 5-1 Debris flow front for test 16 at time 2.263 s

Figure 5-2 Debris flow front for test 16 at time 2.883 s

As discussed by Christiansen (2013) and Laache (2016) , the debris flow front at the beginning is dry and consists of "frozen masses" as called by Christiansen (2013). The same condition of frozen mass has been observed in the test conducted for this thesis as well. The pattern of formation of the frozen mass and its disappearance differ from one test to another. Despite having same test condition, the frozen mass is seen in one test whereas not seen in another test. Referring to Figure 4-3, Figure 4-4 and Figure 5-3 , even though both test 4 and 5 are conducted using 80 kg of material and 20 kg of water, the frozen mass is seen in test 5 and is not seen in test 4. Moreover, the frozen mass was not seen during the test using small volume of debris flow mixture (test with 40 kg of debris flow material). From this discussion, it can be concluded that the formation of frozen mass depends upon the way of mixing of the material. If the mixing is not properly done and the debris flow material gets sink in the bottom while realizing, then it is probable that the frozen mass is seen during the flow.
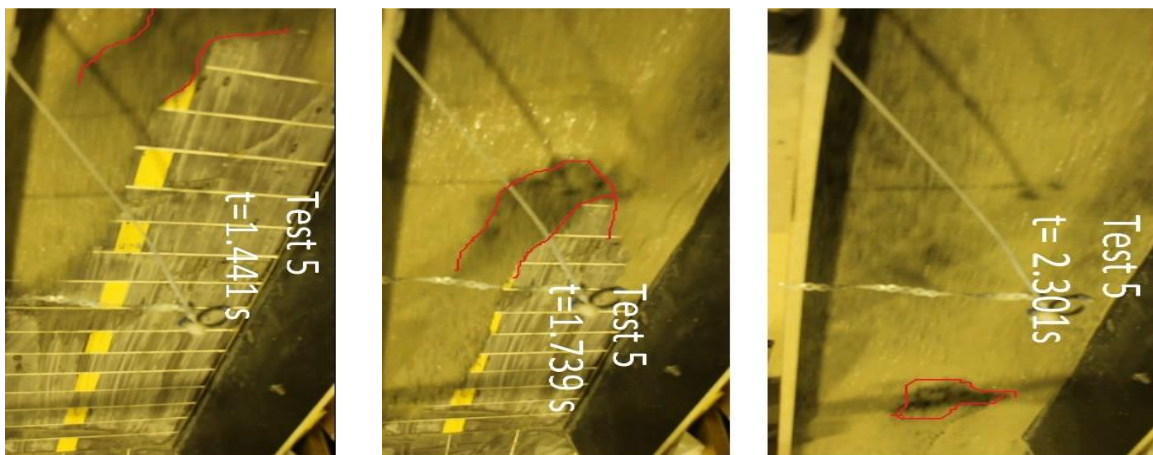
Figure 5-3 Frozen mass seen in test 5

The red line in Figure 5-3 indicates the portion of frozen mass. The frozen mass is seen in the center of the flow path and eventually it is seen to disappear at the bottom of the steep slope. The velocity plot has some sudden peak and the fall which can be because of the pushing effect of the mass behind, which leads the flow front to gain its speed and again slow down. The velocity seems to be decreasing just as the flow passes from the lower slope to the deposition area. The flow changes from supercritical flow to subcritical flow as the flow path changes from sloppy to flat area. Thus, there is generation of hydraulic jump which dissipates most energy in form of heat energy due to its turbulent nature. Moreover, till it reaches the deposition area, there is certain part of kinetic energy that has already been dissipated as heat energy. Hence, this reduces the part of the kinetic energy and the velocity decreases in the deposition area.

Figure 4-5 and Figure 4-8 reveals that when there is change in concentration for given volume of debris flow mixture, the velocity changes significantly for the mixture with lower mass of the debris flow mixture i.e. lower volume of mixture than with higher mass of debris flow mixture i.e. higher volume of mixture. Evidence for this point is that, as concentration increased by 10% from 50% to 60%, for the mixture with 80 kg debris flow material, the velocity decreased by 34% while for the mixture with 40 kg of debris flow material, velocity decreased by 56%. The percentage decrement of velocity for smaller mass of debris flow mixture is very high. This depicts that the effect of change in concentration is comparatively more for lower mass of mixture.
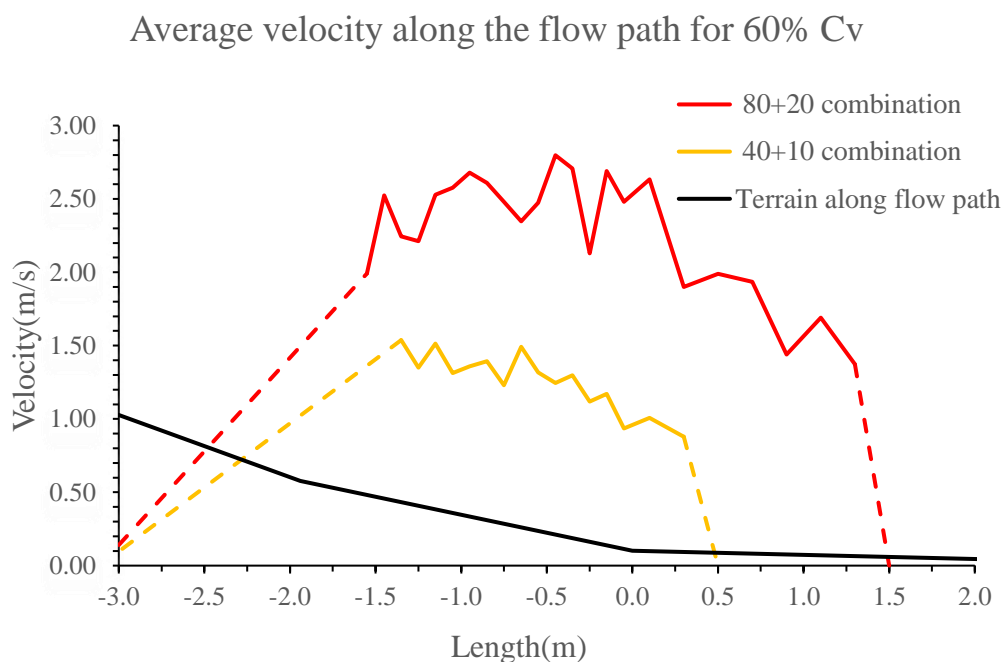
Figure 5-4 Average velocity for the test with 60% concentration

Figure 5-4 shows that reducing the total volume by half from 0.05 m^3 to 0.025 m^3 maintaining same concentration of 60%, the maximum velocity of the debris flow front decreases by 45% whereas for 50% concentration , Figure 5-5 shows that reducing the total volume by half from 0.06 m^3 to 0.03m^3, maintaining the same concentration of 50% , the maximum velocity of the debris flow front decreases only by 14%. The result from Figure 5-4 and Figure 5-5 shows that the effect of change in total volume and total mass of mixture is significant in debris flow mixture with high concentration than for flow with the lower concentration .
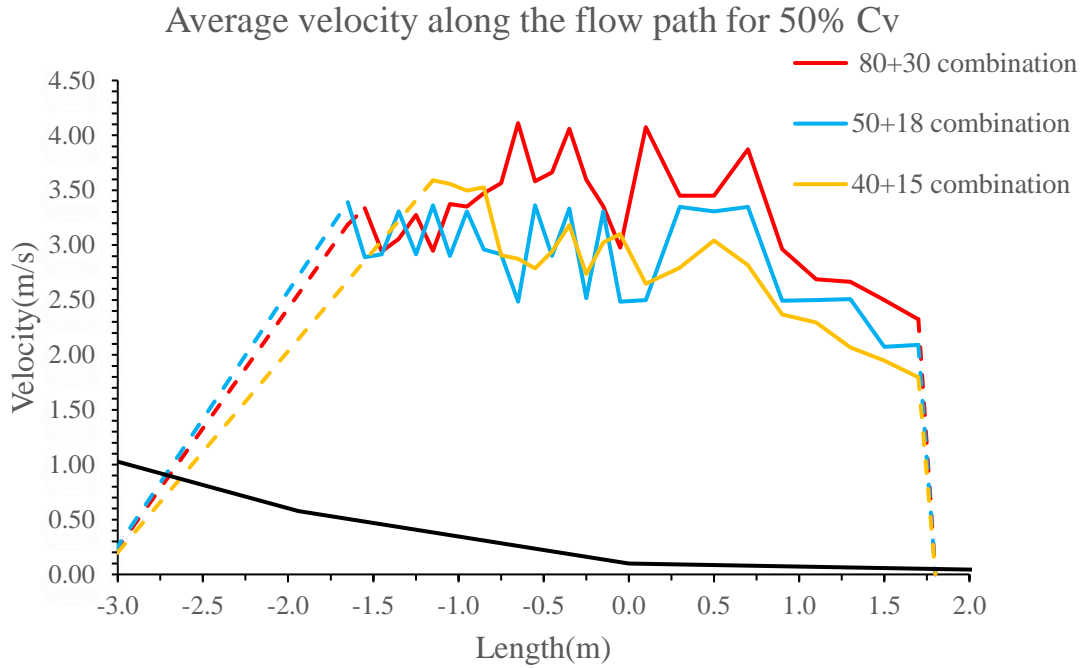
Figure 5-5 Average velocity for the test with 50% Concentration

In an ideal case, for the mass "m" of the debris flow mixture, the conversion of energy from potential energy to kinetic energy is given as

$$mgh = \frac{1}{2}mv_1{}^2 \qquad (5.1)$$

In Equation (5.1), v is the velocity of flow, mgh is the potential energy and $\frac{1}{2}mv^2$ is the kinetic energy. Now when the mass of the mixture is doubled i.e. mass is "2*m" and the height is "β*h". If h_2 is potential height after the volume/mass of mixture doubles, height increment factor "β" is given as: $\beta = \frac{h_2 - h}{h} + 1$. Then, the potential energy and kinetic energy is obtained as Equation (5.2).

$$2 * m * g * \beta * h = \frac{1}{2} * 2 * m * v_2{}^2 \qquad (5.2)$$

In Equation (5.2), the v_2 is the velocity of flow as mass/volumes doubles. The ratio of Equation (5.1) and (5.2) gives Equation (5.3) as:

$$2 * \beta = 2 * \frac{v_2{}^2}{v_1{}^2} \implies v_2 = v_1\sqrt{\beta} \; and \; v_1 = \; v_2/\sqrt{\beta} \qquad (5.3)$$

Decrement in velocity:
$$\frac{v_2 - v_1}{v_2} = \frac{v_1\sqrt{\beta} - v_1}{v_1\sqrt{\beta}} = \frac{\sqrt{\beta} - 1}{\sqrt{\beta}} \qquad (5.4)$$

Equation (5.4) shows that in an ideal case, when there is no any heat energy produced, the velocity change depends only upon the height factor and is equal for same volume/ height of mixture.

However, all potential energy is not converted into kinetic energy and there is always energy dissipation as heat energy due to grain collision and friction between the flow and bed. This dissipation of the energy is more for the high concentrated flow due to the more grain collision as the grains are closer to each other. As the concentration lowers, the intergranular space between grain are occupied by water which prevents the collision of the grain and the energy dissipation as heat energy is mostly due to surges and the friction between the bed and flowing material. Therefore, despite having equal volume and height of the debris flow mixture, in comparison to high concentrated flow, the amount of potential energy converting into kinetic energy is more in case of lower concentrated flow and this resulted in their higher velocity.

The decrement of maximum velocity as volume is reduced by half for flow with lower concentration is 14% (Figure 5-5), which gives the value of height factor "β" as 1.35. This means if the height of the reduced volume is "h" , then the doubled volume has height increment of 35% and height is "1.35*h". From these values, the percentage decrement of the height as total volume gets reduced by half, will be $\frac{1.35h - h}{1.35h} = 26\%$. Suppose that the elevation of the doubled volume of mixture is 1.5 m from the deposition area and if the height gets reduced by 26%, then the height for reduced volume of mixture will be 1.11m i.e. height reduces by 40 cm which is quite reasonable. If is we consider same process of calculation, for 45% decrement of the maximum velocity of higher concentration (Figure 5-4), we get "β" as 3.3. The decrement of height is by 70% which is practically not true. This shows that the ratio of energy dissipated to the potential energy head is more for high concentrated flow with smaller volume of mixture. It can be concluded that the amount of energy dissipated tends to be similar for the high concentrated granular debris flow. While for the granular debris flow with lower concentration, the amount of energy dissipated is governed by the potential head and the ratio between them tends to be almost similar in flow with both high and lower volume. This is the reason behind the high difference in velocity between the flow with lower volume of mixture with varying concentration or between the highly concentrated flow with varying volume of mixture.

The Table 4-1 in Section 4.6 shows that the gradient of the trend line of the energy line goes in decreasing with an increase in volume. This denotes that the loss of energy is gradual as the volume increases. The difference in the gradient of trend line, for 60% concentration as the

volume is doubled, is 7% whereas for 50% concentration, the difference is 4%. This verifies that as the concentration decreases the ratio of amount of energy dissipated to potential head tends to be similar or closer for all volume of mixture.

5.2 Runout

Figure 5-6 shows the trend of runout for the tests with debris slide, which have been conducted only with humid debris flow material. For the coarse debris flow material, the runout increases as the mass of the debris flow material increases and the trend of runout increment is steep. In contrast, the runout of the test with fine material is decreasing as the mass of the material is increasing. But as the trend of decrement is not that significant, it can be considered almost constant.

Debris slide runout of different material
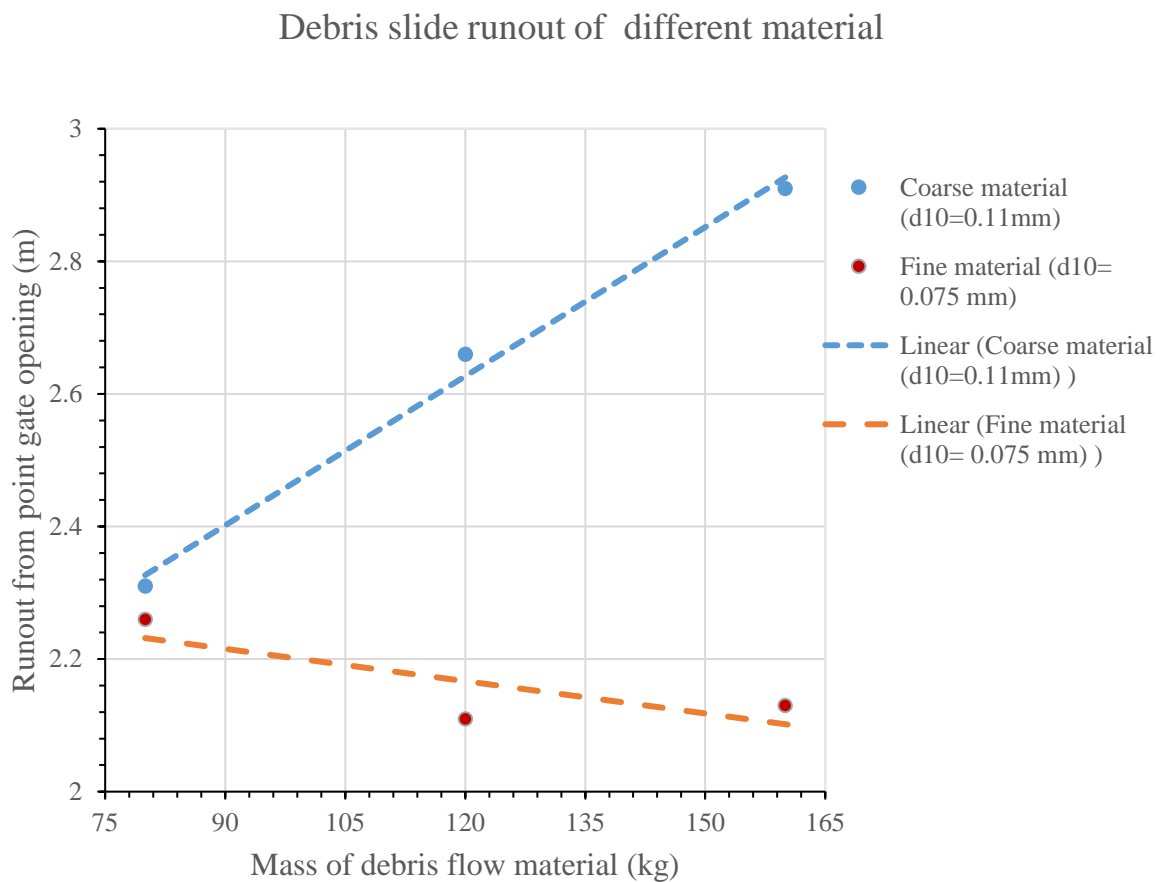
Figure 5-6 Runout for different mass of coarse and fine material

Even though the mass of the debris flow material contributing to slide is taken as 80 kg, 120 kg, 160 kg, the mass is lower than these actual masses of material. This is because in every test, some material is left inside the box. Since, the weight of the material left inside the box is not available for the debris slide tests, it is not certain exactly how much actual weight of debris

flow material is contributing to the slide. In case of fine material, the assumption can be made that comparatively more material is left inside the box than that of coarse material. Thus, the runout may be showing the decreasing trend. Another aspect for this is, the coarse material which has been used for test was sealed in the box and was not exposed to the humid environment unlike the fine material that had been placed open into the humid environment. So, the water content of the fine material is more. It has even more silt content than the coarse particles. According to T. C. Pierson and Scott (1985) , when more amount of silt and /or clay is added into the mixture, the mixture gains the yield strength. The yield stress is dependent on the particle size distribution of mixture as it is generated due to the cohesive forces of fine grained suspensions. As humid fine material has more amount of silt, the cohesive force in the fine material is more than the coarse material which led it to have decreasing trend of runout or almost same trend of runout.

Figure 5-7 shows the plot of the average runout versus average concentration of mixture with 31 kg, 37 kg, and 42 kg mass of debris flow material. The average values are the average of data obtained for the test sets for single test condition. The deviation in concentration is shown by horizontal error-bars and for runout is shown by vertical error-bars. The average plot has been obtained just to see if the plot of average values follows the linear trend of the plot of actual values and it is seen that the average plot follows the linear trend as the actual values.

Figure 5-8 shows the plot of the actual runout as a function of actual concentration and Figure 5-9 shows the plot for actual runout as a function of actual volume of mixture. The actual values are the actual data obtained for the tests. Since, every test is unique with unique concentration and so has the unique runout, the plot with actual values seems more relevant to interpret than the plot with average values. The linear trend line has been drawn to understand the relation between runout, concentration, and total volume.

Even though, every test has unique mass content and concentration, for simplicity and consistency in denotation, the average values of the mass (31 kg, 37 kg, and 42 kg) have been denoted in plot in Figure 5-8 and average value of concentration (57%, 52%, 47%) have been denoted in plot Figure 5-9.
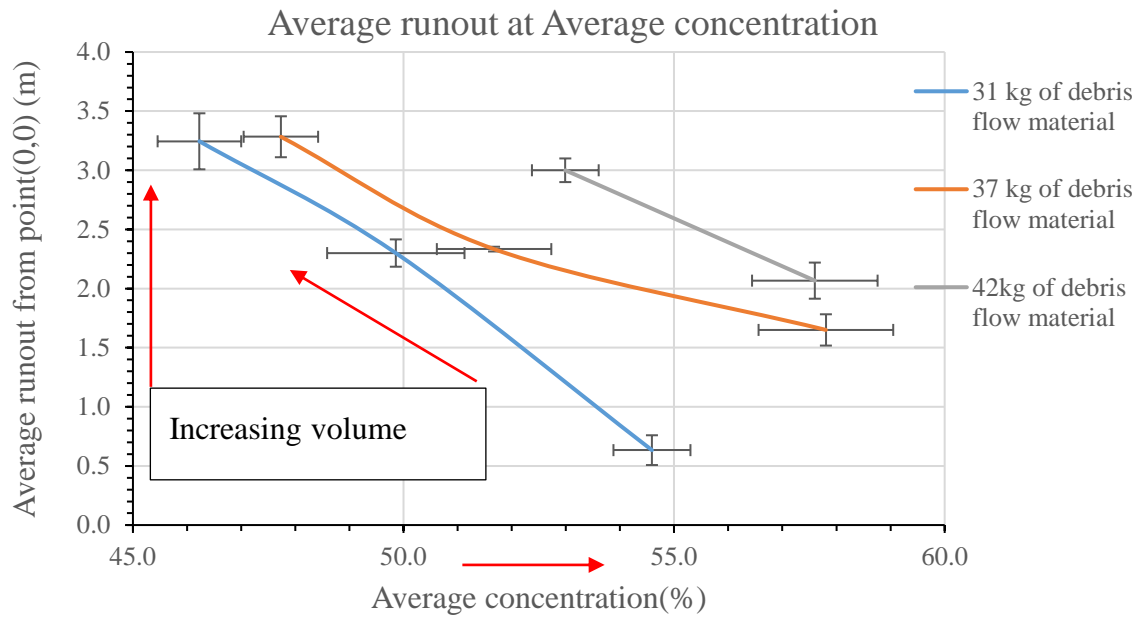
Figure 5-7 Average runout for average concentration of mixture with 31 kg, 37 kg, and 42 kg of debris flow material
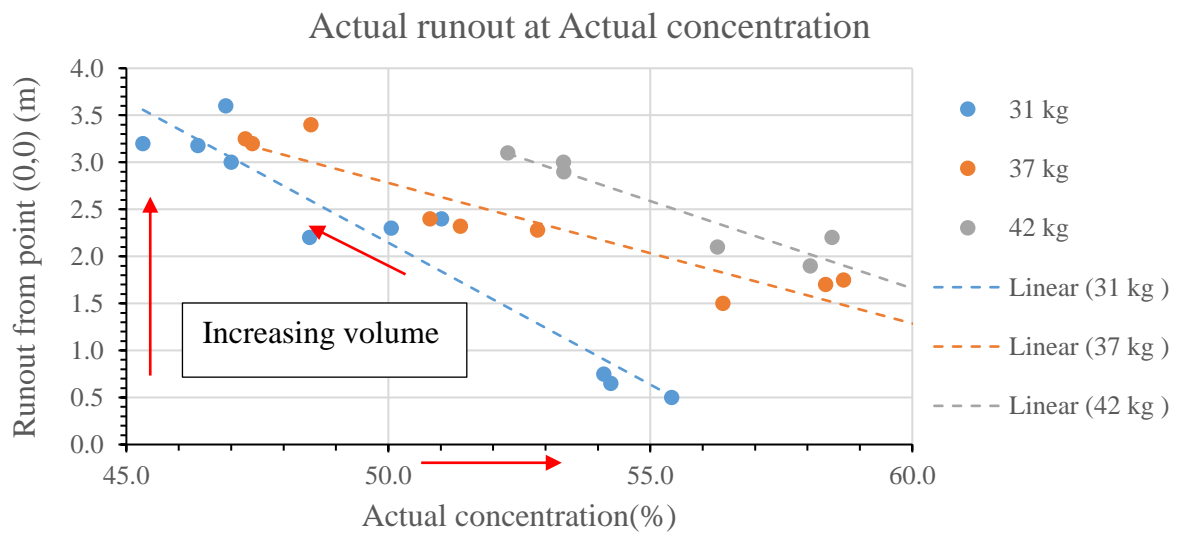
Figure 5-8 Actual runout for actual concentration of mixture with 31 kg, 37 kg, and 42 kg of debris flow material
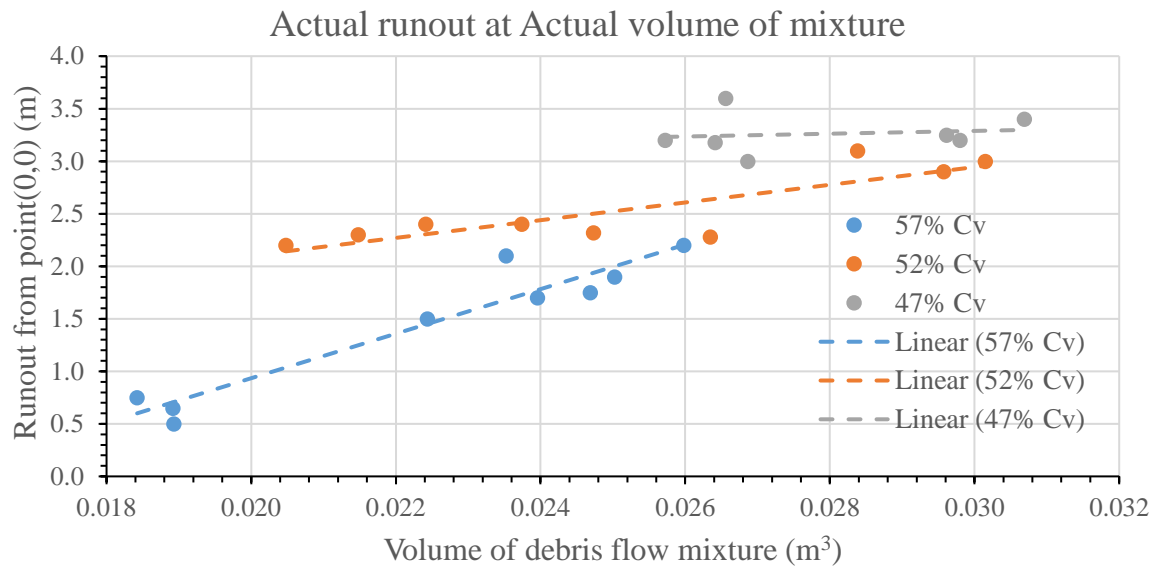
Figure 5-9 Actual runout for actual volume of mixture with 57% concentration, 52% concentration, and 47% concentration

In Figure 5-8 , the higher slope of the runout versus concentration plot shows that the effect of change in concentration in the runout distance is more for the debris flow with smaller mass of the sediment i.e. smaller volume of mixture. Moreover, Figure 5-9 shows that when the total volume of mixture increases, the increase in runout is significant for the higher concentration, unlike for the lower concentration where the increase in runout is moderate. Thus, the effect of volume increment on run-out distance can be observed significantly at same concentration only when the concentration of solids is higher.

Figure 5-8 and Figure 5-9 shows that, at a given volume of mixture, the runout of the debris flow increases as the concentration decreases. This is because when concentration decreases, the yield stress of the debris flow mixture decreases and so does the shear stress of the debris flow which decreases the flow resistance of the mixture. Moreover, as concentration lowers, water fills the inter granular space between grains and the fluidity of the debris flow mixture increases and the intergranular friction between the particles decreases. This leads it to have more runout as the resistant to the flow decreases. As discussed in Section 2.2, one of the stopping mechanism for the debris flow is reduction in the pore pressure created due to fluid mixture of water, fine slit and/or clay and the reduction in the pore pressure helps to gain the internal friction of the debris flow mixture (Costa, 1984). The increase in the water will increase the pore pressure of the mixture during flow. Thus, it will have to flow longer distance to reduce the pore pressure till the level required it to stop. So, the runout increases as the

concentration decreases. However, this effect of change in concentration is observed more in the lower volume of mixture. Discussion presented in Section 5.1 tells that there is high difference in amount of energy dissipated between the flow with different concentration for given smaller volume of mixture, because of which, there is high difference in amount of kinetic energy converted from potential energy between those flows. Another mechanism for stopping debris flow is reducing the internal kinetic energy, that is converted from potential energy, below the level required to maintain the fluid to flow (Calligaris & Zini, 2012). One of the form of reducing kinetic energy is by generating the friction between debris flow and the bed (Takahashi, 2007e) . Thus, the high difference in kinetic energy leads to high difference in requirement of energy dissipation as friction between debris flow and terrain. This demands the need of traveling much farther for the flow to stop in case of the lower concentrated small volume of mixture comparatively to the higher concentrated small volume of mixture. Whereas this difference in the energy dissipation becomes moderate as the total volume increases and thus their difference in the runout length becomes less. Therefore, the effect of change in concentration is prominently seen in smaller volume of mixture than in flow with higher volume of mixture.

Figure 5-8 and Figure 5-9 depicts that, at the given concentration, the runout increases as the total volume of mixture increases. This is simply because as volume of the mixture increases, potential energy increases, which in turn results in increment in kinetic energy. This increase in kinetic energy requires more energy dissipation for debris flow to stop and, therefore leads to high mobility. However, comparatively, the effect of increase in volume is observed distinctly for higher concentrated flow. Same logic as presented in Section 5.1 can be applied in this case as well. The ratio of energy dissipated to the potential energy is high for the smaller volume of densely concentrated flow than for the larger volume of densely concentrated flow. This creates a high difference in the amount of kinetic energy between different volume of densely concentrated flow and therefore there is high difference in the runout length for different volume. This is the reason for more effect seen for the change in total volume in the high concentrated flow.

5.3 Flow height, Deposition height and Deposition pattern

5.3.1 Maximum flow height upstream and downstream

Figure 5-10 shows the plot of the maximum flow height upstream for different mass of debris flow material with varying concentration of mixture. The linear trend line has been drawn to see the relation between concentration and flow height. Since, two plots for 31 kg and 37 kg of debris flow material shows the trend of increasing maximum flow height with increasing concentration, it can be said that the surge height in upstream (transport zone) will be more for highly concentrated flow.
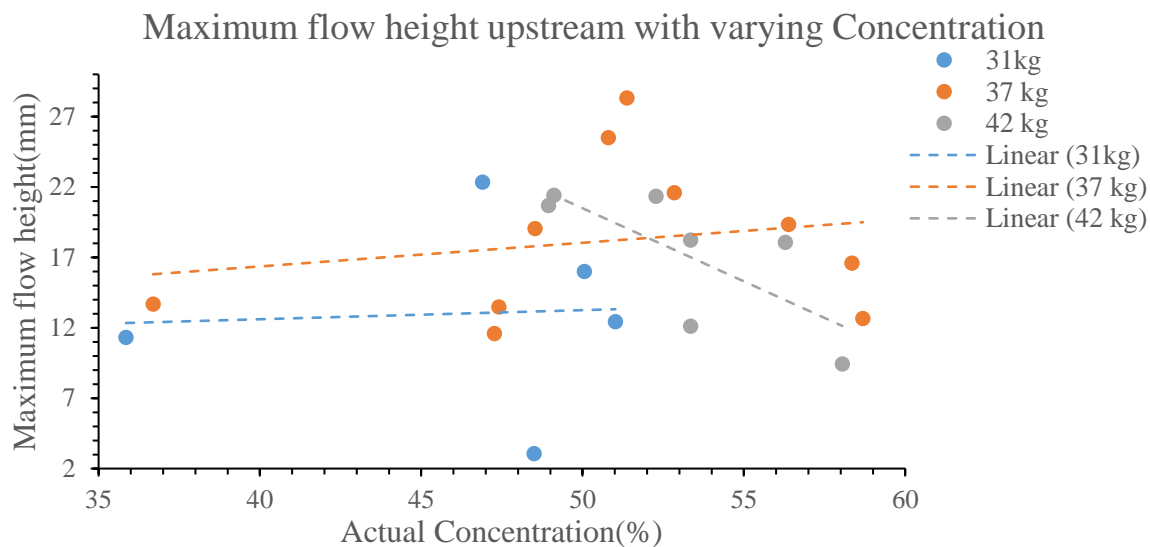
Figure 5-10 Maximum flow height at upstream for different concentration of mixture with 31 kg, 37 kg, and 42 kg of debris flow material.

The plot of the maximum flow height with an increasing volume for different concentration is shown in Figure 5-11. The linear trend line has been used to interpret the graph and to see the relation between total volume and flow height. In all other case, except for the flow with 57% concentration, the maximum flow height shows the increasing trend with an increase in the total volume of the mixture. Thus, it can be inferred that the surge height upstream (transport zone) increases as the total volume of mixtures increases for any given concentration. Figure 5-11 also reveals that the effect of change in concentration is seen more prominent in the flow with higher volume of mixture than for the lower volume of the mixture.

As the concentration increases, the number of particles flowing at a given time increases and thus, the surge will have more height due to the height of the grain particles it carries. When the concentration decreases, the flow behaves more like fluid and the number of particles

flowing at a given time will be less and thus the surge will have less grain particles. This leads it to have lower flow height.
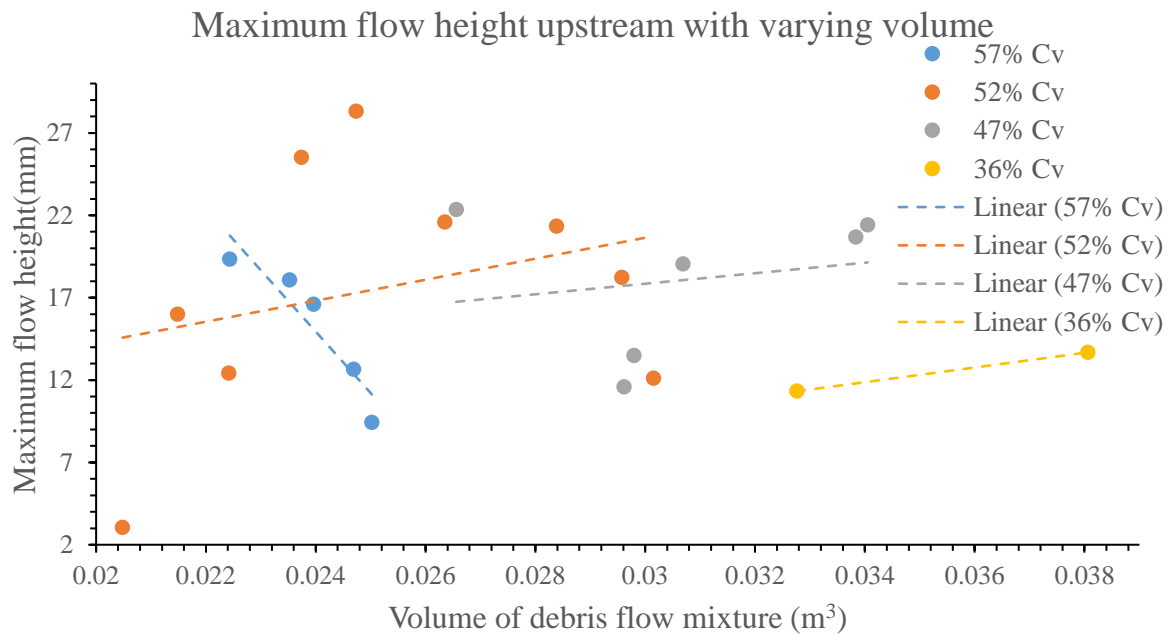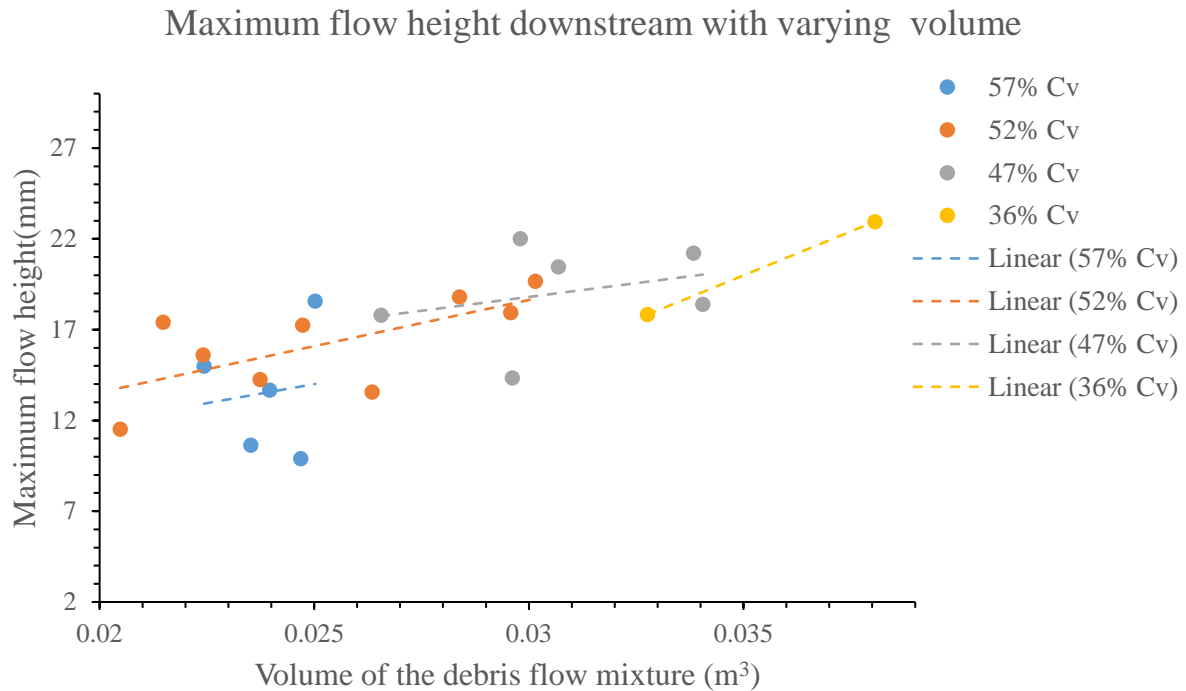

Figure 5-11 Maximum flow height at upstream for varying volume of debris flow mixture with 57% concentration, 52% concentration, 47% concentration and 36% concentration

As the volume of mixture increases, the grain particles it carries at a time will be more. Thus, the surges will have high amount of grain particles at a time which lead it to have a higher maximum flow height. The highest difference between the maximum flow height due to the change in total volume for same concentration is about 7mm (Figure 5-10 and Figure 5-11), which is the largest particle grain size of the mixture. This shows that the rise in flow height due to total volume increment is because of the increase in amount of particle that the flow carries at a given time. Ultimately, any affect in the number of grains flowing at a time will affect the surge height of debris flow in the sloppy terrain or in transport zone.

Figure 5-12 shows the plot of the maximum flow height in the downstream i.e. in the deposition area for varying concentration. The linear trend line has been drawn to interpret the plot. The maximum flow height downstream is found to be decreasing with increase in the concentration. Thus, it can be said that the surge height in beginning of the deposition areas increases as the concentration decreases for a given volume of mixture. The effect of decrease of the concentration in the maximum flow height downstream (deposition area) is seen comparatively more for the mixture with higher volume.
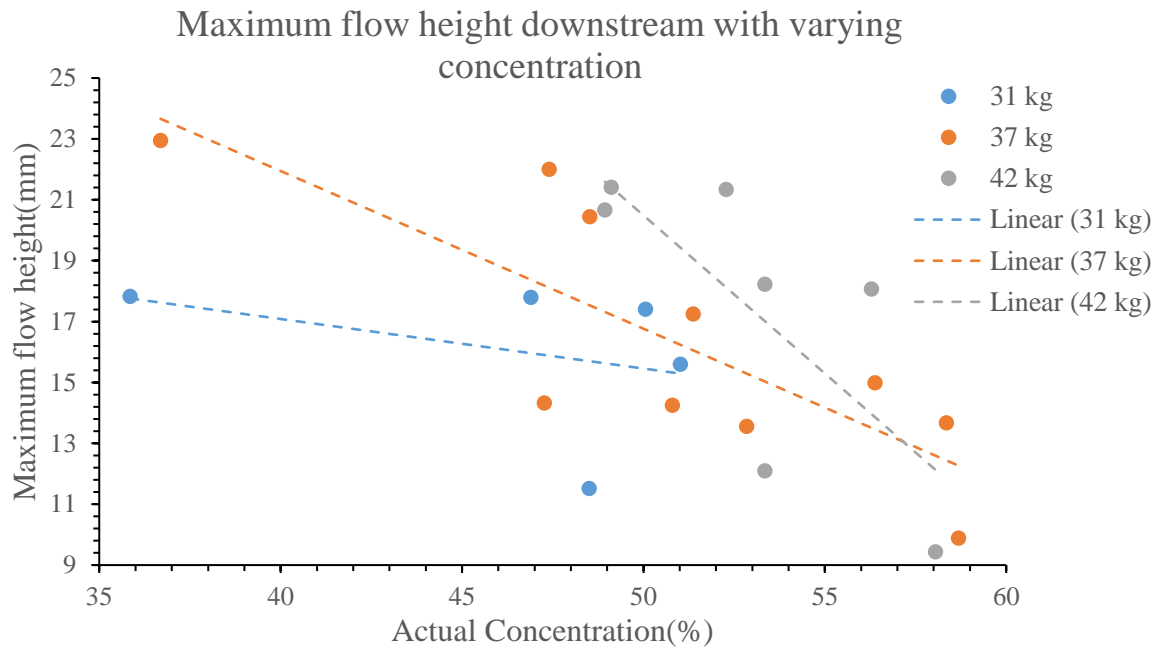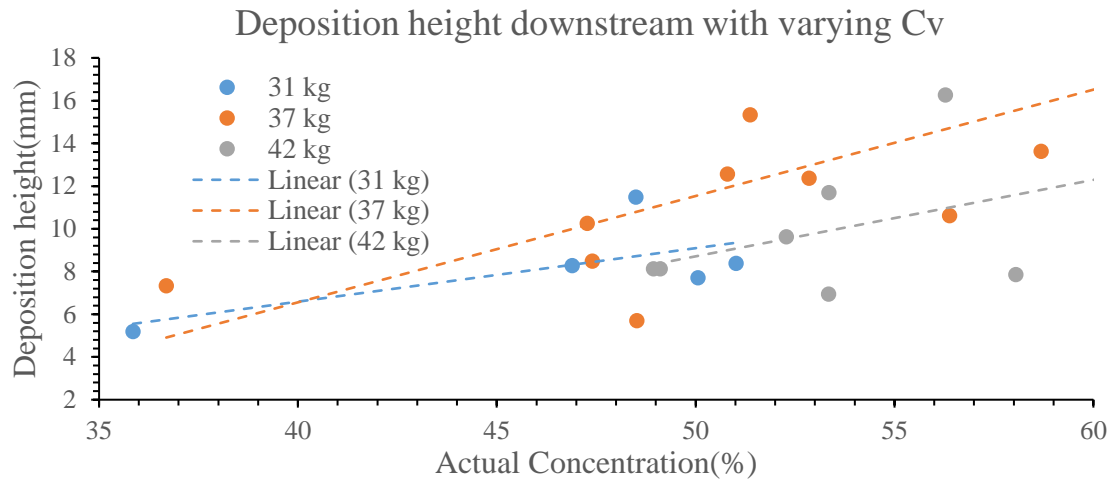
Figure 5-12 Maximum flow height at downstream for different concentration of mixture with 31 kg, 37 kg, and 42 kg of debris flow material.

The plot of the maximum flow height at downstream for increasing volume for different concentration is given in   Figure 5-13. The maximum flow height downstream increases as the volume of mixture increases for a given concentration. It can be thus concluded that the surge height in the beginning of deposition area increases as the total volume of the debris flow increases. The effect in the maximum flow height due to variation in the total volume is prominent for the lower concentration than for higher concentration.

As the debris flow travels from the lower slope to the flat deposition area, it changes its flow regime from supercritical to subcritical flow. This change in flow regime generates the hydraulic jump which is the surge or the flow height. The height of the jump is depended upon the flow velocity in the lower slope. Higher the flow velocity in the lower slope, higher will be the surge height. This is the general mechanism for surge formation in beginning of the depositional area based on the theory of hydraulic jump for fluid flow explained in Chadwick et al. (2013). Likewise, as the concentration decreases and/or total volume increases, the velocity of the flow in lower slope increases. This results in the increasing flow height downstream with decreasing concentration or increasing total volume.
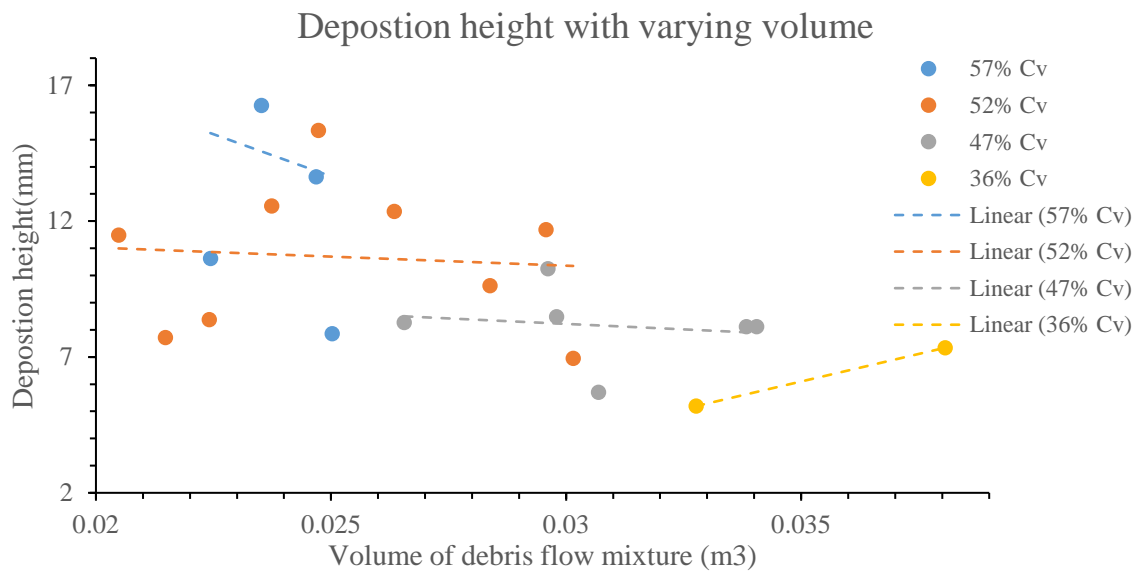
Figure 5-13 Maximum flow height at downstream for varying volume of debris flow mixture with 57% concentration, 52% concentration, 47% concentration and 36% concentration

Even though the total volume of the mixture increases significantly, the flow height downstream doesn't increase much. This is because as the concentration increases, the particles move close due to the cohesive force between the grains, and the number of particles moving at a time is somewhat same independent of the total volume and surge height just varies with few millimeter due to increase in velocity as the total volume increase. However, in case of lower concentration, the particles will move in a dispersive manner. For higher volume of the mixture, the number of particles moving at a time will be more. Thus, the surge consists of high number of particles moving at a given time for the flow with high volume of mixture. Hence, the flow height will be varying significantly for change in total volume. The difference of 7 mm of flow height for 36% concentration (Figure 5-13), which is a maximum size of the coarse particles, verifies that the number of particles moving at time is the determining factor for the surge height.

The debris flow with high volume of mixture gains high velocity with decrease in the concentration because of which it has higher surge height. Thus, the effect of the variation of concentration in flow height downstream (beginning of the deposition area) is more in the flow with high volume of mixture.

The maximum flow height upstream is 17 mm and downstream is 22 mm. The flow height for the down- scaled model as mentioned in Section 3.2 is between 50 mm to 150 mm. Thus, the flow height is lower than the flow height for the actual debris flow event. This might be because of the lower volume of the debris flow mixture used for the test and the wide channel width. Since, the sensor was not available while conducting the test with 80 kg of debris flow material, the data of flow height could not be analyzed for those tests.

5.3.2 Deposition height

The plot of the deposition height for varying concentration of the mixture with 31 kg, 37 kg and 42 kg of the debris flow material is shown in Figure 5-14. Figure 5-15 shows the deposition height for varying volume of debris flow mixture with 57% concentration, 52% concentration, 47% concentration and 36% concentration. The interpretation of relation between deposition height, concentration of mixture and total volume has been done with the help of linear trend line.

From Figure 5-14 and Figure 5-15 , it is observed that the deposition height goes on increasing with increasing concentration. This is because as the concentration increases, the flow height in the downstream decreases and thus, the material swept away is less and the deposition height is more. Another reason could be the highly concentrated flow has more energy is dissipated on the way and this leads it to have smaller coverage of deposition area. Thus, the amount of material accumulated per unit area is more for highly concentrated flow in comparison to lower concentrate flow which ultimately results in the high depositional depth.

For the given total volume of mixture, the deposition height decreased by 2 mm to 5 mm as concentration of the mixture decreased by 5% (Figure 5-15). This decrease in the deposition height is prominent for the lower volume than for the higher volume of the debris flow mixture.

Figure 5-15 shows that for 57% concentration, 52% concentration and 47% concentration, the maximum flow height downstream decreases as the volume of mixture increases. This is because as the total volume increases, the flow height in the downstream increases which leads the flow to wash away the coarser particles farther and reduce the deposition height. However, the effect of decrease in the deposition height due to increase in the volume is not that significant in comparison to the decrease in the deposition height due to decrease in the concentration for any given volume of the debris flow mixture.

Figure 5-14 Deposition height at the downstream for different concentration of mixture with 31 kg, 37 kg, and 42 kg of debris flow material.

Figure 5-15 Deposition height at downstream for varying volume of debris flow mixture of 57% concentration, 52% concentration, 47% concentration and 36% concentration

In contrary, for very low concentration as 36%, the deposition height increases as the volume increases (Figure 5-15). The flow changes its stage from debris flow to hyper-concentrated flow as the water content increases. Thus, the flow mixture acts more like fluid and is not able to take the coarse solid particles in suspension unlike the flow with high concentration. Thus, the coarse solid particles will flow in the bottom and rest in the beginning of deposition area. As the volume increases, the solid particles depositing in the beginning of deposition area is

high. Hence, the deposition height increases as the volume increases in the case of lower concentrated flow.

5.3.3   Deposition pattern

The deposition area is mostly observed as lobate shape for the debris flow tests (Figure 5-17). For a given volume of the debris flow mixture, the width of the middle section of deposition area goes on increasing as the concentration of the mixture decreases. The deposition is seen to have the inverse grading (Figure 5-16) i.e. coarser particles suspended on the top whereas finer particle settling on the bottom until test with 46% concentration. This is due to buoyant forces and dispersive pressures of debris flow (Fisher, 1971). However, as the concentration of the mixture goes very low as 36%, the coarser particles are no more moves suspended on the top and there is no specific segregation pattern seen. This is due to the low material strength of lower concentrated flow (Coussot & Meunier, 1996). Therefore, the deposition pattern is dispersed with both fine and coarse particle mixing together. So, it can be understood that until 46% concentration, flow shows the debris flow behavior, while for the 36% concentration, the deposition pattern no more exhibit inverse grading and thus flow shows behavior of hyper-concentrated flow.

Figure 5-16 shows the inverse grading of the deposition for the "test 24" which is the flow consisting of 27 kg of debris flow material and 11 kg of water and actual concentration as 49%. Figure 5-17 shows the change in deposition pattern for the change in concentration of the mixture. A picture of deposition area for test 16, test 22, test 20 and test 26 are presented in Figure 5-17 as an example to study the effect of concentration in the deposition pattern. The test 16 consists of 29 kg of solid material and 8 kg water with 55% concentration, test 22 consists 29 kg solid material and 11 kg water with 50% concentration, test 20 consists 32 kg solid material and 14 kg water with 45% concentration, test 26 consists 32 kg material and 21 kg water with 36% concentration. The width of the deposition area is increasing as the concentration decreases.

Figure 5-16 Inverse grading of the deposition pattern for test 24 (40+12 combination)
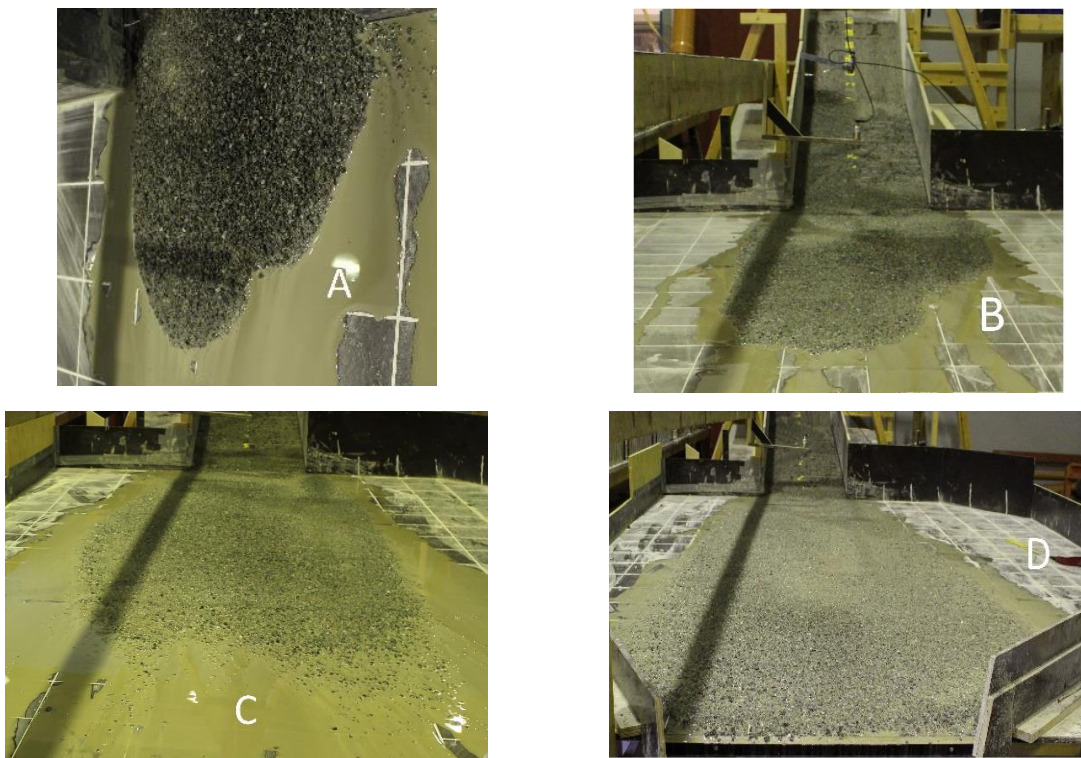
Figure 5-17 Deposition pattern for varying concentration

"A" is for test 16 (55% concentration), "B" is for test 22 (50% concentration), "C" is for test 20 (46% concentration), "D" is for test 26 (36% concentration)

For the debris slide with both coarse material and fine material, the larger particles moved in suspension and the deposition pattern has larger particles on the top layer and finer particles on

the lower layer. Figure 5-18 and Figure 5-19 shows the layering of the deposition section for the debris slide test with coarse material and fine particles. The larger particle is resting on the top whereas the finest particles rest on the bottom layer.
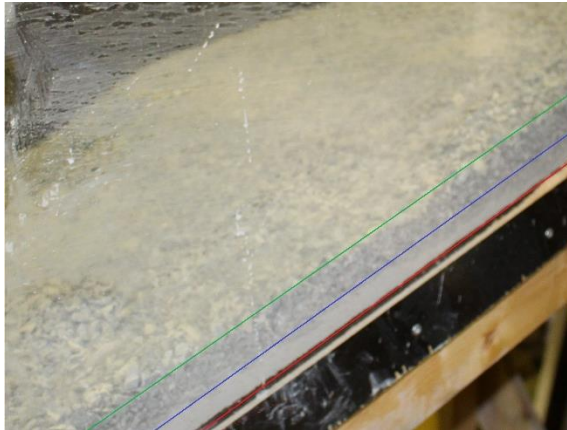
Figure 5-18 Deposition layer for debris slide test with 120 kg of coarse debris flow material
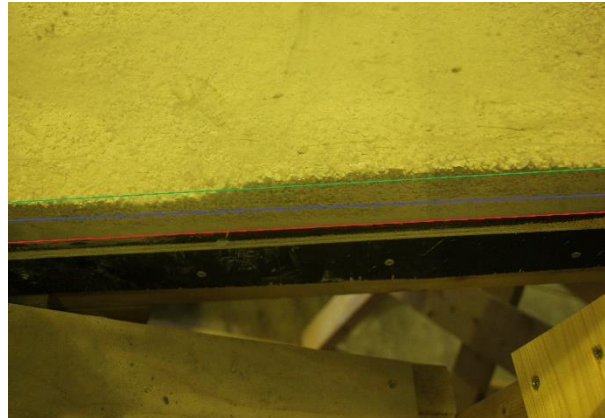
Figure 5-19 Deposition layer for debris slide test with 120 kg of fine debris flow material

In Figure 5-18 and Figure 5-19, the layer of the fine particles is separated by red and blue line and the layer of coarse particle is separated by blue and green line.

5.4 Grain size distribution curve

The GSD curve at beginning, middle and end of deposition area are shown in Figure 5-20, Figure 5-21 and Figure 5-22 respectively for test 35, 36 and 37. The average concentration , material weight and water weight for these tests are 57%, 37 kg and 10 kg respectively.
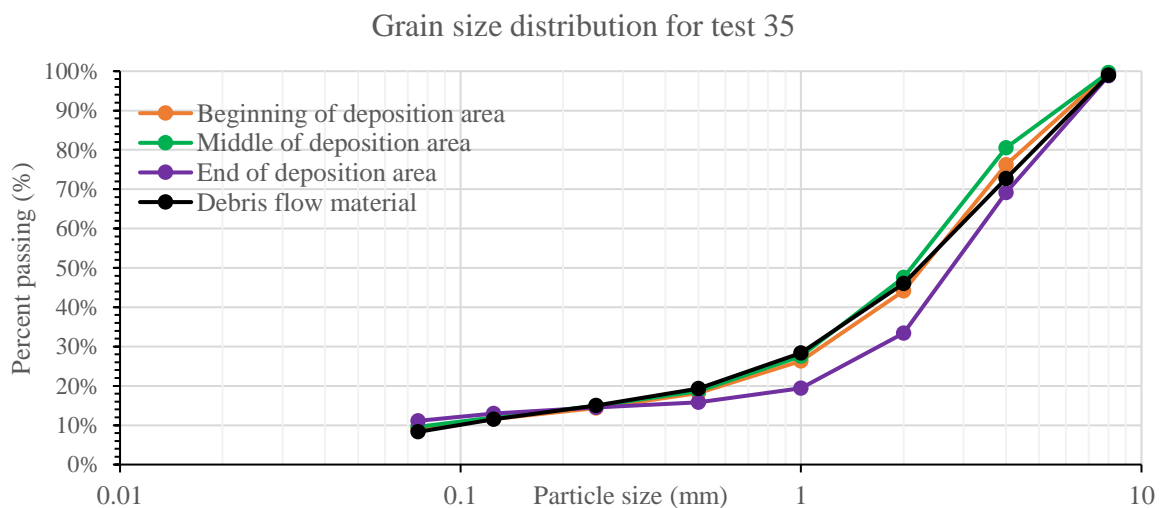
Figure 5-20 GSD curve for debris flow deposition at beginning, middle and end of the deposition area for test 35

Grain size distribution for test 36
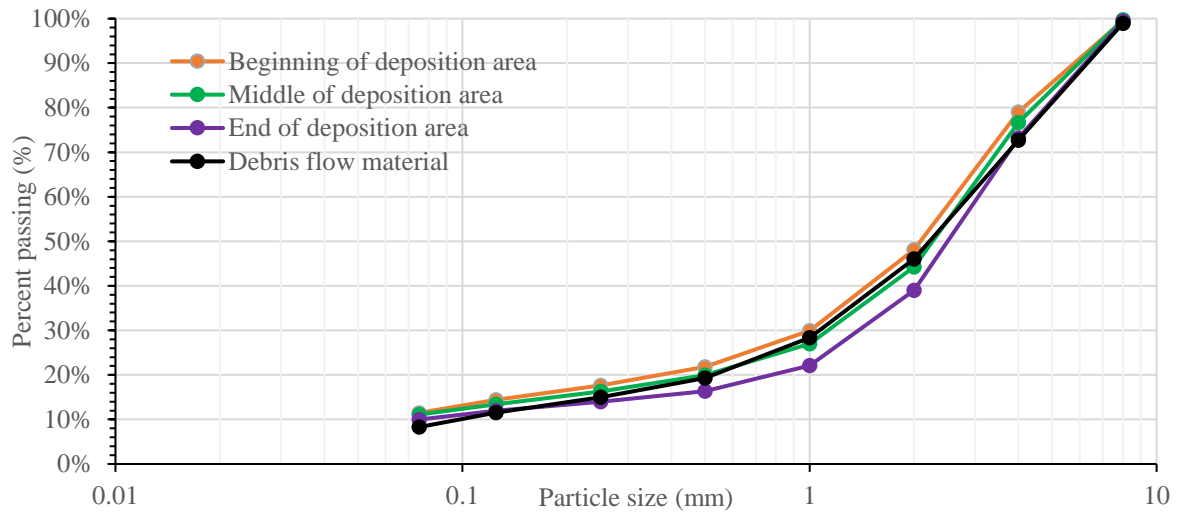
Figure 5-21 GSD curve for debris flow deposition at beginning, middle and end of the deposition area for test 36

Grain size distribution for test 37
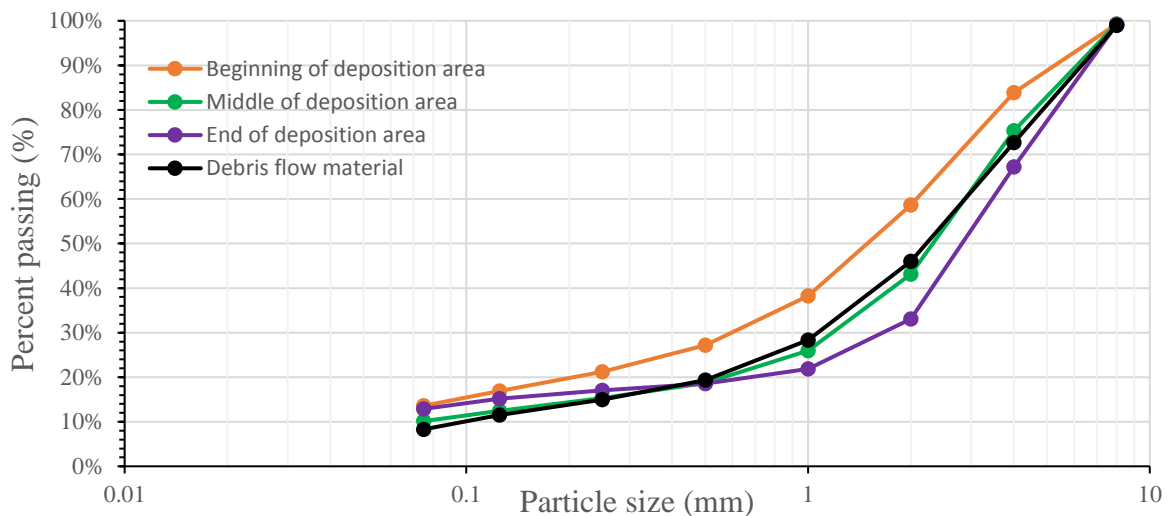
Figure 5-22 GSD curve for debris flow deposition at beginning, middle and end of the deposition area for test 37

Figure 5-20 shows that the GSD in the beginning and middle section of deposition area is similar however, the GSD at the end shows the deposition of coarser particles at the end area.

Figure 5-21 and Figure 5-22 shows that degree of coarseness of the particles goes on increasing from the beginning of the deposition area to the end of the deposition area i.e. the coarser particles gets deposited at the end of the deposition area whereas the fine particles gets deposited at the beginning of the deposition area.
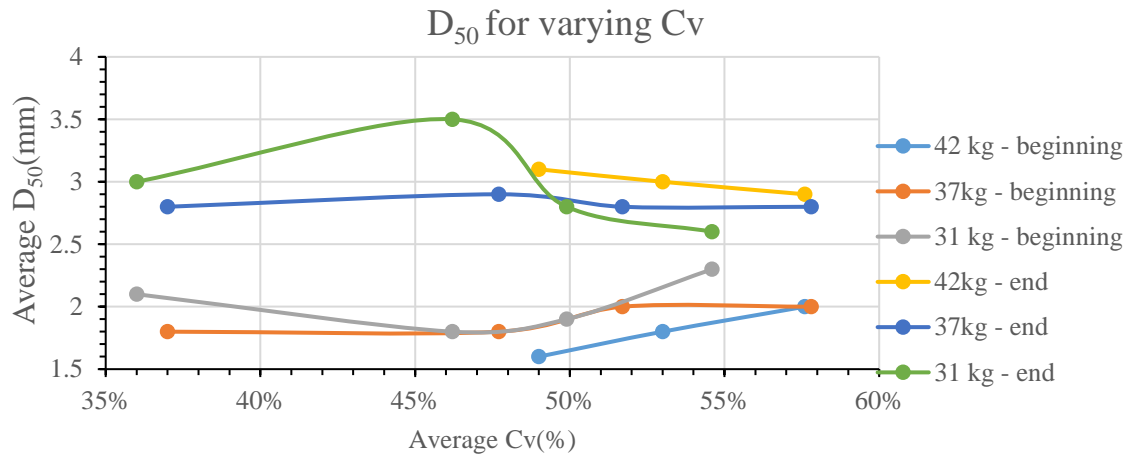
Figure 5-23 D_{50} for the varying concentration of the mixture with 31kg, 37 kg and 42 kg of the debris flow material.

The 50% passing diameter of the particles for varying concentration is given in Figure 5-23. The D_{50} is in the range of 1.6 mm to 2.3 mm for the deposition at the beginning while it is in the range of 2.6 mm to 3.5 mm for the deposition at the end. This also verifies the point that the coarser particles are deposited at the end whereas the finer particles are deposited at the beginning.

From Figure 5-23 it can be observed that with a decrease in concentration until 47% concentration, the D_{50} also goes on decreasing for the deposition of debris flow at the beginning while in contrary, it goes on increasing for the deposition at end. However, further decrease in concentration to 35% shows the increasing trend of D_{50} for the deposition at beginning while it shows decreasing trend for the deposition at end.

Figure 5-23 also shows D_{50} at beginning of deposition area goes on decreasing as the mass of material (i.e. volume of mixture) goes on increasing. While D_{50} at the end of deposition area goes on increasing as mass of material (i.e. volume of mixture) goes on increases until concentration around 47%. However, as the concentration decreases to 36%, the D_{50} at end of deposition area goes on decreasing as the volume of the mixture increases.

The above discussion verifies the theory that the maximum velocity is exhibited on the surface and the velocity goes on decreasing below the surface and is minimum at the bottom of the flow section i.e. at bed on which it flows (Takahashi, 2007a). Since, the density of the coarse particles and fine particles of the mixture are very close, due to the buoyant forces and dispersive pressure, the coarser particle are segregated on the top during the debris flow(Fisher, 1971). Due to the high velocity on the surface, the coarser particles are swept away to the end

of the deposition area leaving behind the fine particles which travels at the bottom during the flow. This gives the trend of increase of coarse particles and D_{50} from beginning of deposition area to end of deposition area. Figure 5-20, Figure 5-21 and Figure 5-22 are the result of this phenomena. Similarly, as the concentration is decreased, the velocity of debris flow increases and so does the surface velocity of the flow. As a result, more coarser particles are swept away till the end of deposition area and leaving behind more fines. Thus, for a given volume of mixture, D_{50} goes on decreasing as concentration decreases at beginning of deposition area, and its vice versa at the end. Similarly, for a given concentration, as the total volume increases, the velocity of flow increase, and so does the surface velocity of flow increases. Thus, the same phenomena result and for increasing volume of mixture, D_{50} at beginning decreases and at end its vice versa.

However, as the concentration decreases to critical value, it is no more debris flow and becomes hyper-concentrated flow where the coarser particles no more flow in suspension due to decrease in the material strength (Coussot & Meunier, 1996). Thus, the coarser particles will fall, stay close to bottom, and settles just as it reaches the deposition area. Hence the finer particles are swept away till the end unlike in debris flow. Thus, as the concentration is lowered to 36%, the D_{50} at the beginning goes on increases and D_{50} at end goes on decreases.

5.5 Impact Force

The magnitude of force measured during the experiment as given in Section 4.7 , is close to the magnitude of the force given by the two-analytical approach, one using hydrodynamic method derived from momentum balance of thrust and another using mixed method. The most fitting formulation for the force measurement is for the mixed method as it does not have any varying coefficient and is based solely on all the flow parameters. The value of coefficient α given in hydrodynamic method fits best for the range given by Bugnion et al. (2012). K value for the hydrostatic approach is out of the range for test 45 whereas almost at the extreme of the given range for test 46. Thus, the mixed method and hydrodynamic method based on momentum balance resembles best for the magnitude of force measured.

From Section 3.2, the dynamic similitude of debris flow gives the magnitude of impact force of natural debris flow event as 8000 times the impact force of debris flow from physical model. Thus, for the test 45 and 46, the magnitude of the natural debris flow is 80 kN and 77.92 kN respectively. This magnitude of the force is very high and can cause huge damage to life and property of people.

6 CONCLUSION AND RECOMMENDATION

The conclusions addressing the objective in Chapter 1 and recommendations for the further work are presented in this chapter.

6.1 Conclusions

The process of debris flow and its mechanism has been understood through debris flow modelling. The evaluation of the debris flow with respect to natural debris flow has been done based on the velocity of the debris flow and the flow height. The velocity of the debris flow front shows that the debris flow test is realistic and the results could be simulated to actual debris flow phenomena. However, the flow height is very low compared to the flow height of the natural debris flow event. Following conclusion can be drawn from the study conducted for this thesis.

1. The effect on velocity due to change in concentration is more in smaller volume of debris flow. The effect on velocity due to change in total volume is more for the higher concentrated mixtures in comparison to lower concentrated mixture.

2. The gradient of the linear trend line of energy head goes on decreasing as the total volume increases for the given concentration. The energy dissipation is rapid for the lower volume of mixture for given concentration.

3. In comparison to debris slide with fine material, the runout length of the debris slide with coarse material increases significantly with the increase in the mass of debris flow material.

4. The runout length of the debris flow increases with increase in total volume and it is more significantly for highly concentrated mixture. Likewise, the runout length of the debris flow increases with decreasing concentration and it is more significantly for smaller volume of mixture.

5. The surge height upstream (transport zone) increases as concentration increases for the given total volume or as volume of debris flow mixture increases for given concentration. The surge height downstream (deposition area) increases as concentration decreases for the given total volume or as volume of debris flow mixture increases for given concentration. The effect of change in concentration on the flow height upstream and downstream is significant for the flow with higher volume of mixture.

6. The deposition height of debris flow increases as concentration increases for the given volume of mixture or as volume of mixture decreases for given concentration. For lower concentration, as 36% which is hyper-concentrated flow, the deposition height increases as the total volume increases.

7. The deposition area of debris flow and debris slide exhibits inverse grading of particle while deposition area of hyper-concentrated flow shows no specific grading. The wide of the deposition area increases as the concentration decreases.

8. The degree of coarseness of the particles goes on increasing from the beginning to the end of deposition area of debris flow. The degree of coarseness of the particles in the end of deposition area increases as the concentration decreases for the given volume of mixture or as the volume of mixture increases for given concentration. It is just vice versa for the deposits at beginning of deposition area. For the hyper-concentrated flow, as the concentration decreases, the degree if coarseness of the particles in beginning of deposition area increases while coarseness at the end decreases.

9. The mixed method of both hydrostatic method and hydro-dynamic method is more reliable for impact force measurement of debris flow.

In overall, the research work for this thesis supports the existing theory of debris flow. Therefore, the results obtained in this thesis can be used to calibrate the numerical model for debris flow.

6.2 Recommendation for further work

Some material was left inside the box for every test, because of which actual concentration deviated from the intended concentration. There was inconsistency of the mass of material, mass of water and concentration between tests of each test sets. This created difficulty in analysis and interpretation of the results. Moreover, the frozen material was seen during the flow in some cases while not in other cases. This depicts that the improve mixing and releasing technique can reduce these frozen materials. So, the proper mixing of the material and release mechanism is recommended.

The velocity has been calculated manually using the video frames. The 50 fps of the video seems insufficient to calculate high velocity as for lower concentrated mixtures. Therefore, the video cameras with high fps is recommended.

The results obtained are based on single material type only. So, the test with other material type is recommended to verify the results obtained.

The higher runout length for lower concentration for given total volume is due to the increase in pore pressure of the flow. However, the pore pressure measurement is lacking in the instrumentation of the model. Thus, the pore pressure measurement is recommended to verify this.

The numerical simulation using existing tools are recommended to see the variation in the results from physical modeling and the numerical modeling.

7 REFERENCES

Bagnold, R. (1968). Deposition in the process of hydraulic transport. *Sedimentology, 10*(1), 45-56.

Bagnold, R. A. (1954). *Experiments on a gravity-free dispersion of large solid spheres in a Newtonian fluid under shear.* Paper presented at the Proceedings of the Royal Society of London A: Mathematical, Physical and Engineering Sciences.

Boniello, M., Calligaris, C., Lapasin, R., & Zini, L. (2010). Rheological investigation and simulation of a debris-flow event in the Fella watershed. *Natural Hazards and Earth System Sciences, 10*(5), 989.

Bugnion, L., McArdell, B. W., Bartelt, P., & Wendeler, C. (2012). Measurements of hillslope debris flow impact pressure on obstacles. *Landslides, 9*(2), 179-187.

Calligaris, C., & Zini, L. (2012). *Debris Flow Phenomena: A Short Overview?* : INTECH Open Access Publisher.

Canelli, L., Ferrero, A., Migliazza, M., & Segalini, A. (2012). Debris flow risk mitigation by the means of rigid and flexible barriers-experimental tests and impact analysis. *Natural Hazards and Earth System Sciences, 12*(5), 1693.

Chadwick, A., Morfett, J., & Borthwick, M. (2013). *Hydraulics in civil and environmental engineering*: Crc Press.

Christiansen, L. F. (2013). *Flomskred: Litteraturstudie og modellforsøk med voller som sikringstiltak.* Institutt for bygg, anlegg og transport.

Costa, J. E. (1984). Physical geomorphology of debris flows *Developments and applications of geomorphology* (pp. 268-317): Springer.

Coussot, P., & Meunier, M. (1996). Recognition, classification and mechanical description of debris flows. *Earth-Science Reviews, 40*(3), 209-227.

Crowe, C. T., Elger, D. F., Williams, B. C., & Roberson, J. A. (2009a). Dimensional analysis and similitude *Engineering fluid mechanics* (pp. 249-273): John Wiley & Sons, Inc.

Crowe, C. T., Elger, D. F., Williams, B. C., & Roberson, J. A. (2009b). The energy equation *Engineering fluid mechanics* (pp. 217-236): John Wiley & Sons, Inc.

Cruden, D., & Varnes, D. (1996). Landslide type and processes, in eds. AK Turner, RL Schuster: Landslides investigation and mitigation, Special Report 247. *Transportation Research Board, National Research Council, National Academy Press, Washington DC*.

Cui, P., Zeng, C., & Lei, Y. (2015). Experimental analysis on the impact force of viscous debris flow. *Earth Surface Processes and Landforms, 40*(12), 1644-1655.

Fisher, R. V. (1971). Features of coarse-grained, high-concentration fluids and their deposits. *Journal of Sedimentary Research, 41*(4).

Fiskum, E. (2012). Flomskred: Testing av ulike sikringstiltak i modellforsøk: Institutt for bygg, anlegg og transport.

Frekhaug, M. H. (2015). *An assessment of prediction tools to Norwegian debris flows.* NTNU.

Håndbok 014: Laboratorieundersøkelser. (2005). Retrieved from Oslo:

. Håndbok v139: Flom- og sørpeskred. (2014). Oslo: Statens Vegvesen.

Heller, P., & Jenssen, L. (2009). *Modellforsøk med flomskred mot bruer : virkning av bruåpning og ledevoller* Teknologi-rapport (online), Vol. nr. 2582.

Huebl, J., & Holzinger, G. Kleinmassstaebliche Modellversuche

zur Wirkung von Murbrechern,.

Hungr, O. (1995). A model for the runout analysis of rapid flow slides, debris flows, and avalanches. *Canadian Geotechnical Journal, 32*(4), 610-623.

Hungr, O., Evans, S., Bovis, M., & Hutchinson, J. (2001). A review of the classification of landslides of the flow type. *Environmental & Engineering Geoscience, 7*(3), 221-238.

Hungr, O., McDougall, S., & Bovis, M. (2005). Entrainment of material by debris flows *Debris-flow hazards and related phenomena* (pp. 135-158): Springer.

Hungr, O., Morgan, G., & Kellerhals, R. (1984). Quantitative analysis of debris torrent hazards for design of remedial measures. *Canadian Geotechnical Journal, 21*(4), 663-677.

Hussin, H. Y. (2011). *Probabilistic run-out modeling of a debris flow in Barcelonnette, France.* M. Sc. thesis, Faculty of Geo-Information Science and Earth Observation (ITC), University of Twente, Enschede, Netherlands, 94 pp.

Hutter, K., Svendsen, B., & Rickenmann, D. (1994). Debris flow modeling: A review. *Continuum Mechanics and Thermodynamics, 8*(1), 1-35. doi:10.1007/bf01175749

Iverson, R. M. (1997). The physics of debris flows. *Reviews of geophysics, 35*(3), 245-296.

Iverson, R. M., Reid, M. E., Logan, M., LaHusen, R. G., Godt, J. W., & Griswold, J. P. (2011). Positive feedback and momentum growth during debris-flow entrainment of wet bed sediment. *Nature Geoscience, 4*(2), 116-121.

Jaedicke, C., Lied, K., & Kronholm, K. (2009). Integrated database for rapid mass movements in Norway. *Natural Hazards and Earth System Sciences, 9*(2), 469-479.

Jakob, M., & Hungr, O. (2005). Introduction *Debris-flow Hazards and Related Phenomena* (pp. 1-7): Springer Berlin Heidelberg.

Johnson, A., & Rodine, J. (1984). Debris flow, Slope Instability D. Brunsden, DB Prior, 257–361: John Wiley, New York.

Laache, E. (2016). *Model Testing of the Drainage Screen Type Debris Flow Breaker.* NTNU.

Major, J. J. (1997). Depositional processes in large-scale debris-flow experiments. *The Journal of Geology, 105*(3), 345-366.

Mangeney, A., Roche, O., Hungr, O., Mangold, N., Faccanoni, G., & Lucas, A. (2010). Erosion and mobility in granular collapse over sloping beds. *Journal of Geophysical Research: Earth Surface, 115*(F3).

Nemec, W., & Postma, G. (1991). *Inverse grading in gravel beds.* Paper presented at the Abstracts IAS 12th Regional Meeting, International Association of Sedimentologists.

Nettleton, I., Martin, S., Hencher, S., & Moore, R. (2005). Debris flow types and mechanisms. *Scottish Road Network Landslides Study*, 45-67.

Pierson, T. (1986). Flow behavior of channelized debris flows Mount St. Helens Washington. *Hillslope processes*, 269-296.

Pierson, T. C. (2005). Hyperconcentrated flow—transitional process between water flow and debris flow *Debris-flow hazards and related phenomena* (pp. 159-202): Springer.

Pierson, T. C., & Scott, K. M. (1985). Downstream dilution of a lahar: transition from debris flow to hyperconcentrated streamflow. *Water resources research, 21*(10), 1511-1524.

Prochaska, A. B., Santi, P. M., Higgins, J. D., & Cannon, S. H. (2008). A study of methods to estimate debris flow velocity. *Landslides, 5*(4), 431-444. doi:10.1007/s10346-008-0137-0

Sandven, R., Senneset, K., Emdal, A., Nordal, S., Janbu, N., Grande, L., & Amundsen, H. A. (2014). *Geotechnics Field and Laboratory Investigations*. Trondheim: Geotechnical Division, NTNU.

Sassa, K., Fukuoka, H., Wang, G., & Wang, F. (2007). Undrained stress-controlled dynamic-loading ring-shear test to simulate initiation and post-failure motion of landslides *Progress in landslide science* (pp. 81-98): Springer.

Sassa, K., & hui Wang, G. (2005). Mechanism of landslide-triggered debris flows: Liquefaction phenomena due to the undrained loading of torrent deposits *Debris-flow hazards and related phenomena* (pp. 81-104): Springer.

Sassa, K., Kaibori, M., & Kitera, N. (1985). *Liquefaction and undrained shear of torrent deposits as the cause of debris flows.* Paper presented at the Proceedings International Symposium on Erosion, Debris Flows and Disaster Prevention.

Sherchan, B. (2016). *Entrainment of Bed Sediments by Debris Flow*. NTNU.

Skilodimou, H. D., & Bathrellos, G. D. Debris flow: categories, characteristics, hazard assessment, mitigation measures.

Solids and Slurries - Definition of Terms. Retrieved from http://www.mrsbme.com/library/articles/goulds/liquids/solids.pdf

Stiny, J. (1910). Die Muren [Debris flows]. *Wagnerschen Univ., Buchhandlung, Innsbruck, Austria.[English translation, EBA Consult., Vancouver, Canada, 1997.].*

Takahashi, T. (1981). Debris flow. *Annual review of fluid mechanics, 13*(1), 57-77.

Takahashi, T. (2007a). Characteristics of fully-developed flow *Debris Flow, 2nd Edition : Mechanics, Prediction and Countermeasures (2nd Edition)* (pp. 170-210). London: London, GBR: CRC Press.

Takahashi, T. (2007b). *Debris Flow Mechanics, Prediction and Countermeasures*. Florence: Florence, KY, USA: CRC Press.

Takahashi, T. (2007c). Initiation and development of debris flow *Debris flow: mechanics, prediction and countermeasures* (pp. 104-167): CRC press.

Takahashi, T. (2007d). Models for mechanics of flow *Debris Flow, 2nd Edition : Mechanics, Prediction and Countermeasures (2nd Edition)*. London: London, GBR: CRC Press.

Takahashi, T. (2007e). What is debris flow *Debris flow: mechanics, prediction and countermeasures* (pp. 1-32): CRC press.

Vagnon, F., & Segalini, A. (2016). Debris flow impact estimation on a rigid barrier. *Natural Hazards and Earth System Sciences, 16*(7), 1691-1697.

VanDine, D. F. (1985). Debris flows and debris torrents in the southern Canadian Cordillera. *Canadian Geotechnical Journal, 22*(1), 44-68.

Varnes, D. J. (1978). Slope movement types and processes. *Special report, 176*, 11-33.

Zhang, S. (1993). A comprehensive approach to the observation and prevention of debris flows in China. *Natural Hazards, 7*(1), 1-23.

APPENDIX A

Results of the water content test

Intended Cv(%)	Test number	Intended solid mass (kg)	Intended water mass (kg)	Material left in the box (kg)	Water content (%)	Actual solid mass (kg)	Actual water mass (kg)	Actual Cv (%)	Standard deviation of Cv(%)	Average Cv (%)
60	16	40	10.0	13.1	14	28.5	8.4	55.4	0.7	54.6
	17			13.5	11	27.9	8.6	54.2		
	18			14.5	12	27.1	8.4	54.1		
	35	45	11.0	8.1	15	37.9	10.0	58.3	1.2	57.8
	36			11.9	12	34.3	9.8	56.4		
	37			6.5	14	39.3	10.2	58.7		
	45	45	11.0	11.5	15	35.0	9.5	57.7	0.1	57.6
	46			10.9	14	35.5	9.6	57.5		
	27	50	12.0	15.8	12	35.9	10.3	56.3	1.2	57.6
	28			10	14	41.2	10.8	58.5		
	29			12.1	14	39.4	10.5	58.1		
	4	80	20.0	-	-	-	-	-	-	-
	5									
	6									
55	22	40	12.0	12.1	12	29.2	10.7	50.1	1.3	49.9
	23			10	12	31.0	11.0	51.0		
	24			14.5	11	27.0	10.5	48.5		
	38	45	13.5	12	14	34.5	12.0	51.4	1.1	51.7
	39			14.1	15	32.7	11.7	50.8		
	40			8.3	15	37.8	12.4	52.8		
	30	50	15.0	11.2	15	40.3	13.5	52.3	0.6	53.0
	31			8.4	17	42.8	13.8	53.3		
	32			7.3	15	43.7	14.0	53.3		
50	19	40	15.0	7.6	13	33.3	14.1	46.4	0.8	46.4
	20			9.3	11	31.7	14.0	45.3		
	21			6.5	14	34.3	14.2	47.0		
	25			7.1	15	33.8	14.1	46.9		
	41	45	16.5	5.3	16	40.4	15.8	48.5	0.7	47.7
	42			7.5	13	38.4	15.6	47.4		
	43			7.9	13	38.0	15.6	47.3		
	33	50	18.0	5.8	15	45.0	17.2	48.9	0.1	49.0
	34			5.3	15	45.4	17.3	49.1		
	13	80	30.0	7.8	14	73.2	29.0	48.1	2.4	45.9
	14			24.6	10	57.6	27.8	43.3		
	15			14.9	12	66.8	28.3	46.4		
40	26	40	22.0	9.1	12	31.9	21.0	35.9		
	44	45	25.0	8	13	37.9	24.1	36.7		

APPENDIX B

Velocity plot of the tests

B.1 Velocity plot of test 4, 5, 6 for 80+20 combination

Velocity along the flow path for 80+20 combination
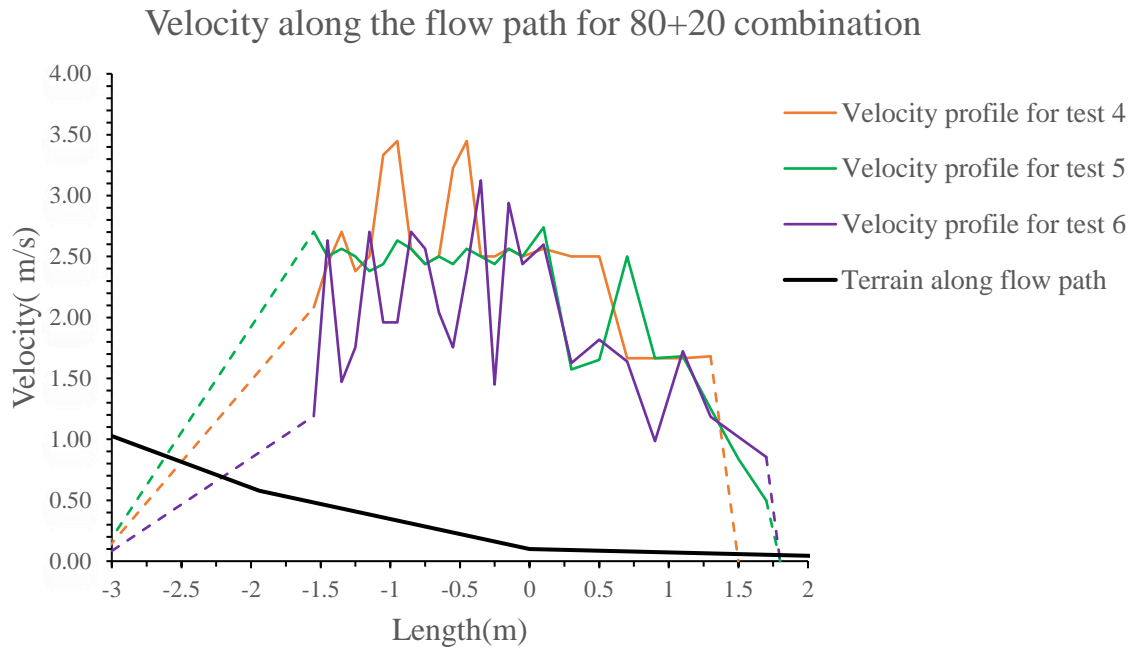
B.2 Velocity plot of test 13,15 for 80+30 combination

Velocity along the flow path for 80+30 combination
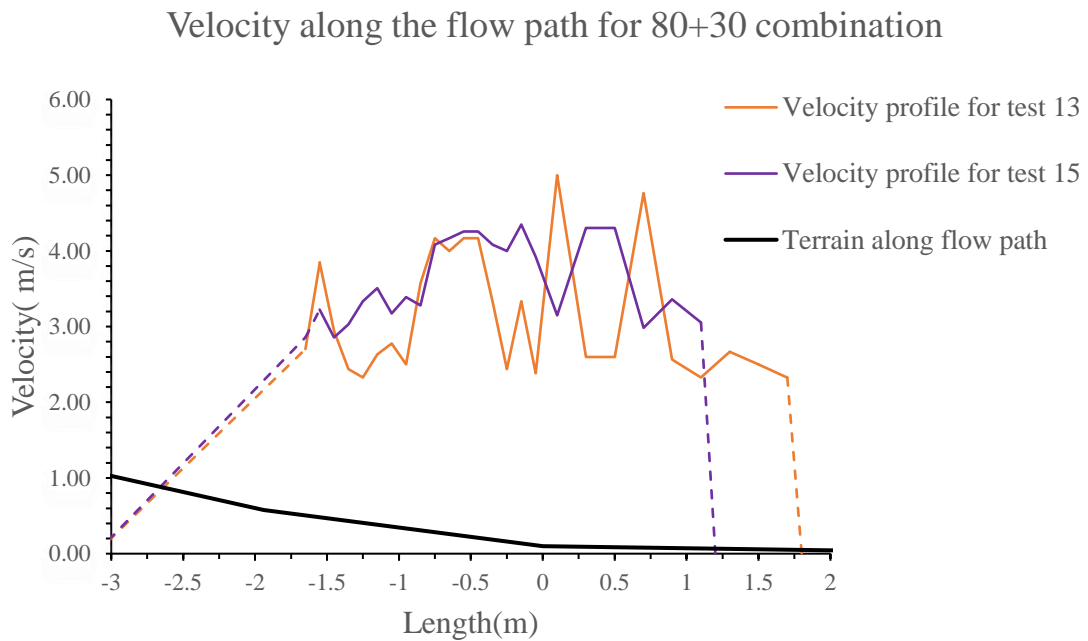
B.3 Velocity plot of test 30,31,32 for 50+15 combination

Velocity along the flow path for 50+15 combination
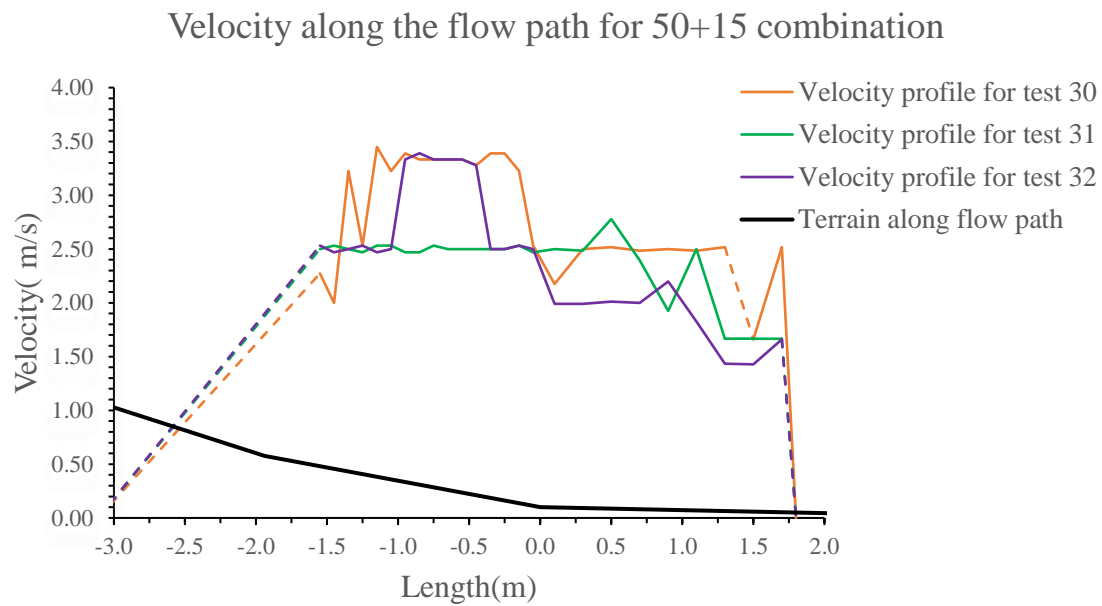
B.4 Velocity plot of test 33,34 for 50+18 combination

Velocity along the flow path for 50+18 combination

B.5 Velocity plot of test 45,46 for 45+11(f) combination
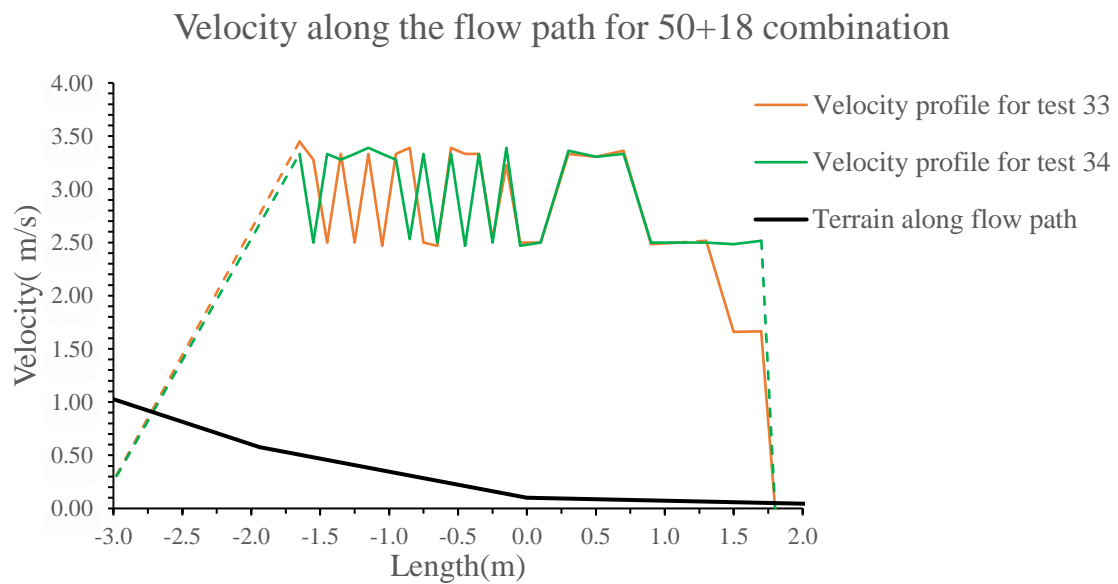
Velocity along the flow path for 45+11combination

B.6 Velocity plot of test 45,46 for 45+16.5 combination
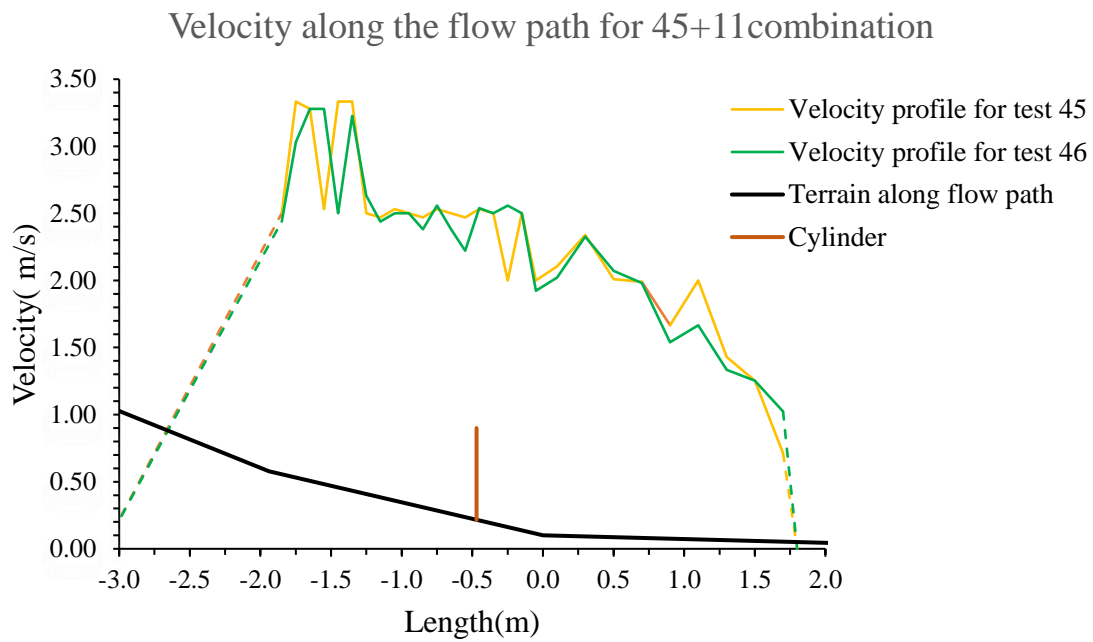
Velocity along the flow path for 45+16.5 combination
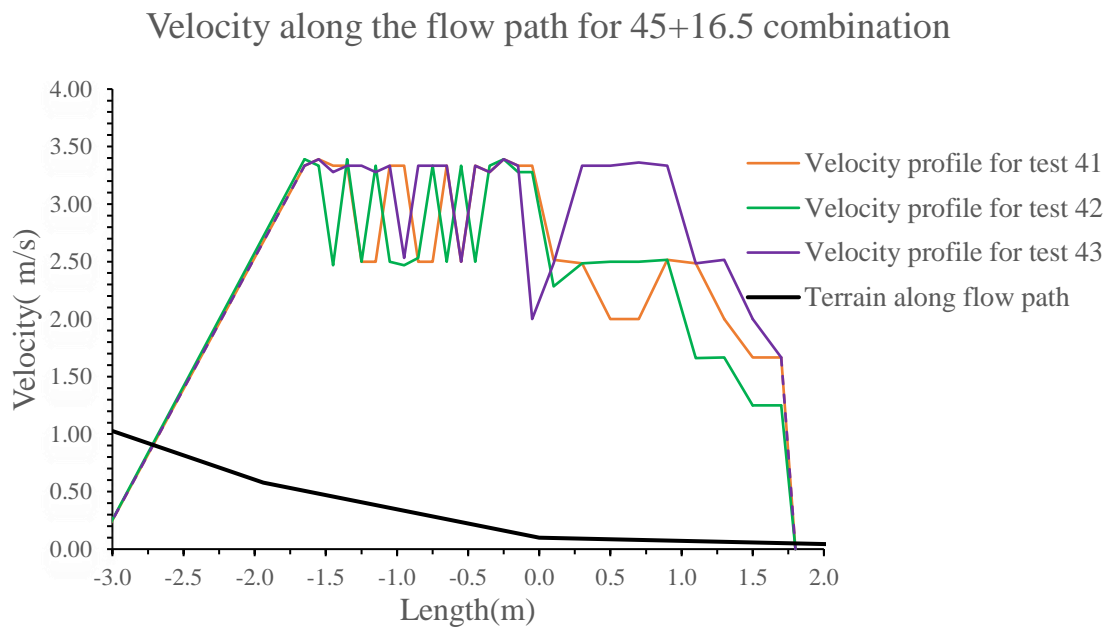
B.7 Velocity plot of test 16, 17, 18 for 40+10 combination

Velocity along the flow path for 40+10 combination
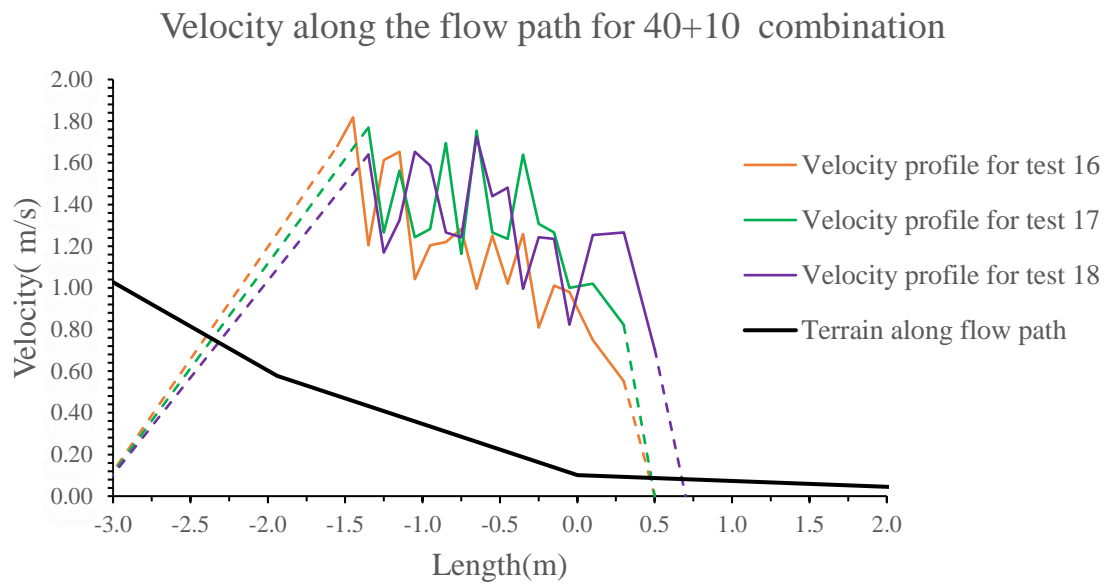
B.8 Velocity plot of test 19,20,21,25 for 40+15 combination

Velocity along the flow path for 40+15 combination
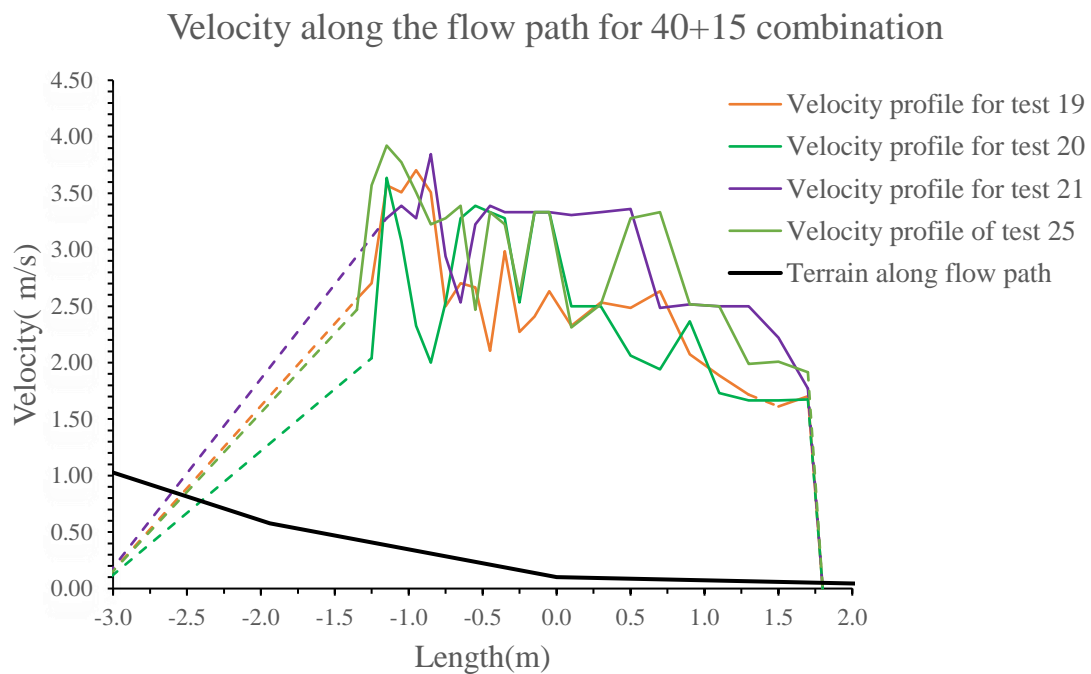
APPENDIX C

Graph of flow height for debris flow test

C.1 Graph of flow height at upstream for debris flow test

C.1.1 Test with 60% Cv

C.1.2 Test with 55% Cv

50+15 (55% Cv)

C.1.3 Test with 50% Cv

40+15 (50% Cv)

45+16.5 (50% Cv)
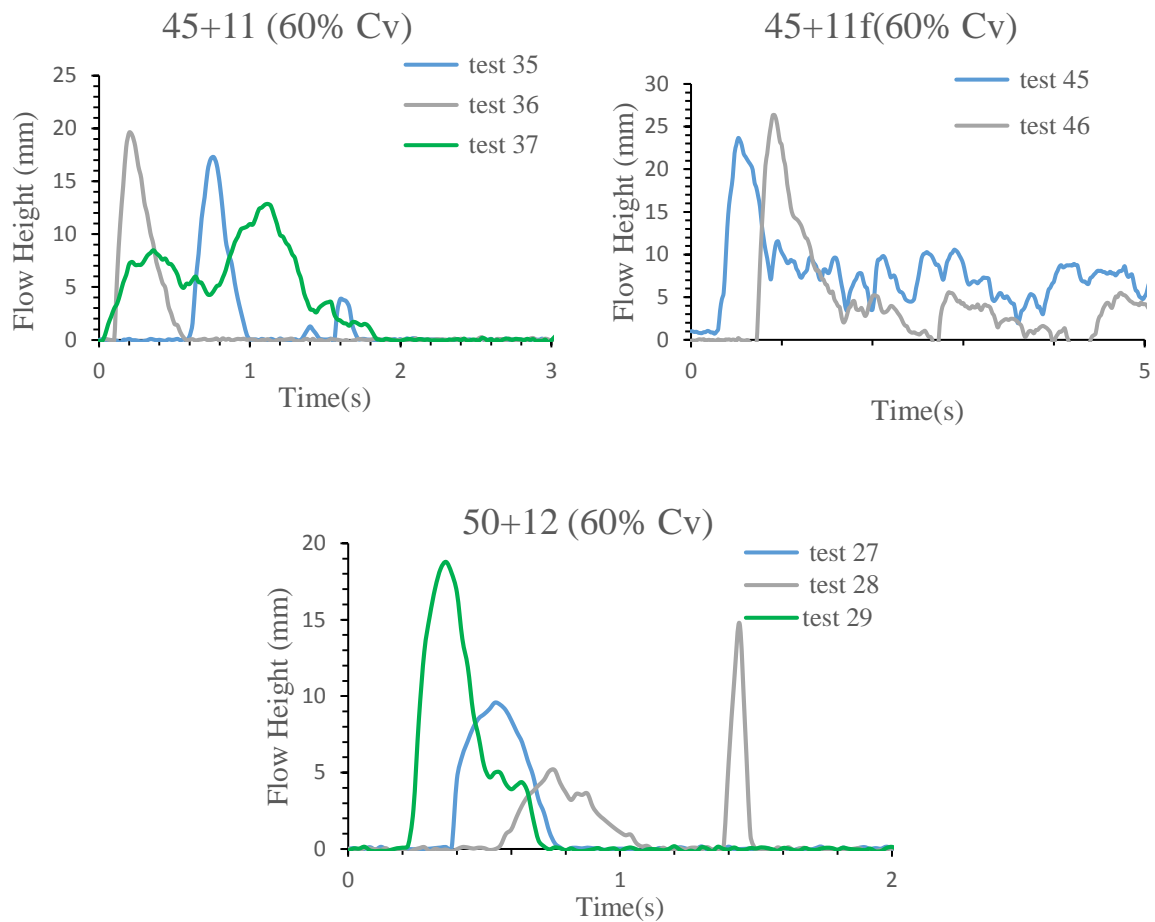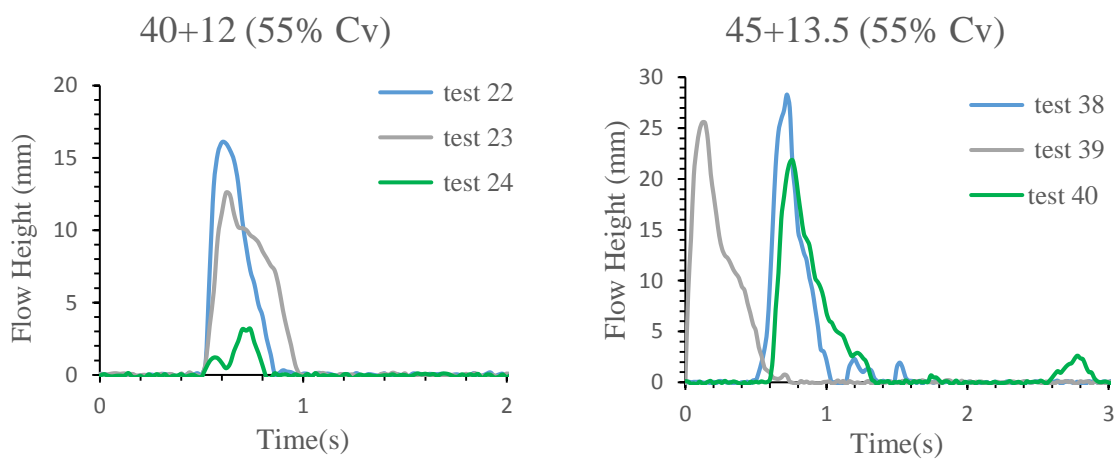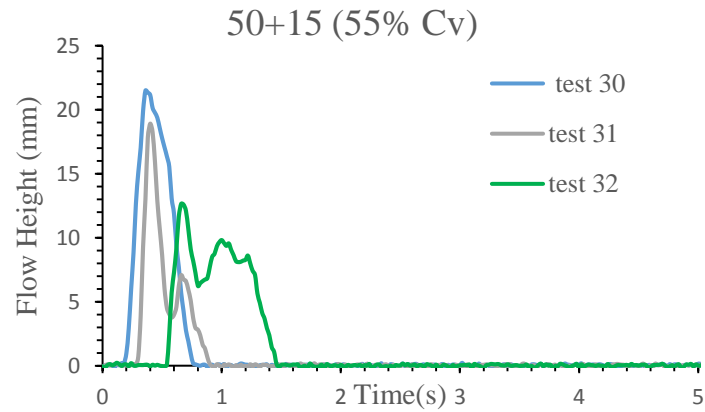
50+18 (50% Cv)

C.1.4 Test with 40% Cv

40+22 (40% Cv)
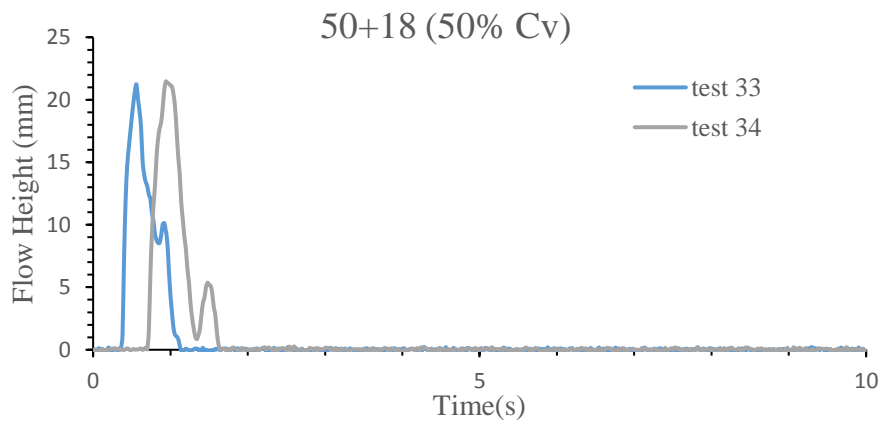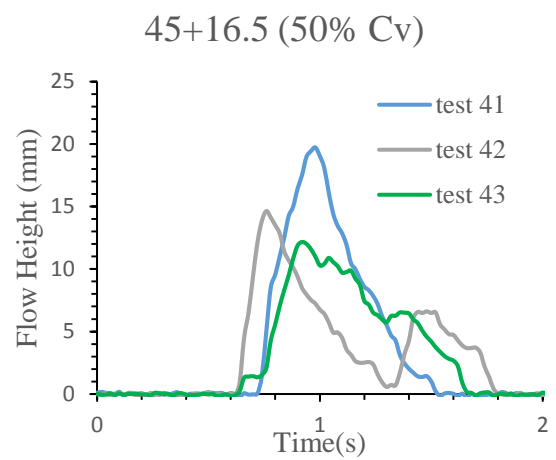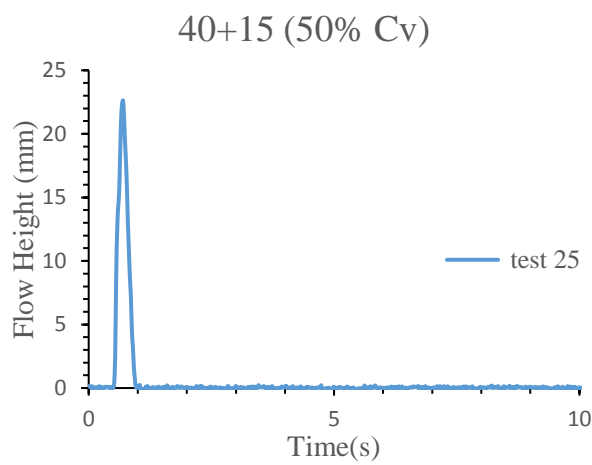
45+25(40% Cv)
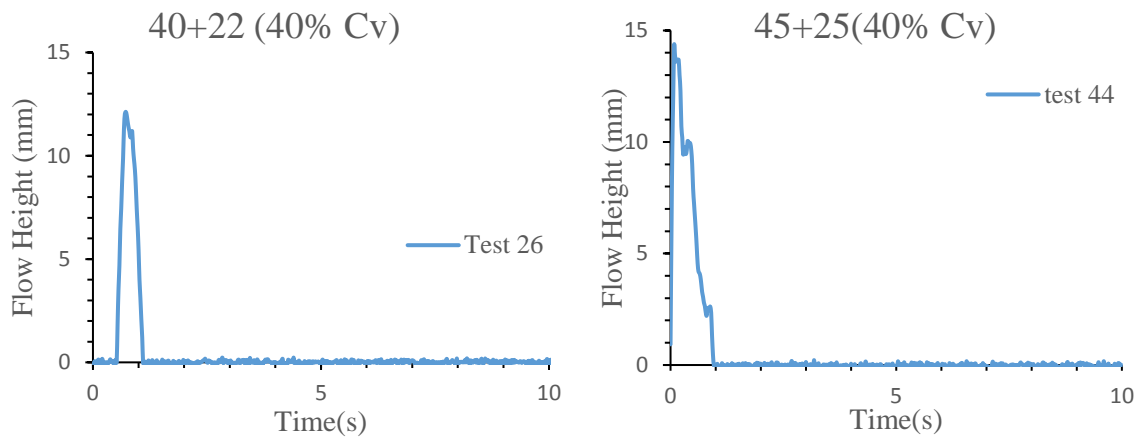
C.2 Graph of flow height at downstream for debris flow test

C.2.1 Test with 60% Cv

45+11 (60% Cv)

45+11f (60% Cv)

50+12 (60% Cv)

C.2.2 Test with 55% Cv

40+12 (55% Cv)

45+13.5 (55% Cv)

50+15 (55% Cv)

C.2.3 Test with 50% Cv

40+15 (50% Cv)

45+16.5 (50% Cv)
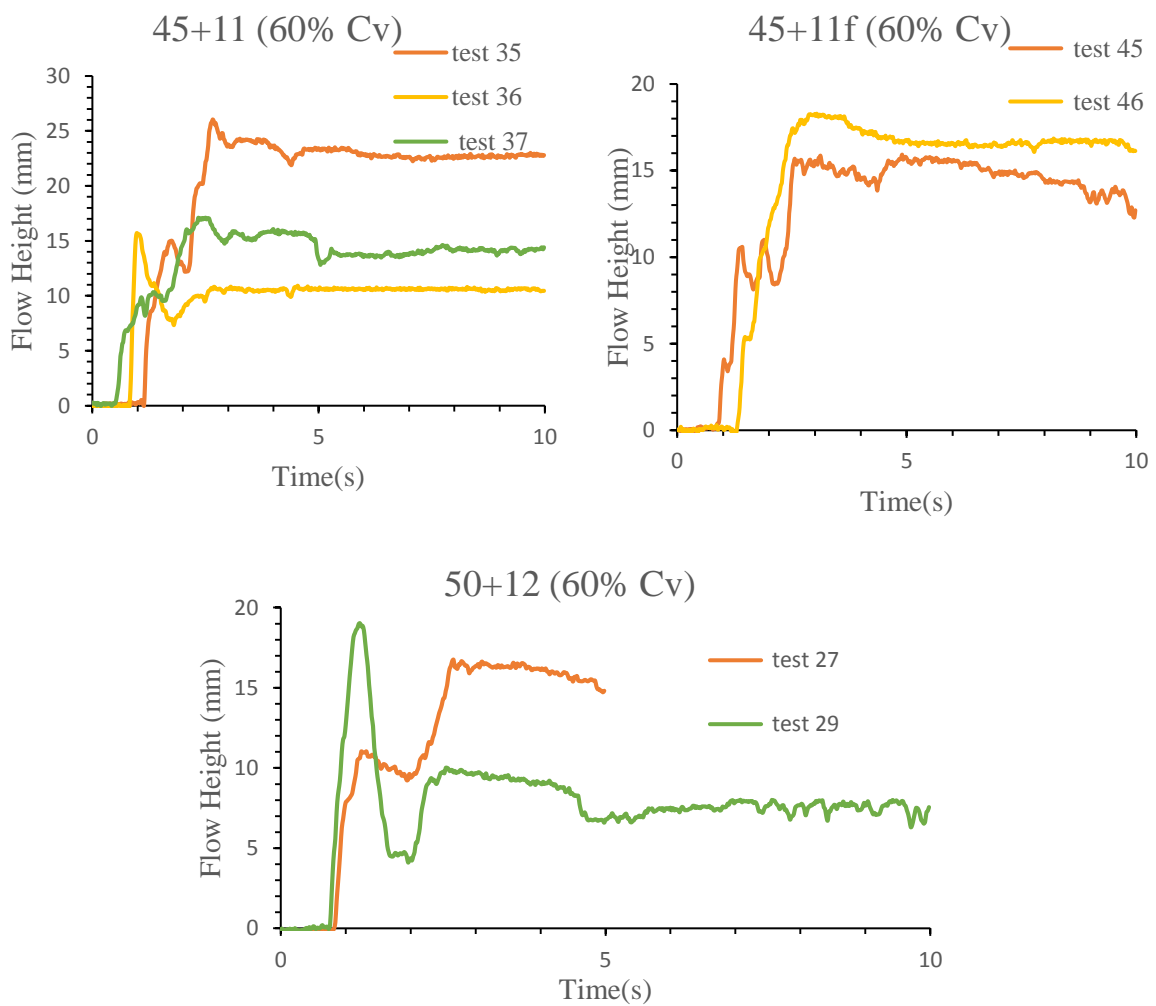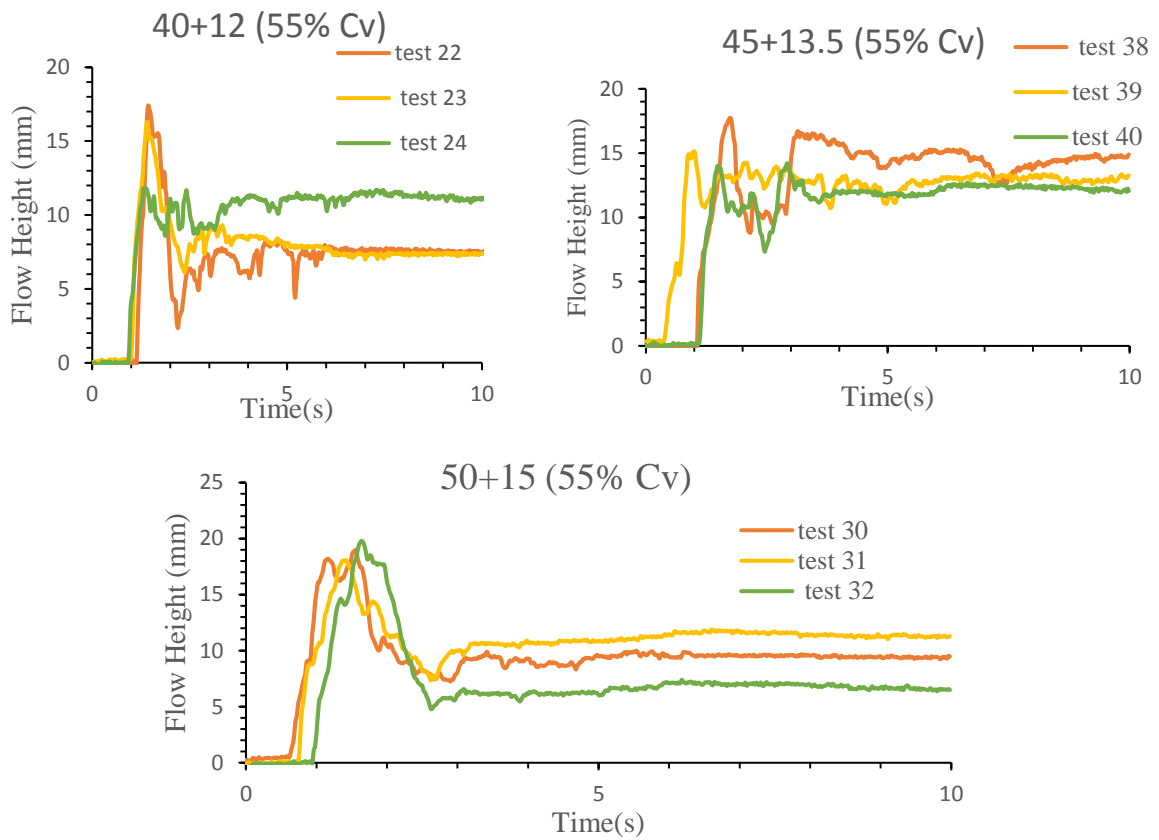
50+18 (50% Cv)
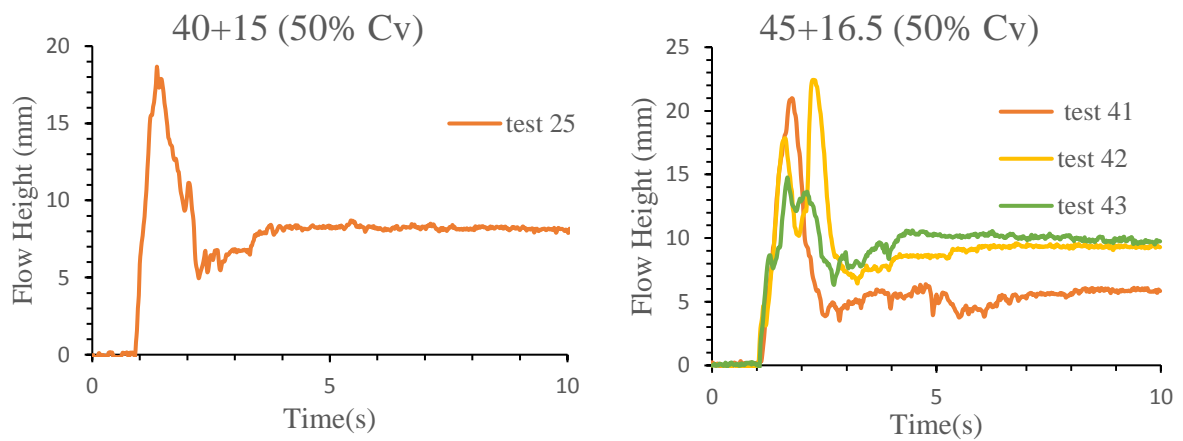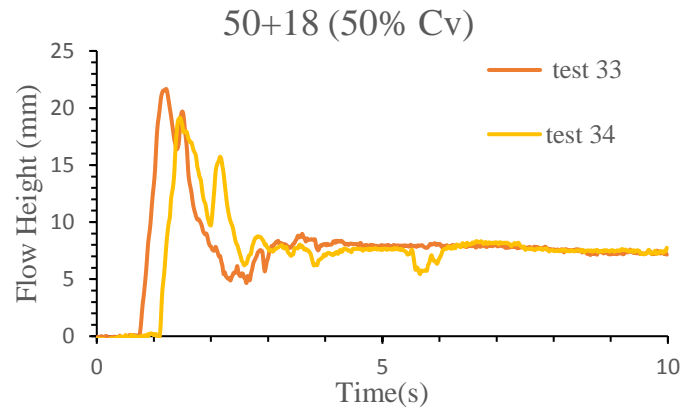
C.2.4 Test with 40% Cv
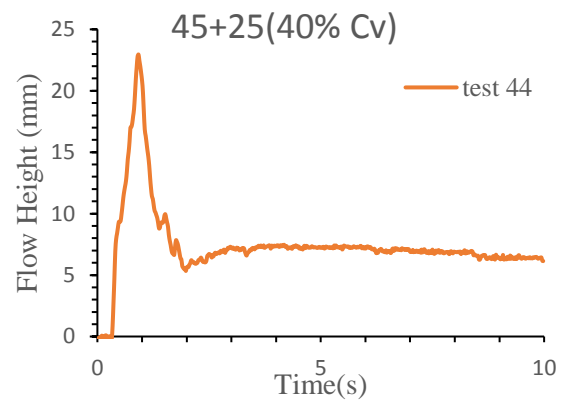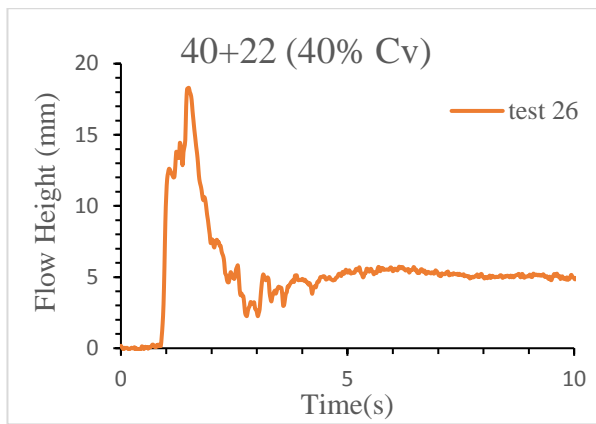
APPENDIX D

Energy line of the tests

D.1 Energy line of test 4, 5, 6 for 80+20 combination

Energy line along the flow path for 80+20 combination
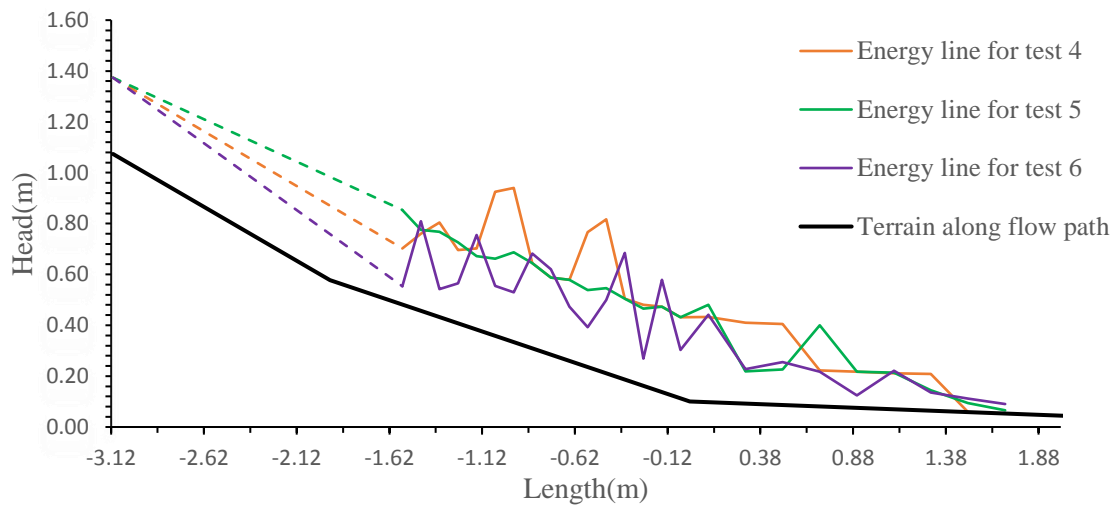
D.2 Energy line of test 13,15 for 80+30 combination

Energy line along the flow path for 80+30 combination
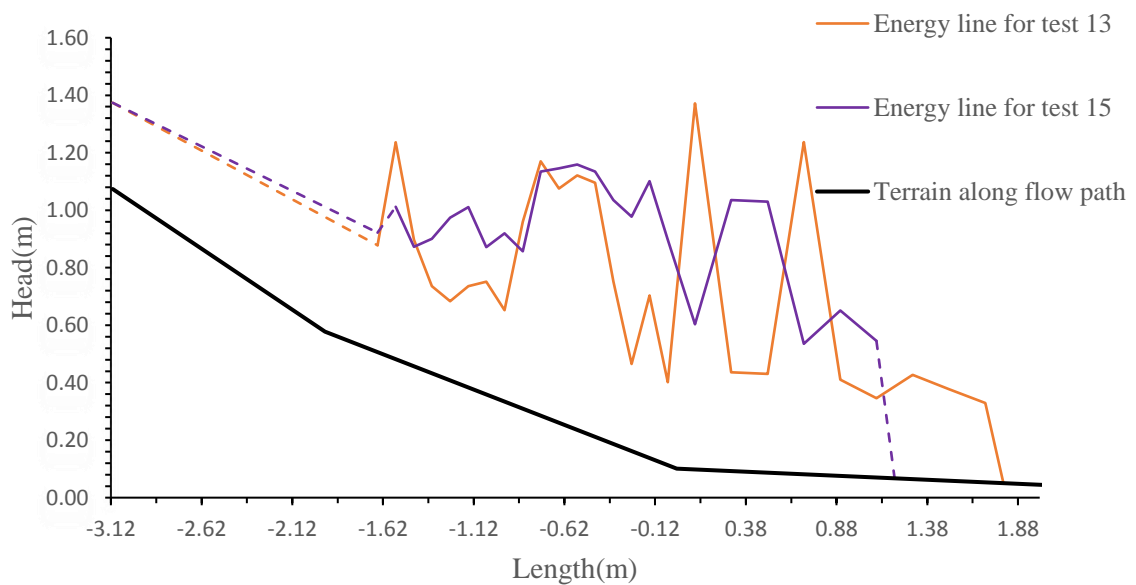
D.3 Energy line of test 30,31,32 for 50+15 combination

Energy line along the flow path for 50+15 combination
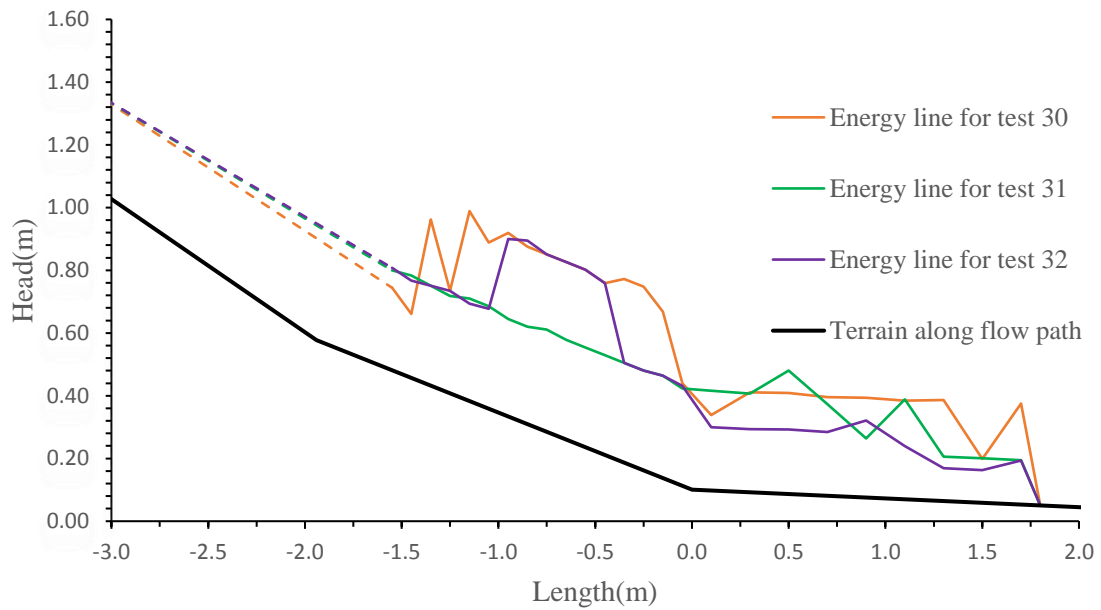
D.4 Energy line of test 33,34 for 50+18 combination

Energy line along the flow path for 50+18 combination
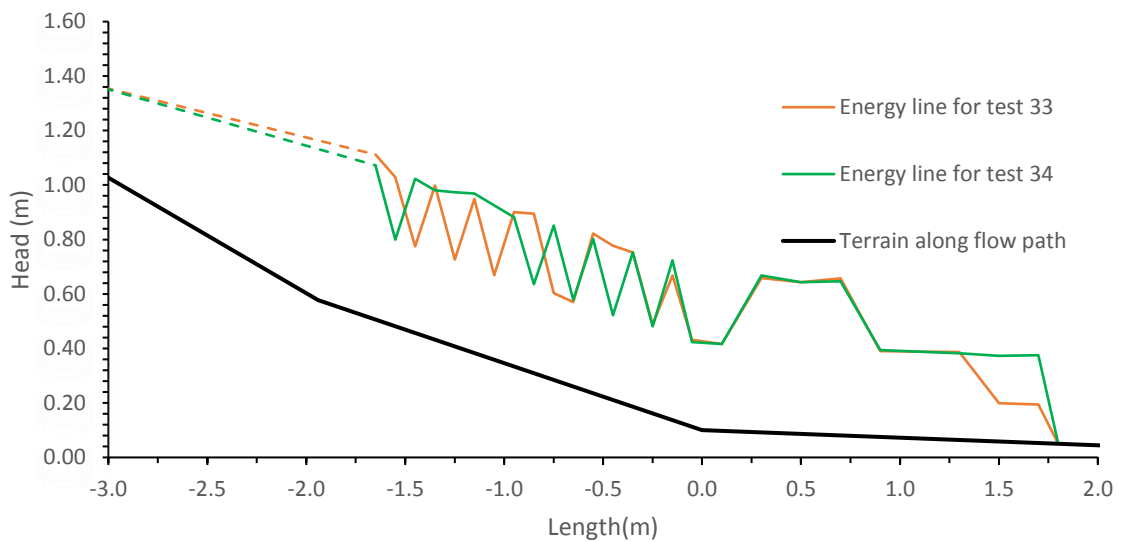
D.5 Energy line of test 45,46 for 45+11(f) combination

Energy line along the flow path for 45+11(f)

D.6 Energy line of test 45,46 for 45+16.5 combination
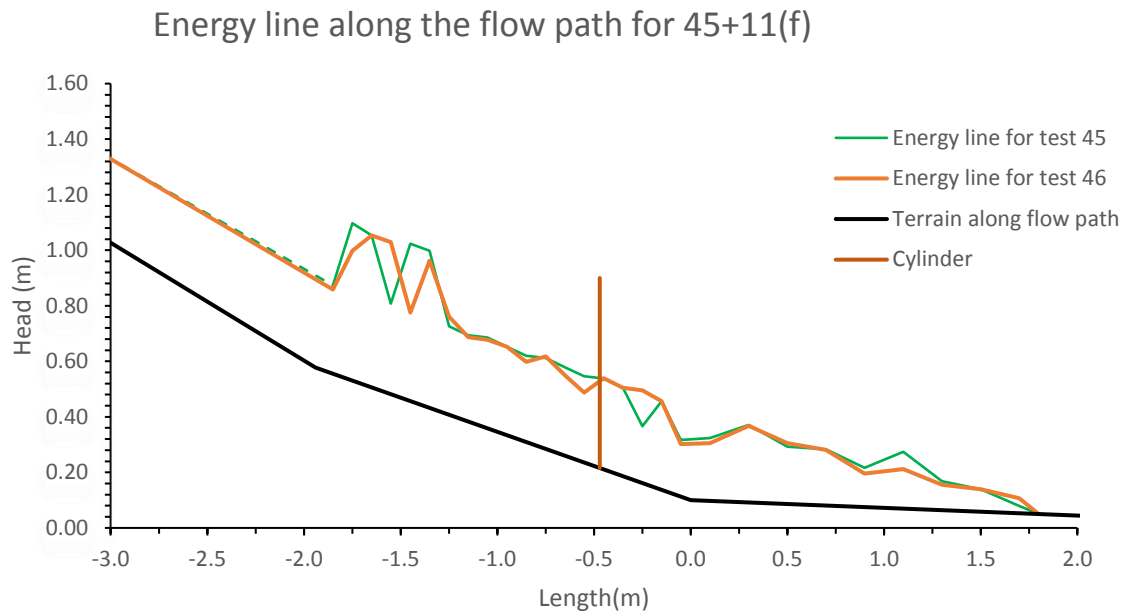
Energy line along the flow path for 45+16.5 combination
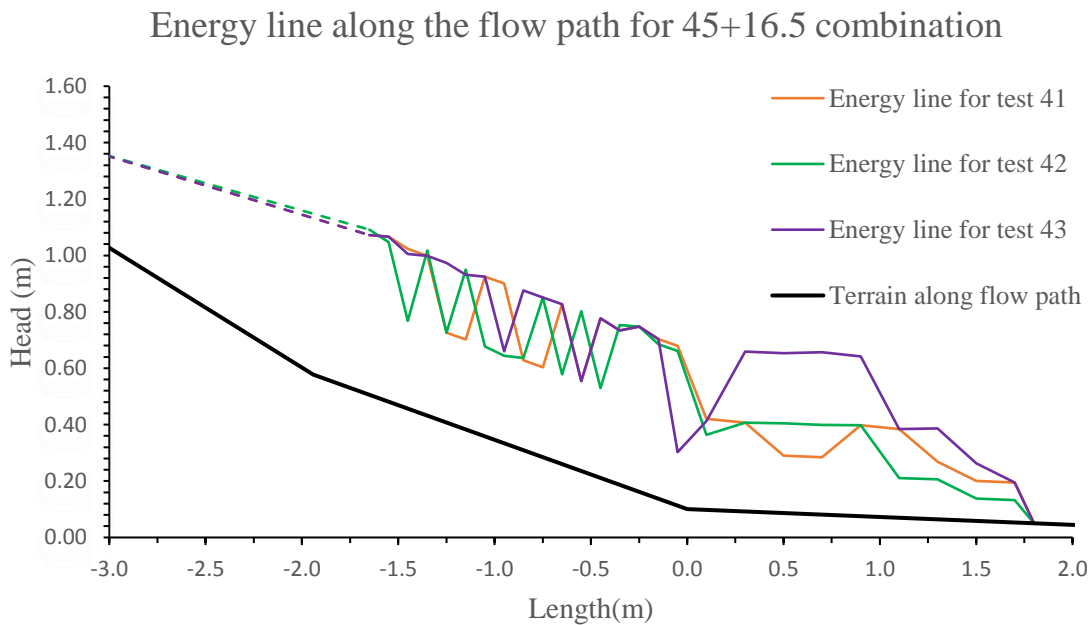
D.7 Energy line of test 16, 17, 18 for 40+10 combination

Energy line along the flow path for 40+10 combination
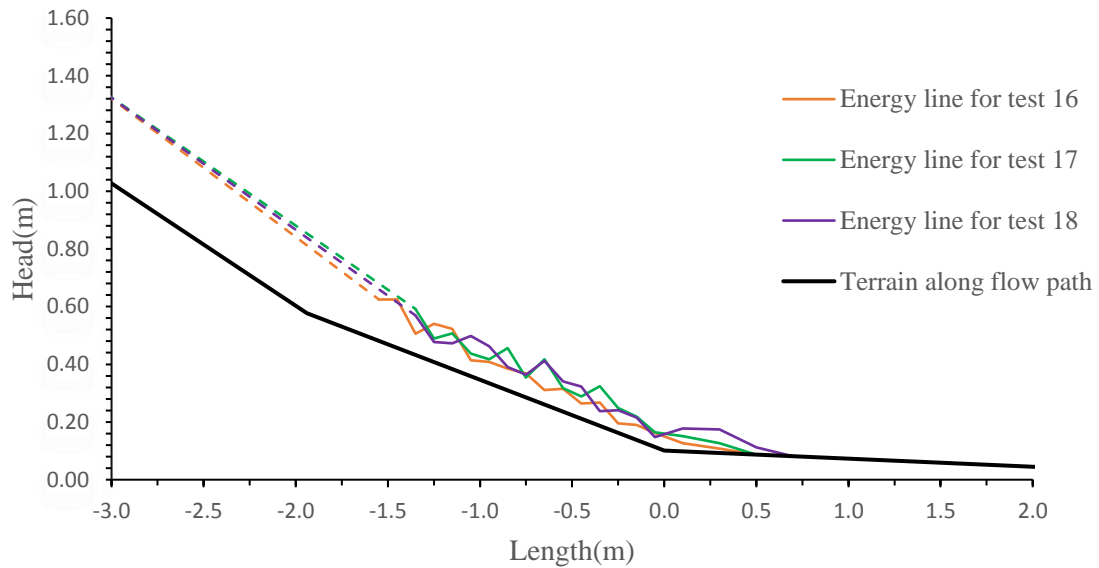
D.8 Energy line of test 19,20,21,25 for 40+15 combination

Energy line along the flow path for 40+15 combination
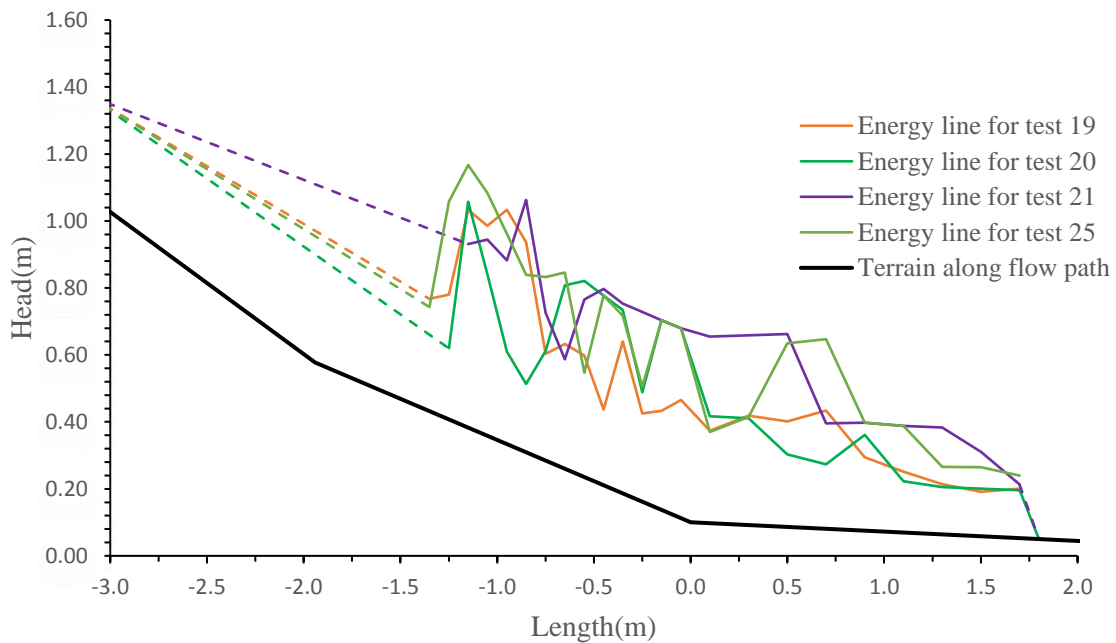
APPENDIX E

Grain size distribution

E.1 GSD for test with 80 kg debris flow material
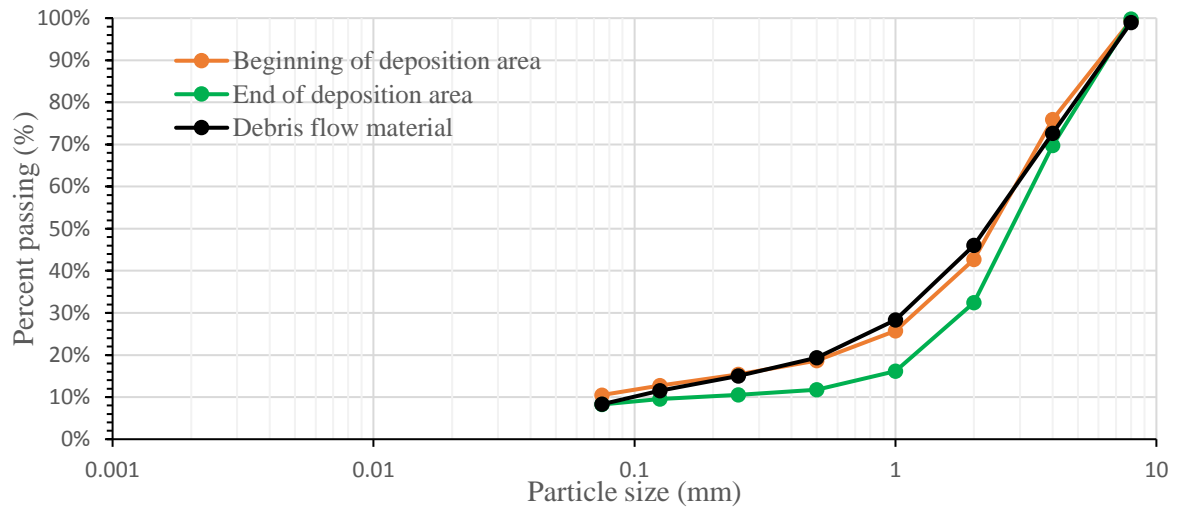
E.1.1 GSD for test 13, 14, 15 with 80+30(50% Cv) combination

Grain size distribution for test 13
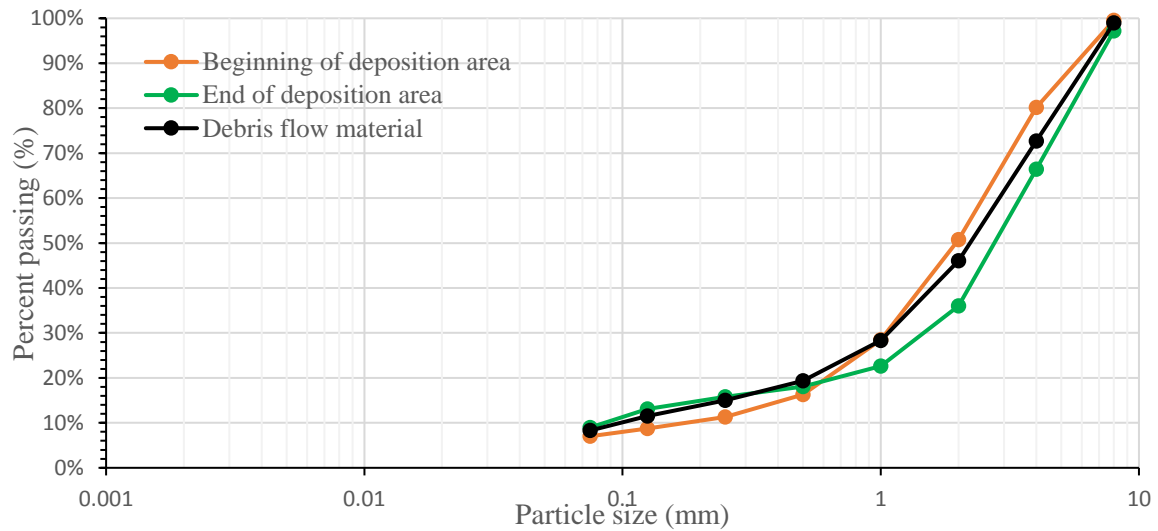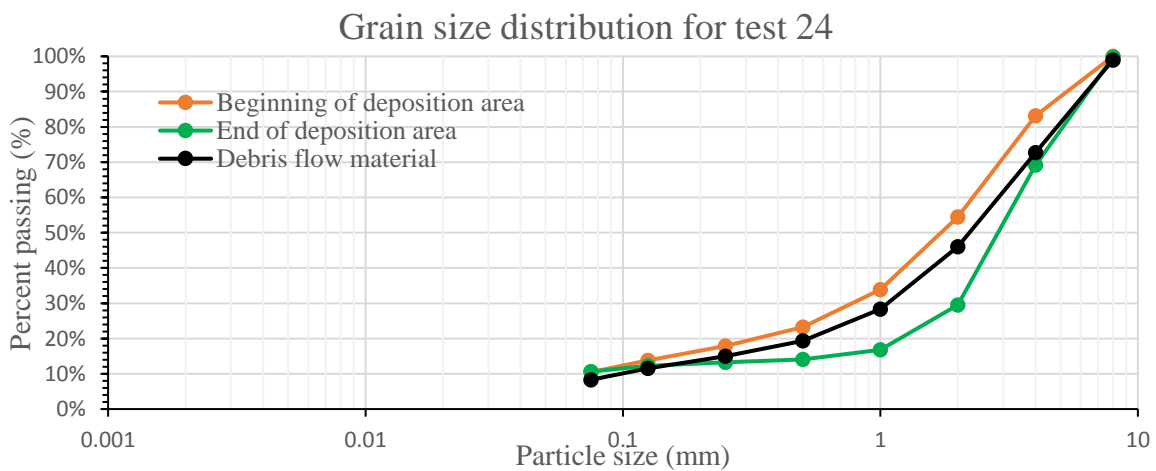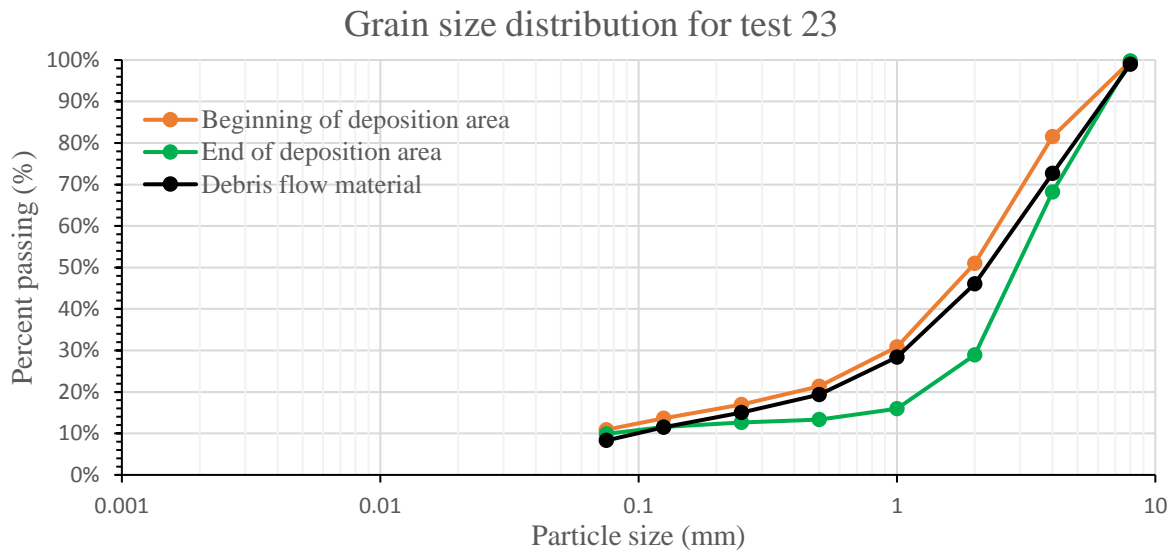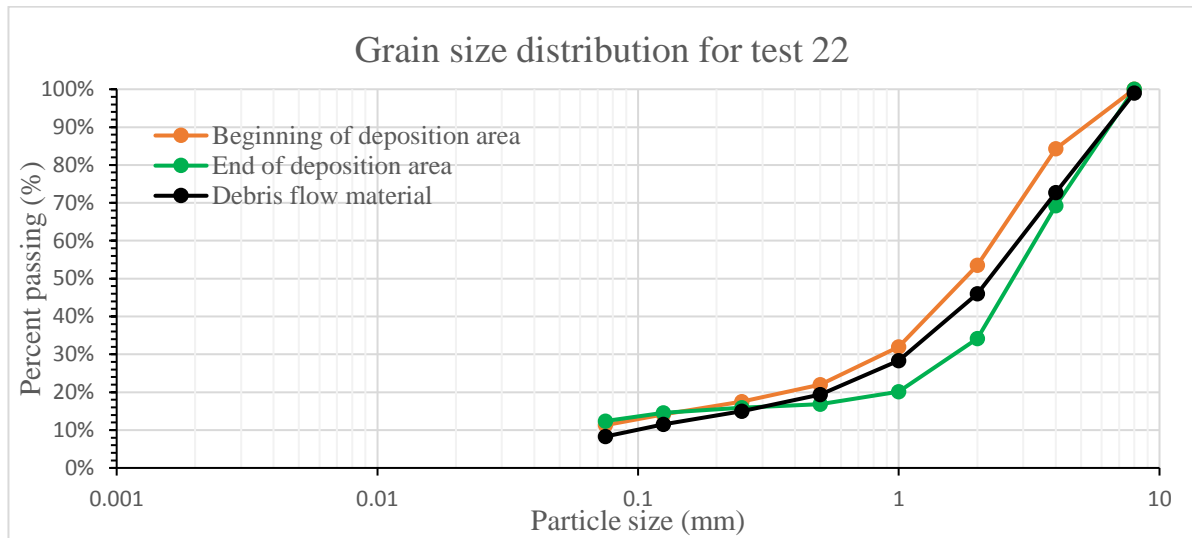

Grain size distribution for test 14
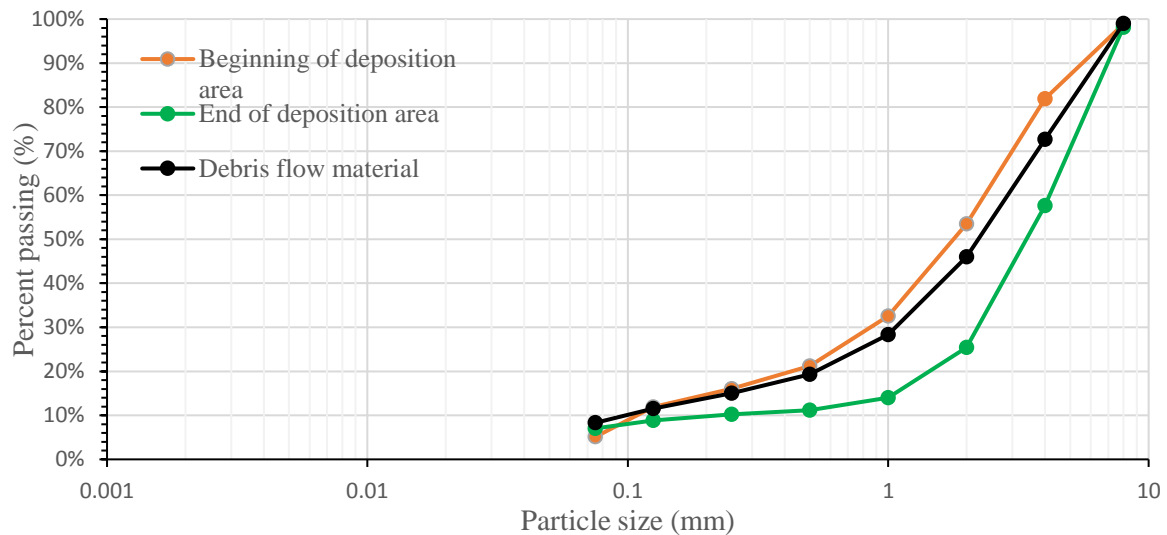
Grain size distribution for test 15
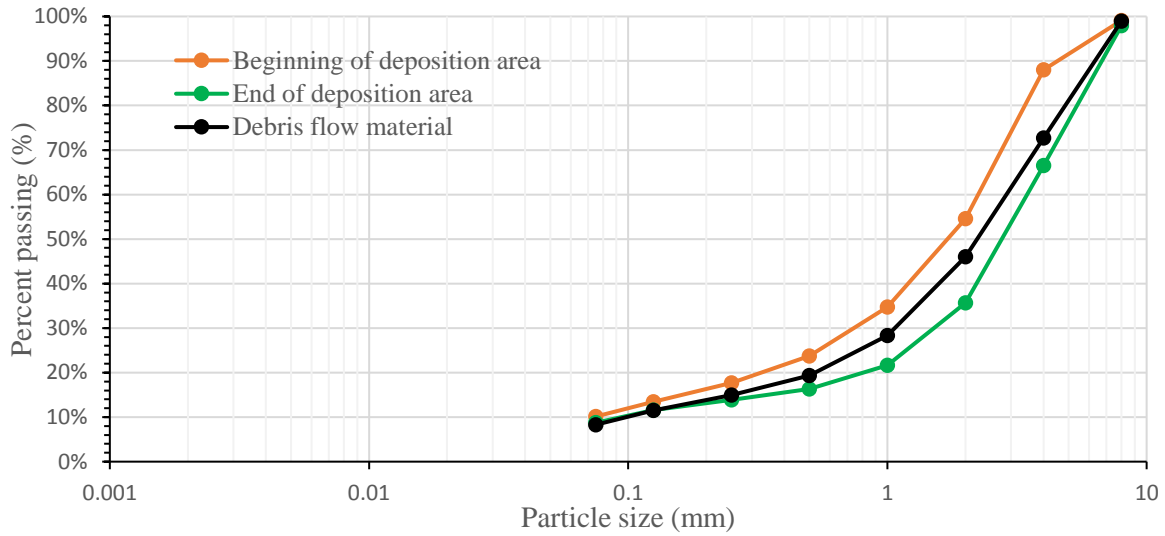
## E.2 GSD for test with 50 kg debris flow material

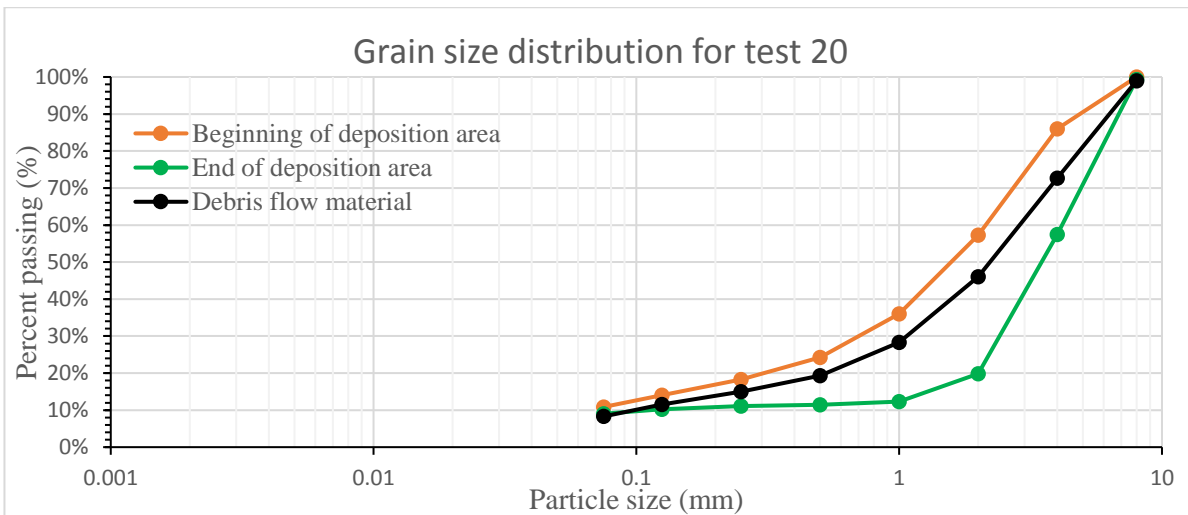## E.2.1 GSD for test 27, 28, 29 with 50+12(60% Cv) combination

Grain size distribution for test 27
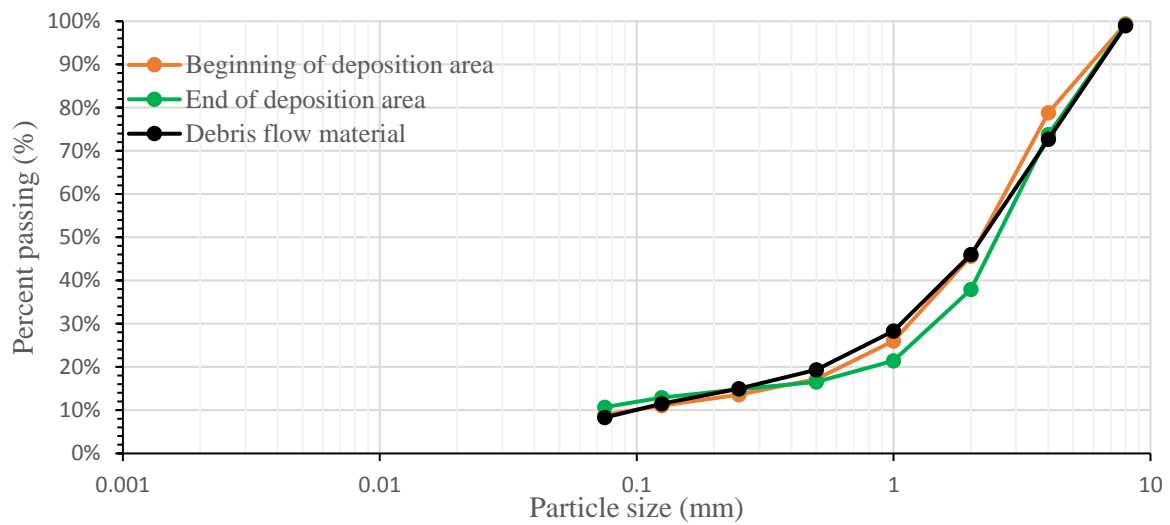
Grain size distribution for test 28
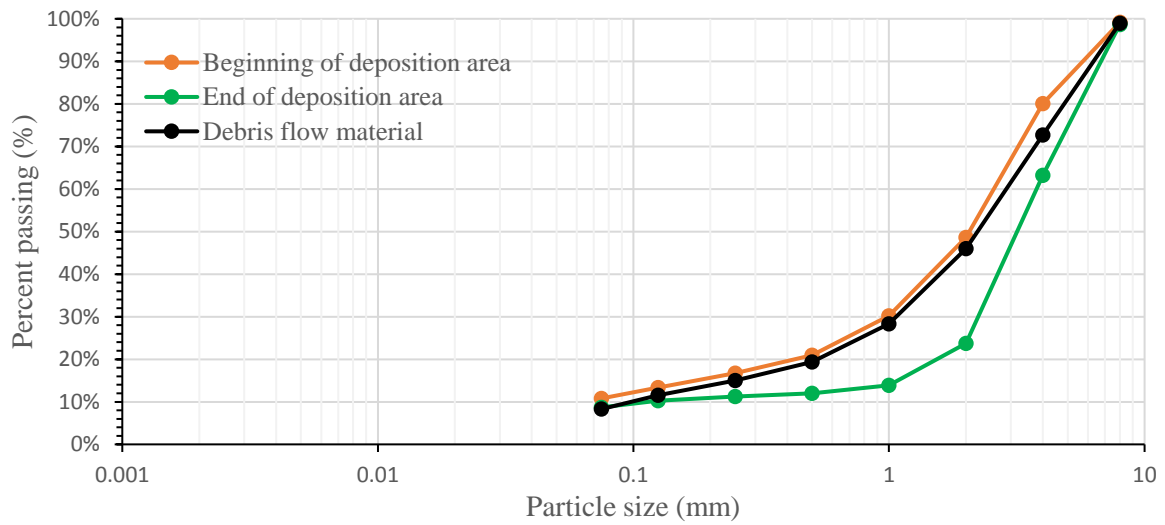
Grain size distribution for test 29
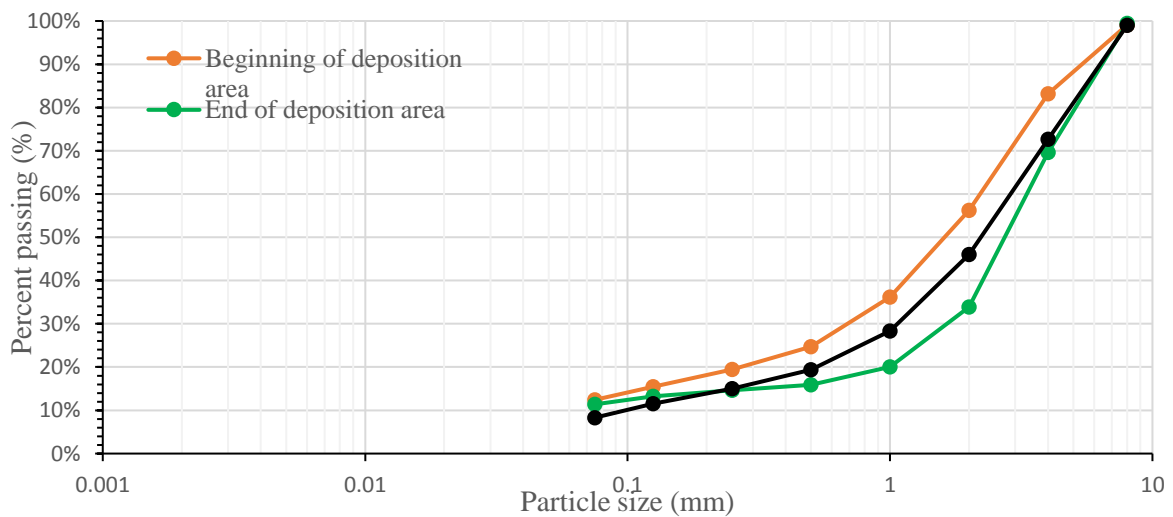
E.2.2 GSD for test 30, 31, 32 with 50+15(55% Cv) combination

Grain size distribution for test 30
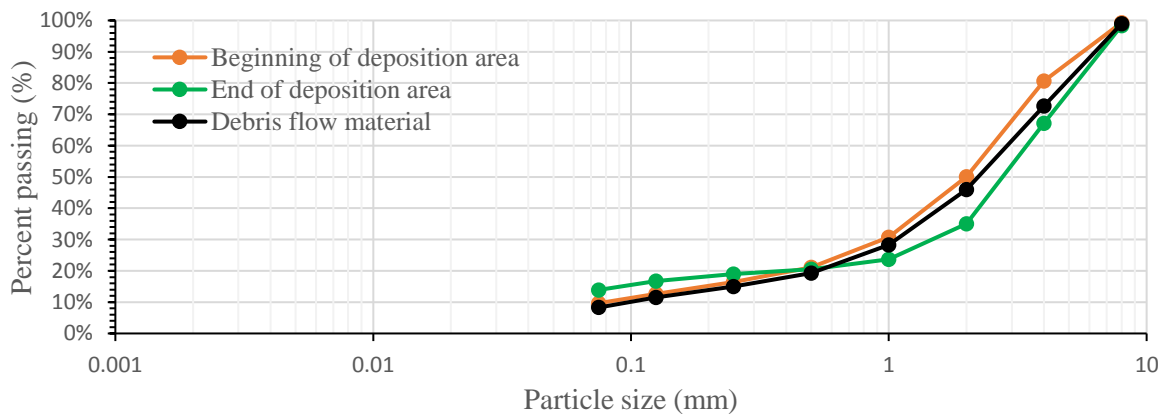
Grain size distribution for test 31
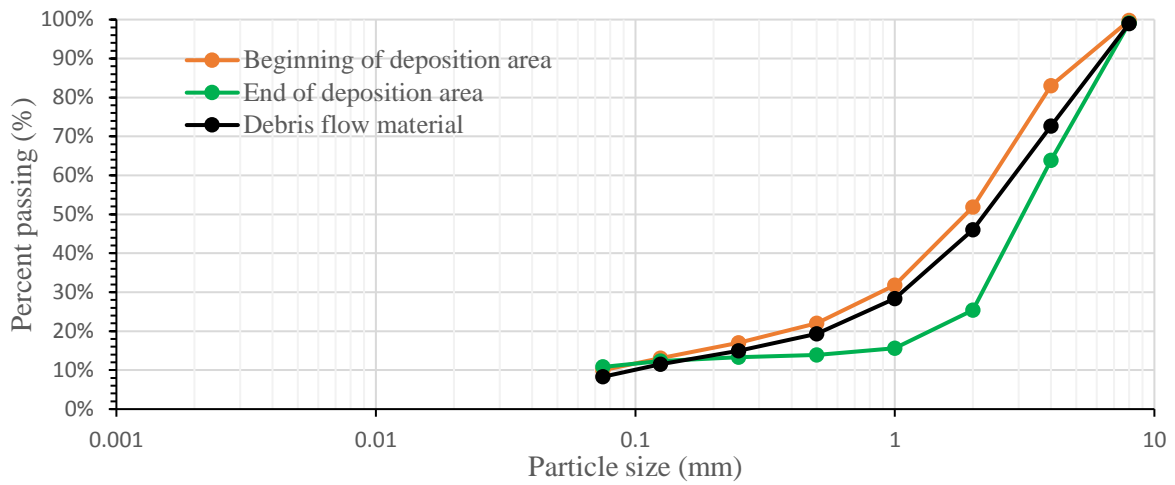
Grain size distribution for test 32
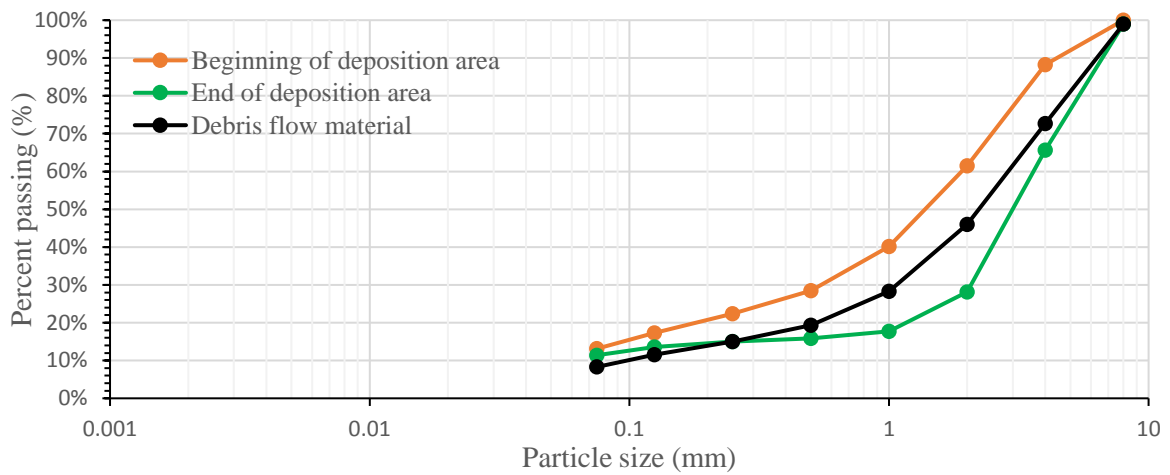
E.2.3 GSD for test 33,34 with 50+18(50% Cv) combination

Grain size distribution for test 33
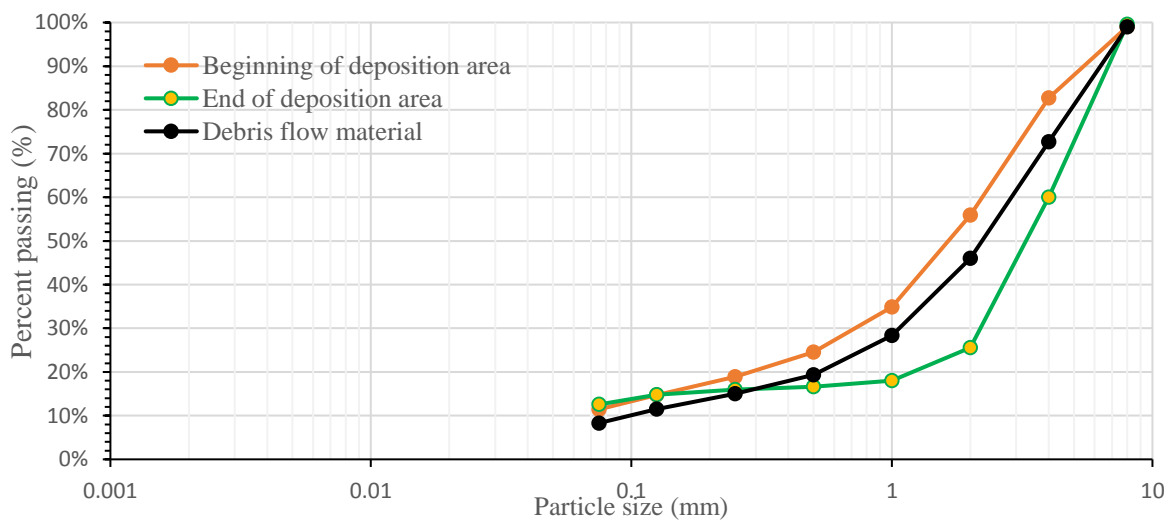
Grain size distribution for test 34
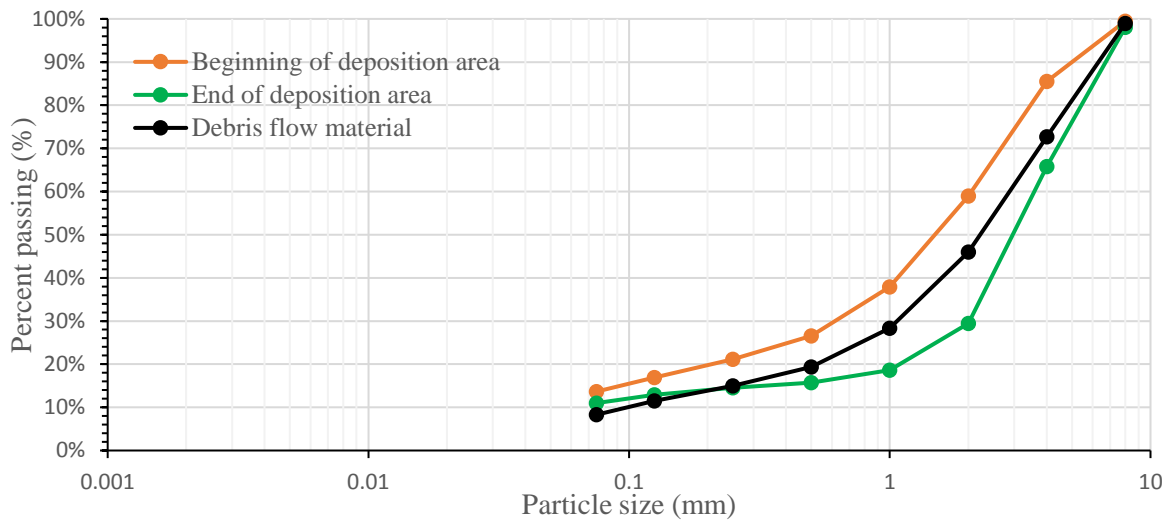
E.3 GSD for test with 45 kg debris flow material

E.3.1 GSD for test 35, 36, 37 with 45+11(60% Cv) combination

Grain size distribution for test 35
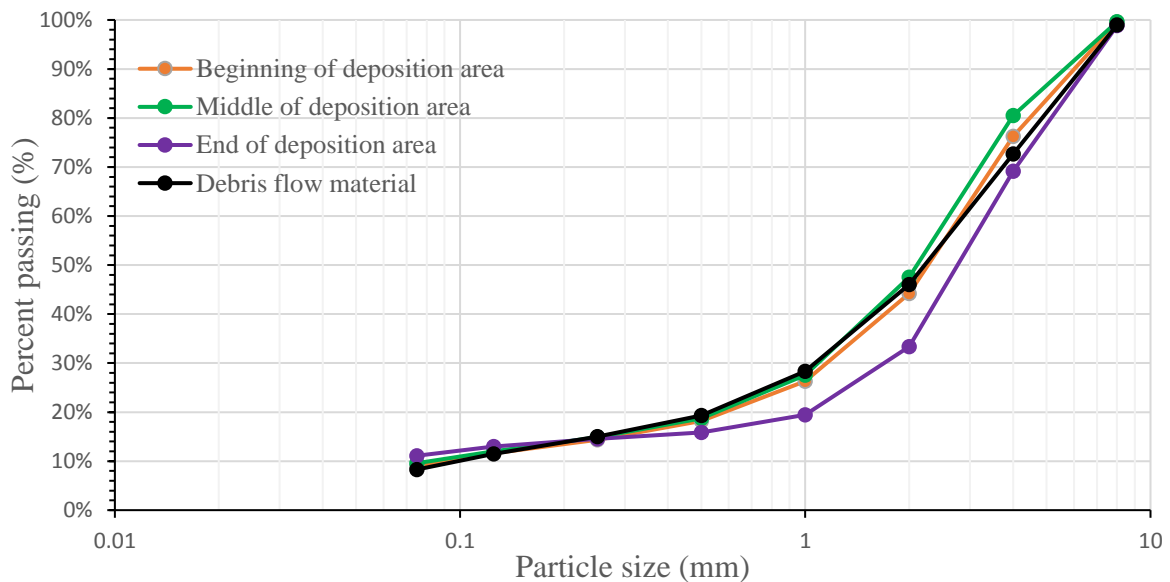
Grain size distribution for test 36
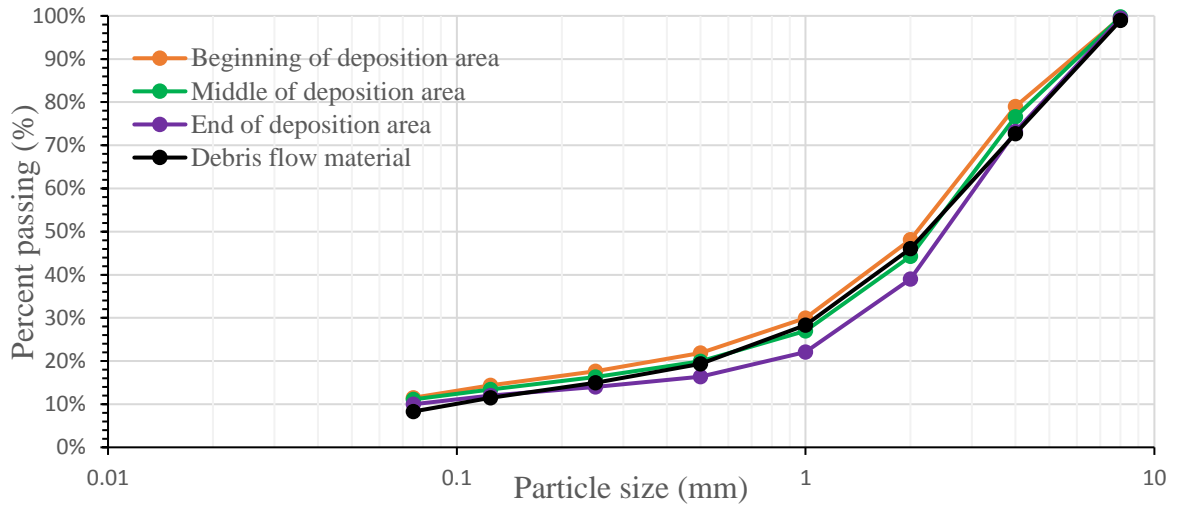
Grain size distribution for test 37
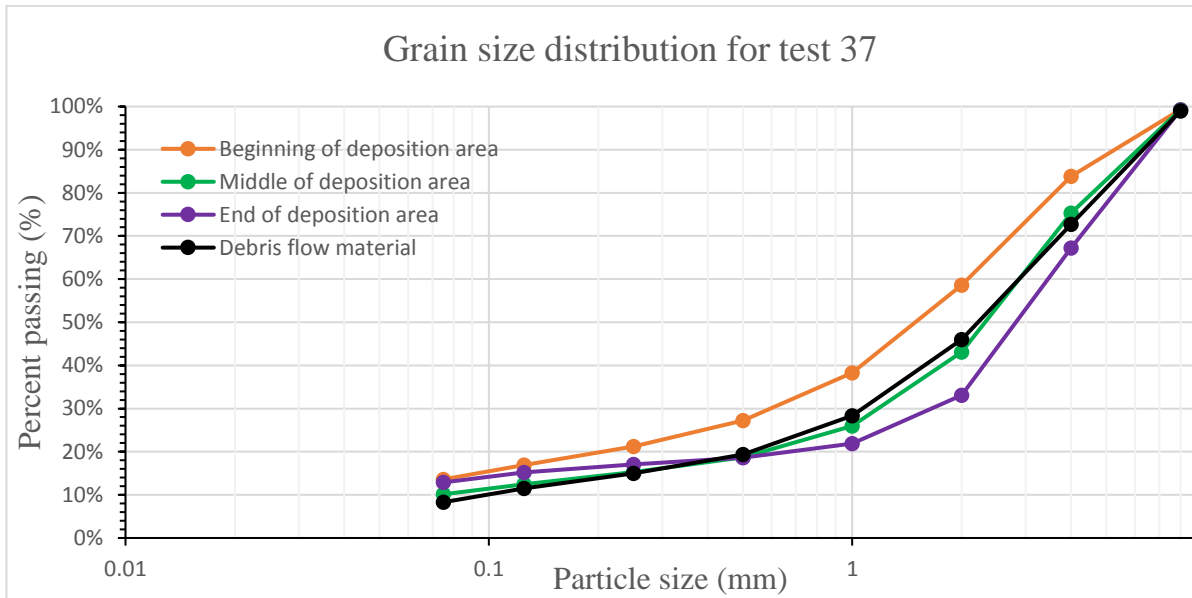
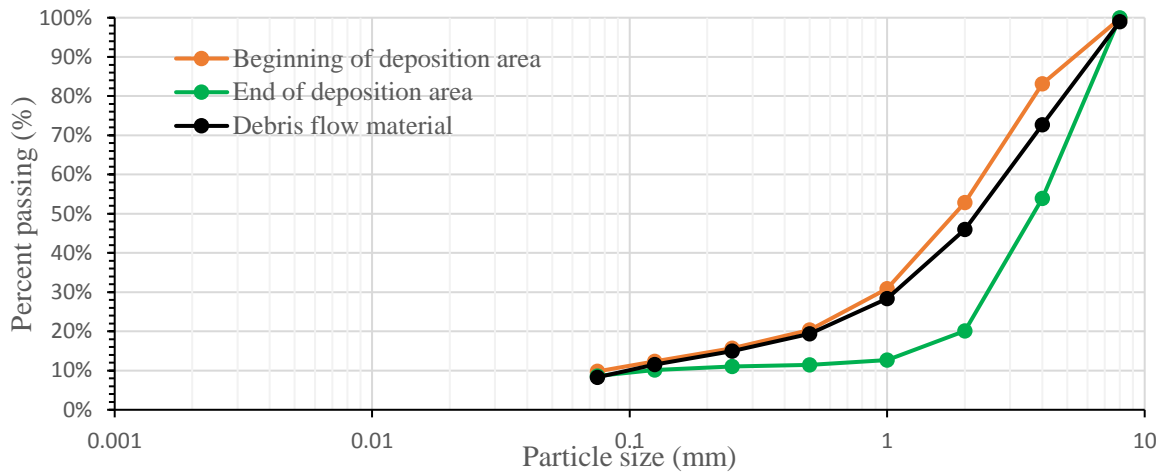### E.3.2 GSD for test 38,39,40 with 45+13.5(55% Cv) combination

Grain size distribution for test 38
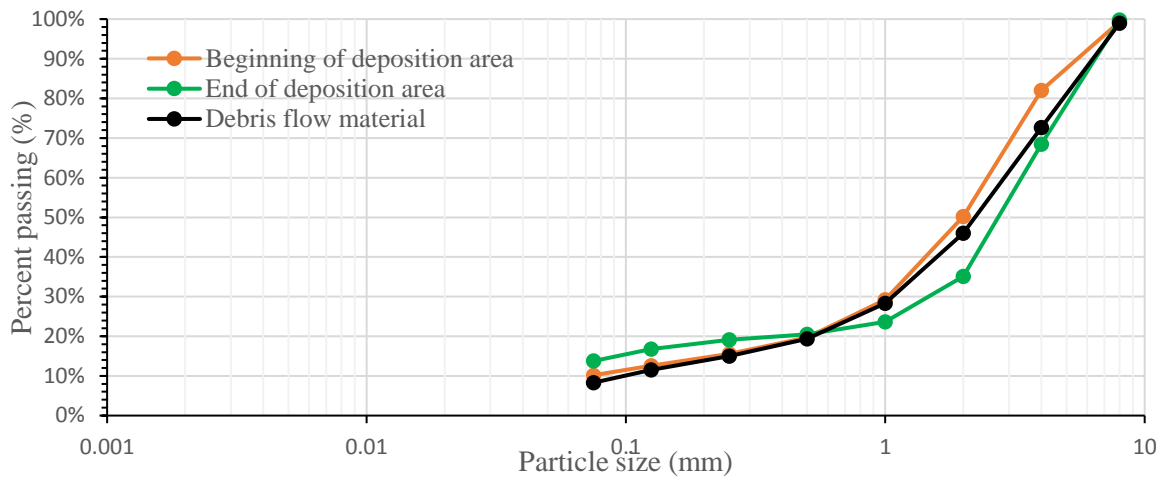
Grain size distribution for test 39
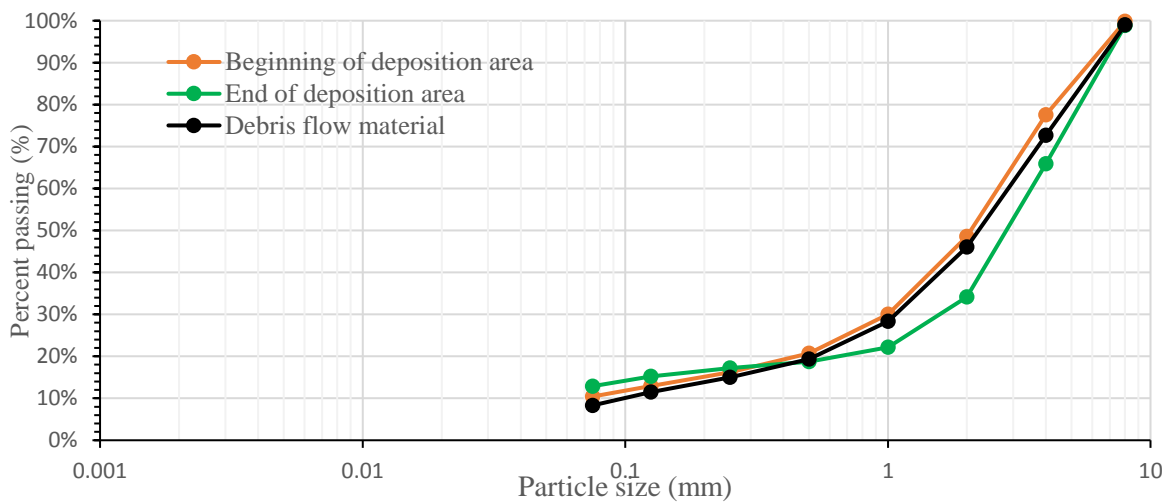
Grain size distribution for test 40
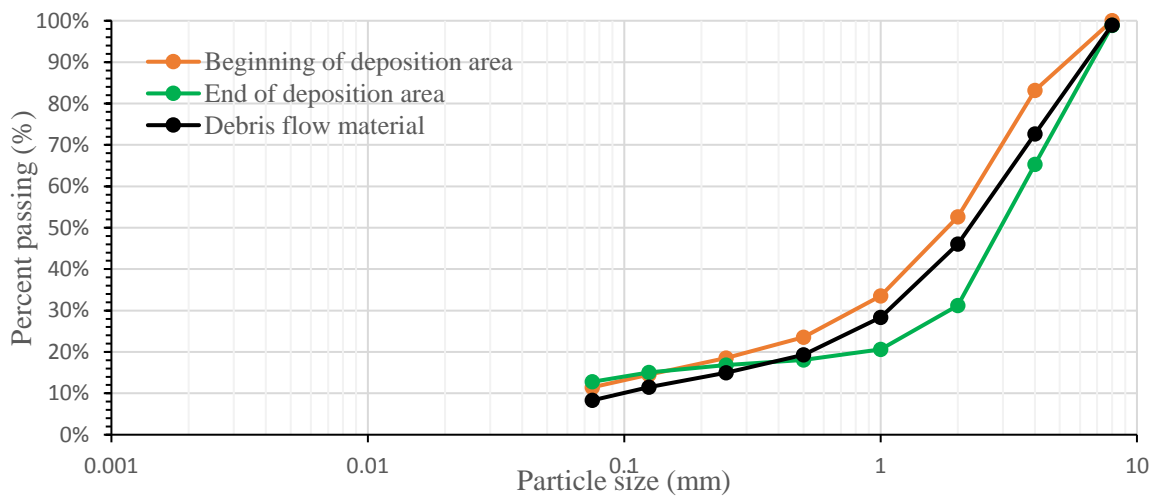
E.3.3 GSD for test 41,42,43 with 45+16.5(50% Cv) combination

Grain size distribution for test 41
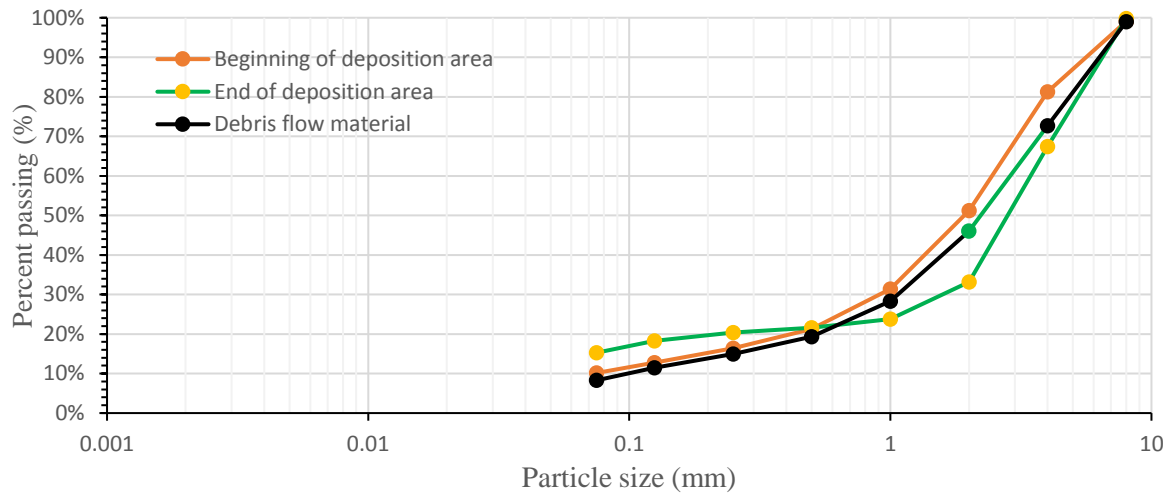
Grain size distribution for test 42
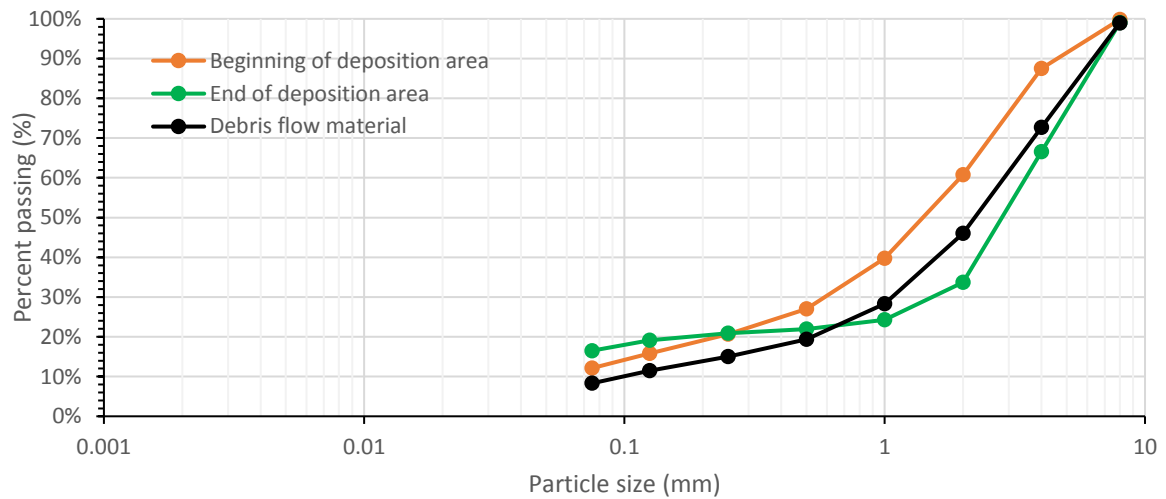
Grain size distribution for test 43
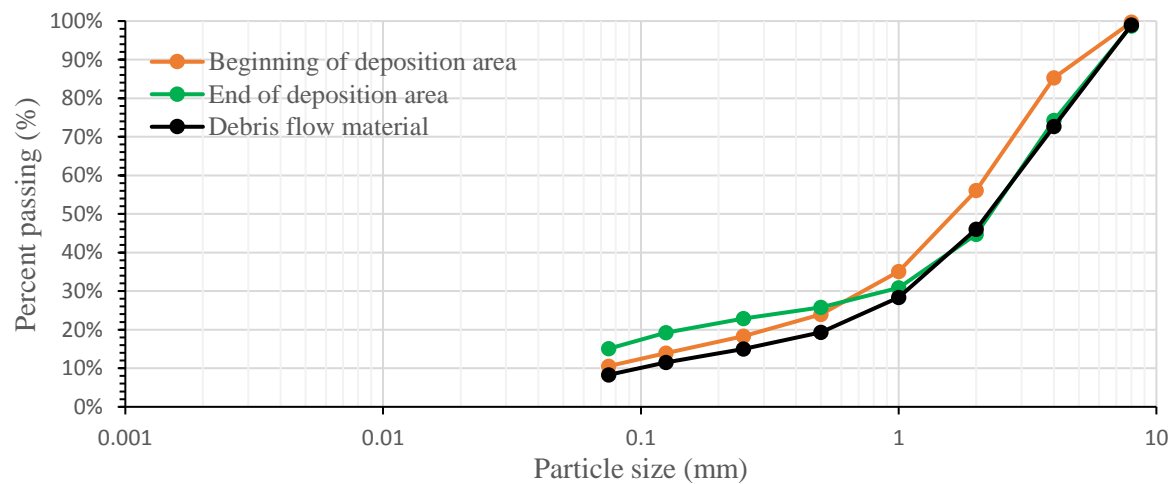
### E.3.4 GSD for test 44 with 45+25(40% Cv) combination

Grain size distribution for test 44
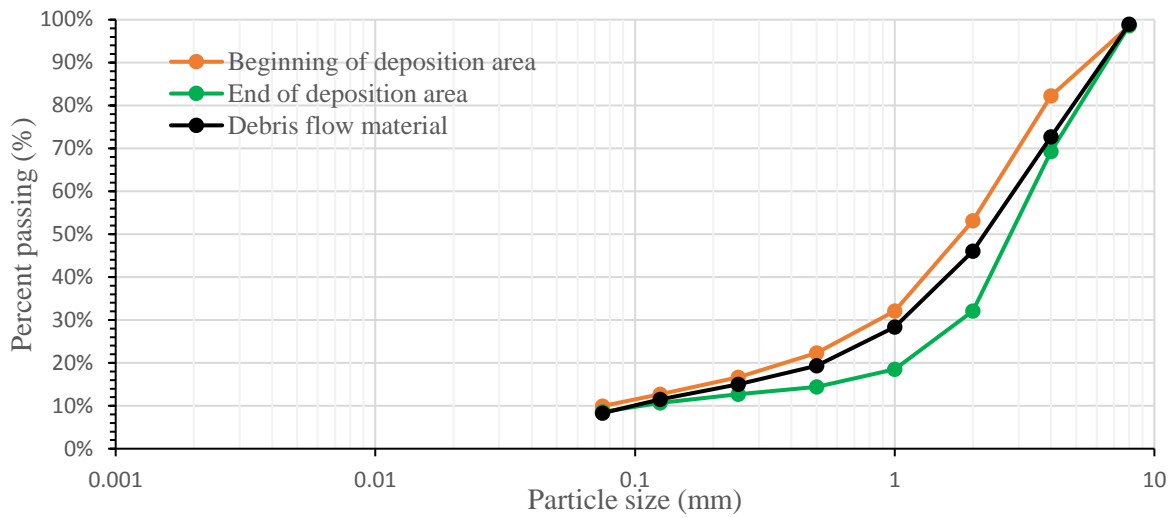
E.4 GSD for test with 40 kg debris flow material

E.4.1 GSD for test 16,17,18 with 40+10(60% Cv) combination

Grain size distribution for test 16
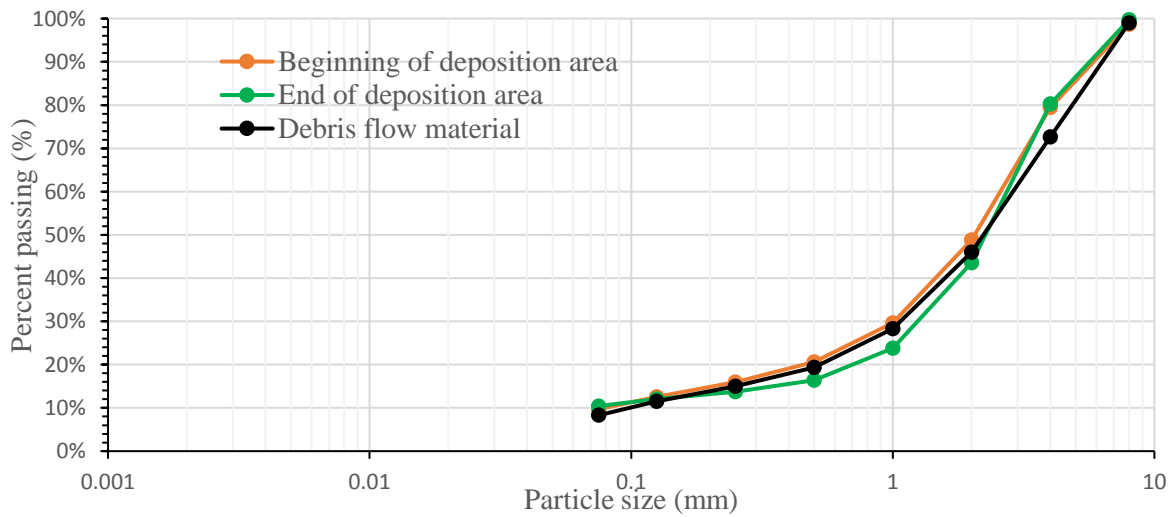
Grain size distribution for test 17
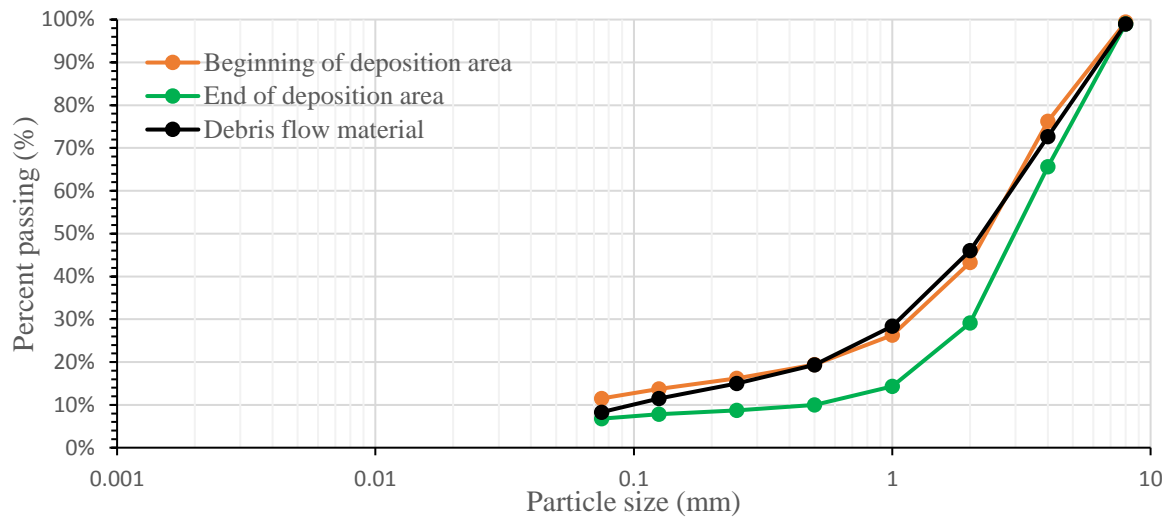
Grain size distribution for test 18

E.4.2 GSD for test 22,23,24 with 40+12(55% Cv) combination

Grain size distribution for test 22

Grain size distribution for test 23

Grain size distribution for test 24

E.4.3 GSD for test 19, 20, 21, 25 with 40+15(50% Cv) combination

Grain size distribution for test 19
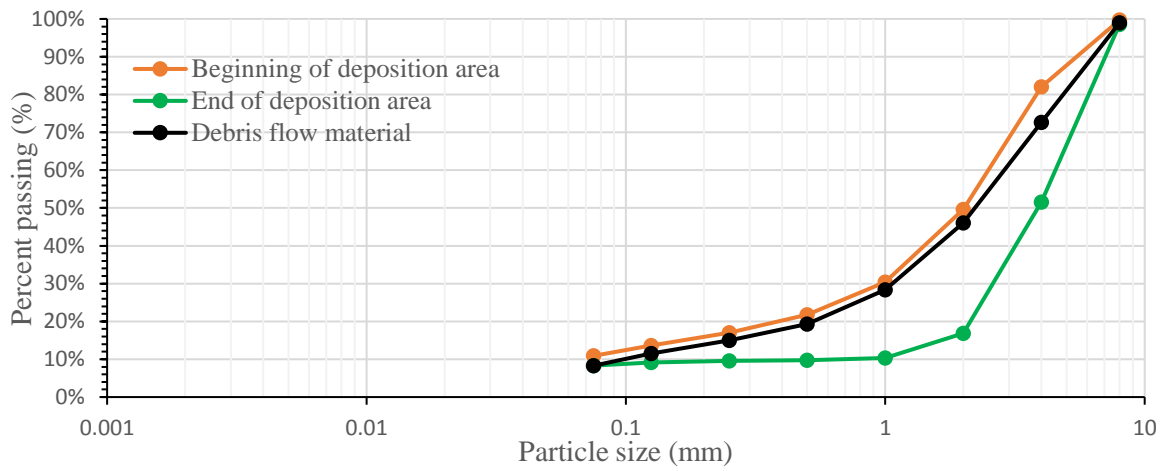
Grain size distribution for test 20

Grain size distribution for test 21
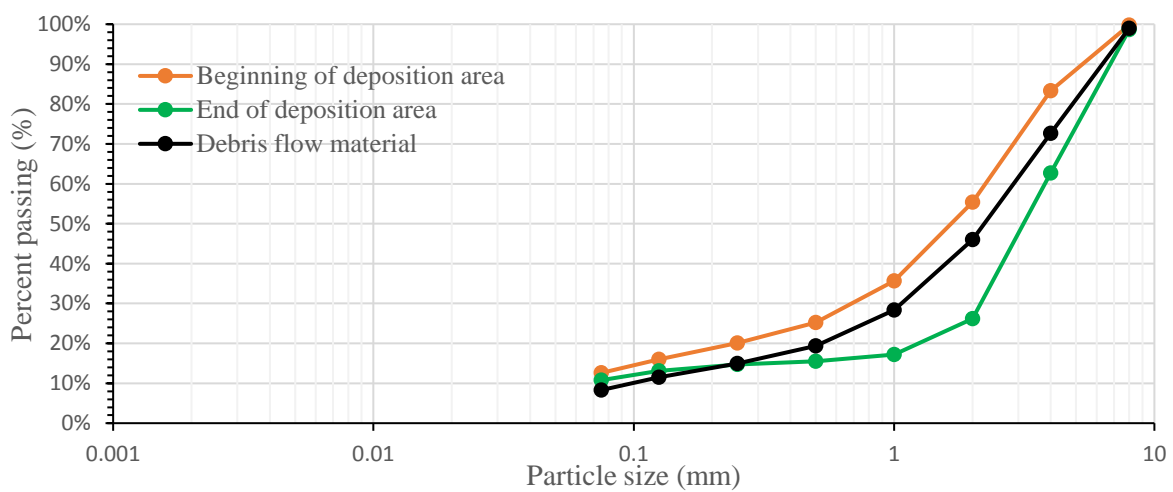
Grain size distribution for test 25

E.4.4 GSD for test 26 with 40+22(40% Cv) combination

Grain size distribution for test 26
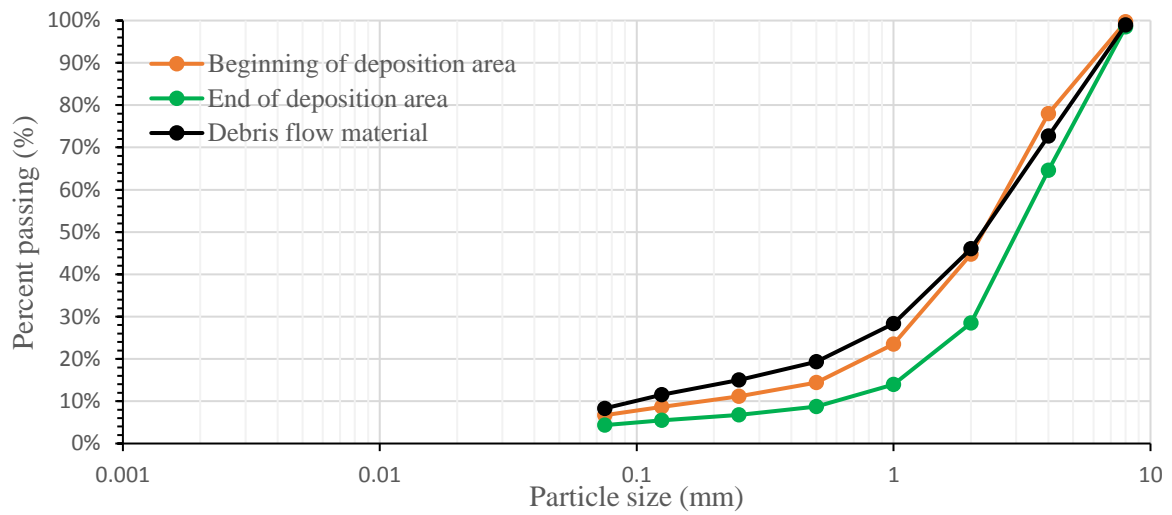
APPENDIX F

Runout length

F.1 Runout length for debris slide test with coarse material(test 1,2,3)
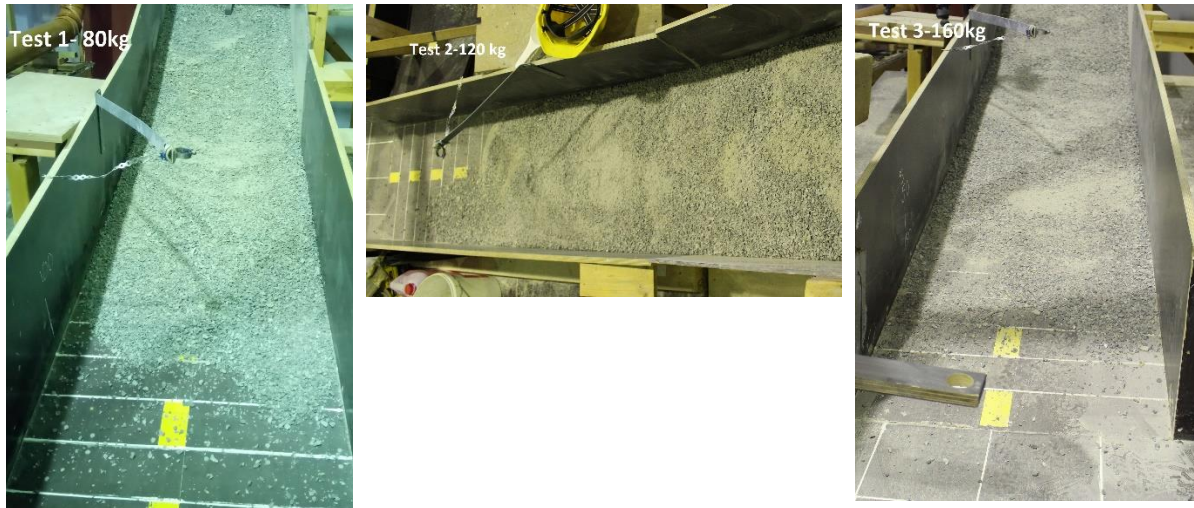
F.2 Runout length for debris slide test with fine material(test 7,8,9)

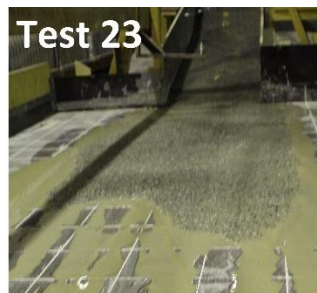### F.3 Runout length for 80+20 combination (test 4,5,6)
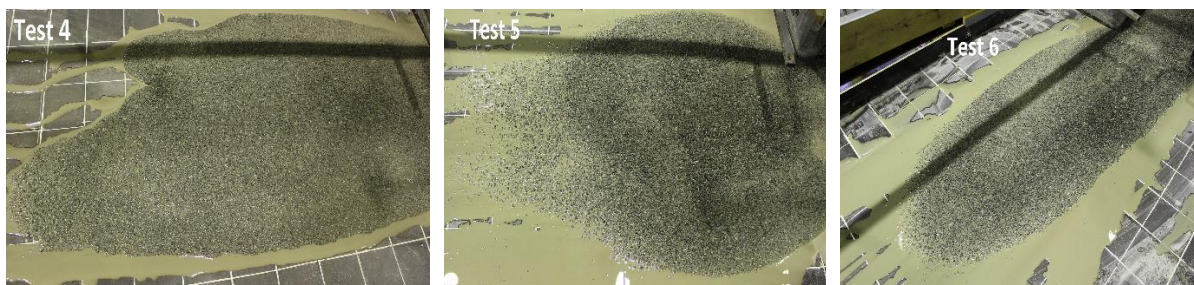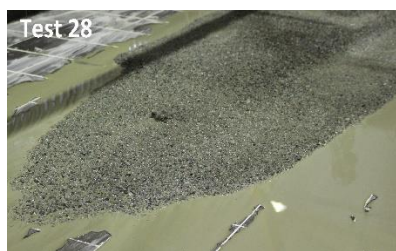
F.4 Runout length for 40+10 combination

F.5 Runout length for 40+15 combination
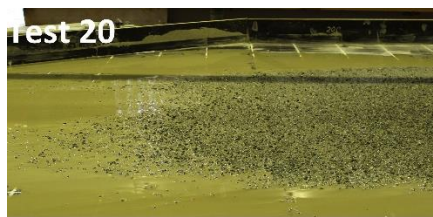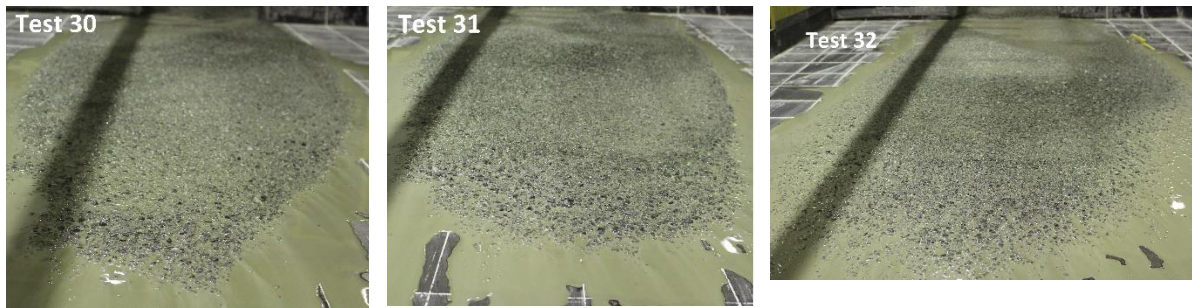

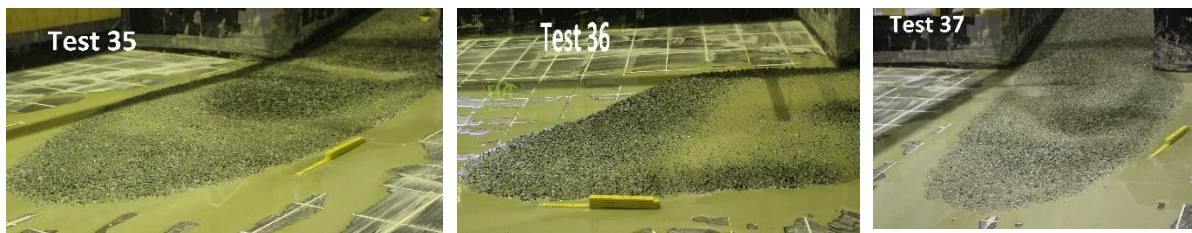### F.6 Runout length for 40+12 combination

F.7 Runout length for 50+12 combination

F.8 Runout length for 50+15 combination

F.9 Runout length for 45+11 combination

F.10 Runout length for 45+13.5 combination

F.11 Runout length for 45+16.5 combination

F.12 Runout length for 45+11(f) combination

APPENDIX G

Test Videos and Pictures

All videos and pictures for debris slide tests and debris flow tests (only with coarse material) are attached as zip files on DAIM.